# COMPARATIVE STUDY OF TURKISH EARTHQUAKE CODE 2007 AND TURKISH BUILDING EARTHQUAKE CODE 2018

A THESIS SUBMITTED TO
THE GRADUATE SCHOOL OF NATURAL AND APPLIED SCIENCES
OF
MIDDLE EAST TECHNICAL UNIVERSITY

BY

İSMAYIL ASGAROV

IN PARTIAL FULFILLMENT OF THE REQUIREMENTS
FOR
THE DEGREE OF MASTER OF SCIENCE
IN
CIVIL ENGINEERING

NOVEMBER 2022

Approval of the thesis:

**COMPARATIVE STUDY OF TURKISH EARTHQUAKE CODE 2007 AND TURKISH BUILDING EARTHQUAKE CODE 2018**

submitted by **İSMAYIL ASGAROV** in partial fulfillment of the requirements for the degree of **Master of Science** i**n Civil Engineering, Middle East Technical University** by,

Prof. Dr. Halil Kalıpçılar
Dean, Graduate School of **Natural and Applied Sciences** _____

Prof. Dr. Erdem Canbay
Head of the Department, **Civil Engineering** _____

Prof. Dr. Özgür Kurç
Supervisor, **Civil Engineering, METU** _____

**Examining Committee Members:**

Prof. Dr. Ahmet YAKUT
Civil Engineering, METU _____

Prof. Dr. Özgür KURÇ
Civil Engineering, METU _____

Prof. Dr. Yalın ARICI
Civil Engineering, METU _____

Prof. Dr. Murat Altuğ ERBERİK
Civil Engineering, METU _____

Asst. Prof. Dr. Berat Feyza SOYSAL ALBOSTAN
Civil Engineering, ÇANKAYA UNIVERSITY _____

Date: 24.11.2022

**I hereby declare that all information in this document has been obtained and presented in accordance with academic rules and ethical conduct. I also declare that, as required by these rules and conduct, I have fully cited and referenced all material and results that are not original to this work.**

Name Last name : İsmayıl Asgarov

Signature :

## ABSTRACT

### COMPARATIVE STUDY OF TURKISH EARTHQUAKE CODE 2007 AND TURKISH BUILDING EARTHQUAKE CODE 2018

Asgarov, İsmayıl
Master of Science, Civil Engineering
Supervisor: Prof. Dr. Özgür Kurç

November 2022, 108 pages

This thesis compares the complete analysis and design procedure of TEC 2007 and TBEC 2018 for an archetype reinforced concrete building with three different story configurations (three-story, six-story, twelve-story), and the structures are analyzed and designed at three locations in Türkiye (Istanbul, Ankara, Adana). The study focuses on the differences between the defined approaches in the mentioned codes regarding seismic load calculation, finite element model preparation, and reinforced concrete member design. The results are summarized, and necessary conclusions are derived for the changes that cause the differences between the codes. The effect of updates made to the new seismic code shows variation between the structure heights and locations.


Keywords: Seismic Codes, Comparative Analysis, Reinforced Concrete Design, Equivalent Force Method Analysis.

# ÖZ

## TÜRKİYE DEPREM YÖNETMELİĞİ 2007 VE TÜRKİYE BİNA DEPREM YÖNETMELİĞİ 2018 KARŞILAŞTIRILMASI

Asgarov, İsmayıl
Yüksek Lisans, İnşaat Mühendisliği
Tez Yöneticisi: Prof. Dr. Özgür Kurç

Kasım 2022, 108 sayfa

Bu tez, üç farklı kat konfigürasyonuna (üç katlı, altı katlı, on iki katlı) sahip arketip betonarme bina için TDY 2007 ve TBDY 2018'in tam analiz ve tasarım prosedürünü karşılaştırıyor ve yapılar Türkiye'de üç lokasyonda (İstanbul, Ankara, Adana) analiz edilip ve tasarlanıyor. Çalışma, sismik yük hesabı, sonlu eleman modeli hazırlama ve betonarme eleman tasarımı ile ilgili olarak belirtilen kodlarda tanımlanan yaklaşımlar arasındaki farklılıklara odaklanmaktadır. Sonuçlar özetlenip ve kodlar arası farklılıklara neden olan değişiklikler için gerekli çıkarımlar yapılmıştır. Yeni deprem yönetmeliğinde yapılan bazı güncellemelerin etkisi, yapı yükseklikleri ve konumları arasında farklılık göstermektedir.

Anahtar Kelimeler: Sismik Kodlar, Karşılaştırmalı Analiz, Betonarme Tasarım, Eşdeğer Kuvvet Yöntemi Analizi.

To my family and friends

## ACKNOWLEDGMENTS

The author wishes to express his deepest gratitude to his supervisor, Prof. Dr. Özgür Kurç, for his guidance, advice, criticism, encouragement, and insight throughout the research.

The technical assistance of Prof. Dr. Ahmet Yakut is gratefully acknowledged.

The author is grateful for the support and encouragement of his family, friends, and colleagues.

## TABLE OF CONTENTS

## LIST OF TABLES

TABLES

## LIST OF FIGURES

FIGURES

# CHAPTER 1

# INTRODUCTION

The nature of seismic loads requires the design of structures according to the standards that preserve life safety while maintaining an economical design. Some of the factors that determine the magnitude of lateral seismic load are the following:

a) Location: the site's proximity to the nearest fault lines determines the required accelerations the building must resist.
b) Soil strata: the intensity transferred to the building through ground motion depends on the soil.
c) Lateral force resisting system: the structure's response to the earthquake depends on the lateral force resisting system and materials used.
d) Height, Stiffness: The structure's height and lateral stiffness determine its response mode. The arrangement of appropriate lateral stiffness for the size of the structure is crucial to achieving a safe and economical design.

Considering the variability of the listed points above, it is apparent that before the structural designers start their work, information from the following disciplines is required:

Geotechnical engineers: classify the soil type,

Earthquake engineer: report the probabilities of seismic events and their return intervals,

The multi-disciplinary nature and uncertainty of seismic loads require the use of guidelines that structural engineers can follow in the design of buildings for all materials, heights, stiffnesses, and locations within the code's jurisdiction.

In Türkiye, the first earthquake code was established in the 1940s (Işık, 2021), and updates were made throughout the years to implement the latest technological advancements. Before the Turkish Building Earthquake Code 2018 (TBEC 2018), the latest change was made in 1997. The Turkish Earthquake Code 2007 (TEC 2007)

has an additional chapter for the assessment of existing buildings; the rest of the principles were carried over from the 1997 code.

The 21-year gap between the revision of the seismic code resulted in a notable change in the core approach to the seismic load determination and requirements of these codes. Unfortunately, the effect of these changes for different structural systems on the cost, safety, and serviceability of the buildings have never been fully studied.

## 1.1 Objectives & Scope

The main purpose of this study is to better understand the impact of these major changes on the reinforced concrete buildings. For this purpose, archetype buildings with a lateral system consisting of reinforced concrete shear walls and moment frames are analyzed and designed utilizing both TEC 2007 and TBEC 2018. These buildings have three, six, and twelve stories to consider the effect of building height in the analysis. Three locations were chosen: Istanbul, Ankara, and Adana. Although the seismic design category (SDC) in TBEC 2018 depends on more factors, for comparison, the seismic design category can be divided into four for both codes. Istanbul corresponds to SDC 1, which results in the highest seismic load among other locations, Adana is in SDC 2, and Ankara is in SDC 3 which represents a region with low seismic activity.

The archetype buildings will be analyzed and designed for three seismic design categories having three different heights according to TEC 2007 and TBEC 2018. The analysis results will be compared in terms of seismic load calculations, member design loads, capacity design equations, reinforcement detailing requirements and total weight of the major reinforcement. The main steps of this comparative study are listed below:

a. An archetype floor plan is utilized to generate structural models of three, six, and twelve story buildings. The buildings have lateral force resisting systems of moment frames and shear walls.
b. All buildings are analyzed and designed according to both TEC 2007 and TBEC 2018. The analysis is based on equivalent static loads and linear elastic analysis. The analyses and design calculations for the frame members are performed with ETABS v19.
c. The analysis results are compared in terms of base shears, member forces, total reinforcement weight, total material cost and drift.

# CHAPTER 2

# LITERATURE REVIEW

The structural design of buildings against an earthquake load is a complex procedure. Seismic codes simplify the process by using the latest advancements in the literature to provide a reasonable approach for determining the variables involved in the seismic design of structures. As the literature progresses, the need arises to update the seismic codes according to the latest findings. A comparison is made between the seismic codes to determine the significance of each change. The comparative analysis determines the impact of the latest findings on the design process. The available literature that compares the seismic codes is discussed, and their findings are presented.

Akkar et al. (2018) have studied the evolution of seismic hazard maps in Türkiye. They have found that the ground-motion amplitudes have increased for locations closer to the fault zones. According to the results of Akkar et al. (2018), the increase in amplitude has increased the earthquake load demand on structures with short spectral periods compared to TEC 2007, while for moderate to high periods, the increase in the demand decreases due to the differences in the response spectrum definitions in TBEC 2018.

Nemutlu and Sarı (2018) have compared four and nine-story reinforced concrete structures with respect to TEC 2007 and TBEC 2018. They have used modal response spectrum analysis to compare the base shears. The analyzed building's soil category is Z3 for TEC 2007, and ZD for TBEC 2018. Their results show that the base shear increases by 10% in both directions from TEC 2007 to TBEC 2018.

Aksoylu et al. (2020) have studied the differences between ASCE 7-16, TBEC 2018, and TEC 2007. The comparisons are made for seismic load calculations, base shears, drifts, and non-linear performance of reinforced concrete structures. The structures of three, five, seven, and nine stories are analyzed with varying soil classifications

depending on the code. The lateral resisting system of all structures is moment-resisting reinforced concrete frames. The acceleration determination procedures are similar in TBEC 2018 and ASCE 7-16. In TEC 2007, the acceleration is obtained from the seismic region map of Türkiye, while TBEC 2018 and ASCE 7-16 both use site-specific maps that give spectral acceleration coefficients corresponding to a 0.2-second short and a 1-second-long period. These spectral acceleration coefficients are modified by multiplying them with $F_s$ and $F_1$ factors dependent on the site's soil characteristics. The equivalent lateral force method (ELFM) is used to apply the seismic load for linear design. The study shows that the design response spectrum preparation procedure is similar in TBEC 2018 and ASCE 7-16, with an additional factor of 2/3 that is multiplied by the spectral acceleration coefficients in ASCE 7-16.

Additionally, the structure's weight is determined from the sum of dead load and a percentage of the live load in TEC 2007 and TBEC 2018. The percentage of live load applied depends on the usage class of the structure. However, in ASCE 7-16, the live loads are not included, but additional requirements are given for storage areas and partition loads, resulting in less seismic weight than the other two codes (Aksoylu et al., 2020). The analysis is based on a site located in Istanbul/Avcilar. The soil class is a variable, and the same analysis procedure is performed for all soil classes. The author concludes that the spectral acceleration coefficient decreases as the soil gets weaker from ZA to ZE in TBEC 2018.

According to Aksoylu et al. (2020), decreasing member stiffnesses in TBEC 2018 results in increased periods, in the calculation of periods for ASCE 7-16 minimum periods governs which changes the results. TEC 2007 governs at almost all soil classes for shorter buildings, while TBEC 2018 governs for taller buildings and strong soils. TEC 2007 reports higher forces for structures in weaker soils, and ASCE 7-16 results in lower or equal forces at all building heights and soil classes compared to the other two codes. The drifts are also calculated, and the study revealed that TBEC 2018 drift results are generally smaller than the other two codes except for the weakest soil and three-story structure. TEC 2007 drifts are generally larger or equal

to ASCE 7-16 drifts except for seven and nine-story structures in Z1 (ZB, B) and nine-story structures in Z2 (ZC, C) soil.

Aksoylu et al. (2020) have also conducted a performance evaluation using a nonlinear pushover analysis procedure for all three codes. The static pushover analysis is performed for all structures. The author mentions that the design of members was not changed between the codes, even in the case of failure to ensure that the comparison focuses only on the other differences between the codes. The considered design earthquake corresponds to the seismic event with a return period of 475 years. ASCE 7-16 performance displacements are lower than the other two codes, and for higher story structures, TBEC 2018 results are lower than TEC 2007. The performance demands are closer for weaker soils. The author reports that the pushover analysis resulted in ductile behavior at all structure and soil combinations, and the plastic hinge formations started from the beams.

The study compared three seismic codes: ASCE 7-16, TEC 2007, and TBEC 2018. The obtained results indicate that the soil class at the site is a significant factor affecting the trends of the results between the codes. The study focuses on reinforced concrete structures with a lateral system of moment frames at a single location.

Akansel et al. (2020) have compared the TEC 2007 seismic zone map with the TBEC 2018 seismic hazard map in terms of spectral acceleration intensity (SAI) by using 475-year return period accelerations in Türkiye. The author states that the study aims to identify the change in seismic hazard levels across the country between the codes. The study considers 4000 points on TEC 2007 map and 14000 points on TBEC 2018 map to obtain the peak ground acceleration (PGA) and SAI ratios of the two seismic codes. The maps are iterated for each soil category defined in both codes. The author finds that there is an average of 50% increase in PGA values from 2007 to 2018 code averaged across all points. They add that the increase is especially significant in low seismic zones defined in TEC 2007 and locations close to a fault line. The author’s results show that the maximum increase in SAI is observed for weak soils, and they speculate that the updates to the seismic code will increase the cost for buildings located on weak soils.

Işık (2021) has performed a study on the previous five seismic design codes (1968, 1975, 1998, 2007, and 2018). The variations in size and material quality of structural components like columns and beams have been compared for each code. A four-story reinforced concrete model was assessed by three distinct analysis methods, including eigenvalue, pushover, and dynamic time history, using the minimum requirements for the members in each code. The five seismic codes to be analyzed are given in Table 2.1.

Table 2.1. The codes to be used in the study. (Table 2, Işık, 2021)

| Year | Code | Abbreviation (in Turkish) |
|---|---|---|
| 1968 | Specification for Structures to be Built in Disaster Areas | ABYYHY-1968 |
| 1975 | Specification for Structures to be Built in Disaster Areas | ABYYHY-1975 |
| 1998 | Specification for Structures to be Built in Disaster Areas | ABYYHY-1998 |
| 2007 | Turkish Earthquake Code | DBYBHY-2007 |
| 2018 | Turkey Building Earthquake Code | TBDY-2018 |

The author lists each code and briefly details the improvements made compared to the previous versions. A four-story reinforced concrete structure is considered for the analysis. The structure's performance is assessed by pushover and time history analysis. The author presents the time history analysis results as shown in Table 2.2, with load factor being used to reach the target displacement and total support force and moment shown for each code. Table 2.2 shows that throughout the revisions made to the code, total support force and moment carrying capacity of the structures are increased when specified target displacements are reached.

Table 2.2. Time history analysis results. (Table 8, Işık, 2021)

| Code | X Direction | | | | Y Direction | | | |
|---|---|---|---|---|---|---|---|---|
| | Total Support Force | | Moment | | Total Support Force | | Moment | |
| | Load Factor | Total Support Force (kN) | Load Factor | Moment (kN·m) | Load Factor | Total Support Force (kN) | Load Factor | Moment (kN·m) |
| 1968 | 4.15 | 414.163 | 4.096 | 845.394 | 4.151 | 414.163 | 3.745 | 844.957 |
| 1975 | 4.975 | 497.071 | 4.506 | 905.650 | 4.969 | 496.896 | 4.402 | 905.592 |
| 1998 | 5.933 | 592.373 | 5.157 | 1066.483 | 7.3741 | 733.06 | 6.7398 | 1319.594 |
| 2007 | 7.112 | 711.298 | 6.8787 | 1281.552 | 9.0158 | 901.587 | 8.8904 | 1579.939 |
| 2018 | 12.432 | 1243.393 | 12.373 | 2094.214 | 12.8585 | 1285.857 | 12.3514 | 2126.838 |

The author reports that the building period values have dropped because each revised code has stingier requirements which leads to the design of structures that are more resilient against seismic events. Throughout the updates to the seismic codes, the structure's performance has improved, and the target displacement values have been reduced. Between the first and the last code, the period value changes by 27%. The difference between the seismic load carrying capacity of the codes from 1968 and 2018 was estimated to be over 200%.

Büyüksaraç et al. (2022) focus on locations in the same seismic design category in TEC 2007 and compare them with the newly introduced seismic parameters for the same locations in TBEC 2018. The differences in seismic parameters between the seismic codes are highlighted, and pushover analysis is performed to assess the performance of analyzed structures. The study is conducted for a reinforced concrete seven-story structure that consists of moment frames. The chosen locations for analysis are Adana, Erzurum, Ankara, Bursa, Kütahya, Diyarbakır, and Samsun. The authors report that according to TEC 2007, all locations are in the same seismic region. However, in TBEC 2018 the seismic parameters are different for each location due to the usage of a site-specific hazard map introduced in the latest code. The findings of Büyüksaraç et al. (2022) also support the results of Akkar et al. (2018), initial peak ground accelerations are higher in some locations for TBEC 2018, but when the design spectral accelerations are compared, the TEC 2007 design spectral accelerations are higher at all locations. Figures 2.1 and 2.2 demonstrate the results found in the study for peak ground accelerations and reduced design spectral accelerations. The reduced design spectral accelerations shown in Figure 2.2 are obtained by using a reduction factor of eight for both codes.

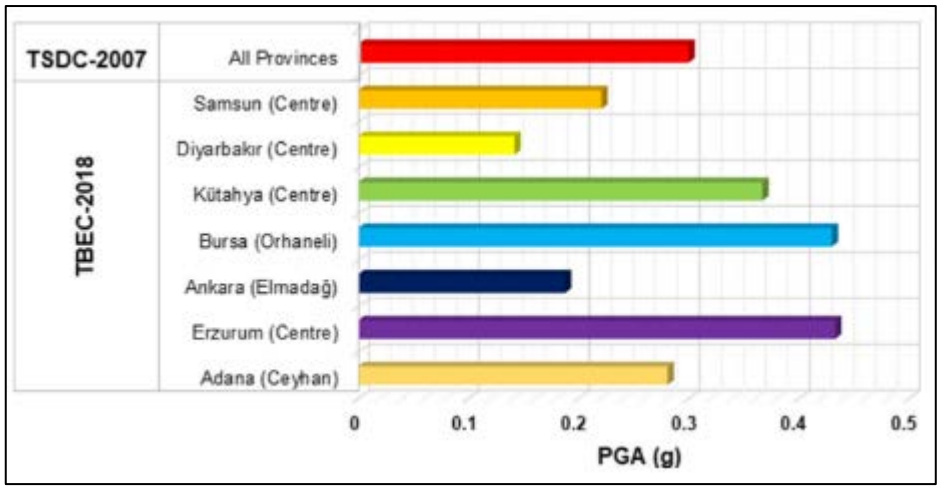


Figure 2.1. Comparison of PGA for selected locations. (Büyüksaraç et al., 2022)

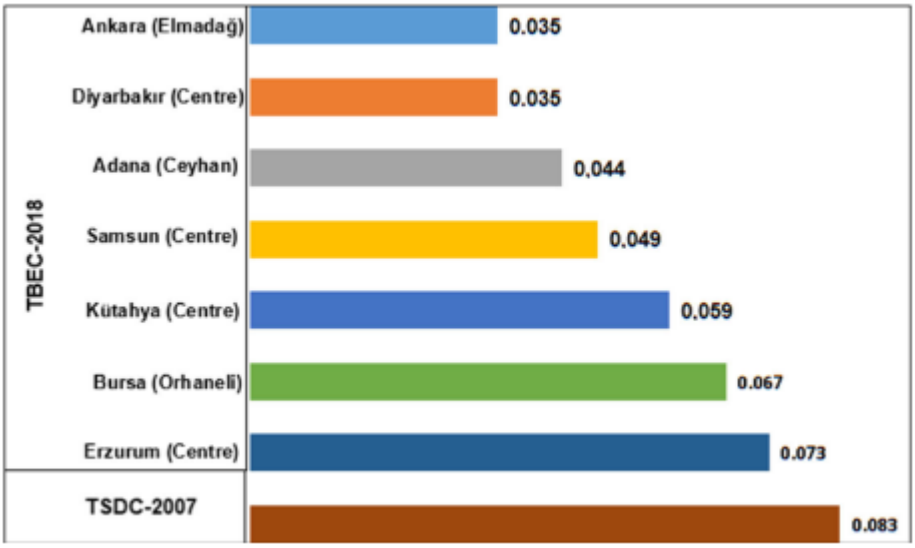


Figure 2.2. The comparison of the reduced design spectral accelerations. (Büyüksaraç et al., 2022)

From Figures 2.1 and 2.2, Büyüksaraç et al. (2022) conclude that the usage of site-specific seismic parameters significantly impacts the seismic analysis of structures. The use of seismic zones in TEC 2007 results in over estimation of the design spectral acceleration, while the use of site-specific data results in the formation of a spectral response spectrum that is more accurate. The study is limited to seven locations and one seismic region defined in TEC 2007. Additionally, the structure model uses the same effective stiffnesses for both codes to eliminate the differences arising from this change.

## 2.1 Summary

The changes between the TEC 2007 and TBEC 2018 have resulted in extensive research into the topic. The papers discussed in this chapter have shown the changes in obtaining accelerations, structure modeling, analysis, and seismic performance.

The consensus in the literature is that the new TBEC 2018 seismic code has resulted in a more accurate estimation of the seismic loads due to the usage of the seismic hazard map. The updates made to the response spectrum preparation are the starting point for the differences between the codes. The members are also modeled considering their cracked sections which add to the change in response spectrum by modifying the period and stiffness of the structure.

This study will add to the literature by considering the moment frame and shear wall dual lateral resisting reinforced concrete system. Including both moment frames and shear walls will consider the effect of using a dual system on the compared results. Additionally, three locations are chosen according to their seismic design category, resulting in a comparison that includes structures in high, moderate, and low seismic regions. Three different structure heights are chosen to represent the differences according to the changing building height. Also, the members are designed according to both codes, and the sections are modified if a failure condition occurs.

# CHAPTER 3

# PROPERTIES OF ARCHETYPE BUILDING AND DESIGN PARAMETERS

This study includes the analysis and design of reinforced concrete structures located in Istanbul, Ankara, and Adana. The analyzed archetype structures are three, six, and twelve-stories. The building heights and locations are varied to include their effect in comparisons made between TEC 2007 and TBEC 2018. The information about the material properties, gravity loading, finite element model (prepared in ETABS v19.0.0) of the archetype structure, and additional information about the chosen locations for analysis and design are presented. The analysis is performed under gravity and seismic loads, other are outside the scope of this study.

## 3.1 Building Floor Plan

Figure 3.1 shows the archetype structure framing layout which was taken from Example 7B (Yakut et al., 2018) and slightly modified. The green, red, and blue colors indicate reinforced concrete beams, columns, and shear walls. The typical floor plan consists of reinforced moment frames around two U-shaped shear walls. The overall dimensions of the building are nineteen meters in the X-direction (East/West) and fourteen meters in Y-direction (North/South). The beam spans are 1.5, 3, 4, 4.5, and 5 meters. The first story's height is 3.5 meters; the other stories are 3 meters. There are four shear walls with 2-meter lengths each in the X-direction and two with 3-meter lengths each in the Y-direction. The member sizes for each structure will be discussed in detail in the succeeding chapters. The total height of each structure is given in Table 3.1. The number of stories and total structure heights.. Additionally, 3D models of the buildings are given in Figure 3.2.

Table 3.1. The number of stories and total structure heights.

| Number of Stories | Total height (m) |
|---|---|
| 3 | 9.5 |
| 6 | 18.5 |
| 12 | 36.5 |

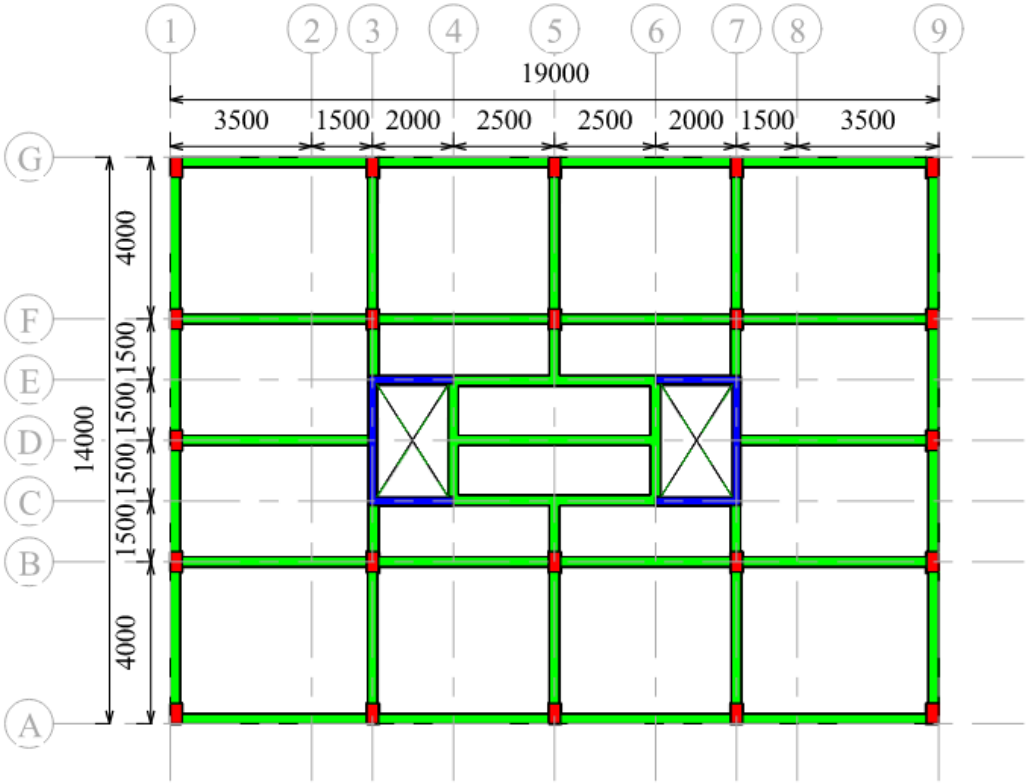


Figure 3.1. Floor plan of the archetype structure used in the study.

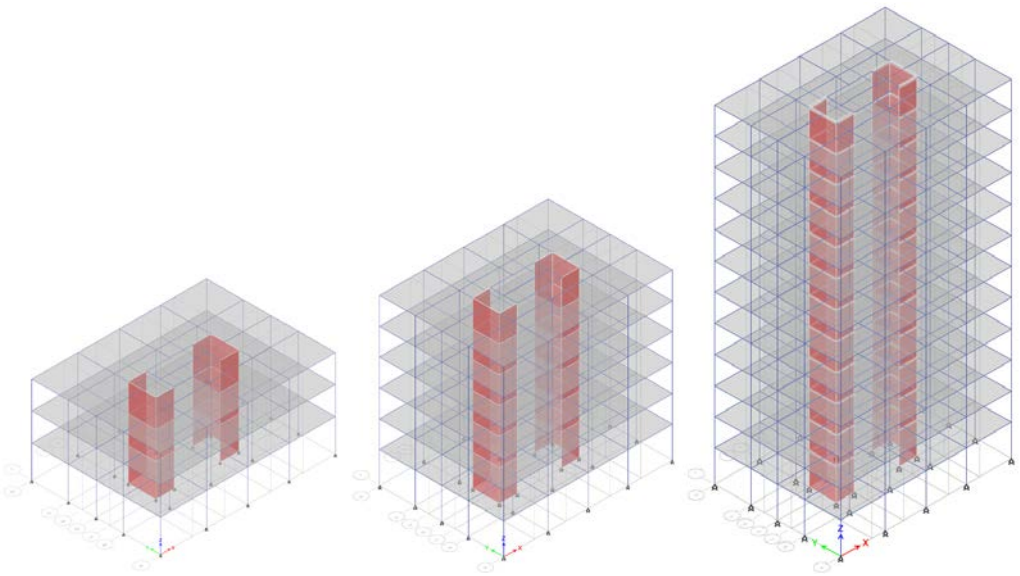

Figure 3.2. Three, six, and twelve-story building 3D models.

## 3.2 Locations

Three locations are chosen for the study: Istanbul, Ankara, and Adana. The locations correspond to three different seismic design categories (SDC). Figure 3.3 shows the locations and their seismic design categories.

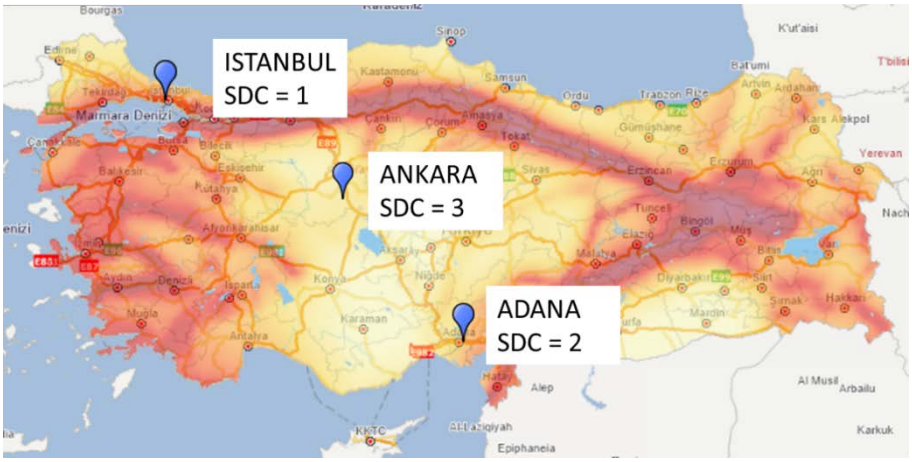


Figure 3.3. Locations and seismic design categories (DEMC, 2020).

In TEC 2007, the seismic design parameters change according to the seismic zone map that divides the country into predetermined zones without considering the

variability in the soil conditions. The code defines a constant acceleration for each zone, and it is used to construct the response spectrum. With TBEC 2018, an online seismic hazard map tool is introduced to read the seismic parameters from the coordinate location of the buildings. The map provides the response spectrum for gravity and lateral seismic loads. Table 3.2 shows the locations and their coordinates alongside the seismic category definition according to each code. The seismic parameters to be used in the load calculation will be discussed in detail in Chapter 4.

Table 3.2. Archetype building locations, coordinates, and seismic design parameters.

| Location | Coordinates (Latitude/ Longitude) | TEC 2007 | TBEC 2018 |
|---|---|---|---|
| Istanbul | 40.9900/ 28.8900 | Zone 1 | SDC 1 |
| Ankara | 39.3890/ 32.7800 | Zone 3 | SDC 3 |
| Adana | 36.9925/ 35.4547 | Zone 2 | SDC 2 |

## 3.3 Material Properties

The used material properties are given in Table 3.3 for concrete and Table 3.4 for steel reinforcement.

Table 3.3 Concrete material properties.

| Property | Value |
|---|---|
| Material Strength | C30 ($f_{ck}$ = 30 MPa, $f_{cd}$ = 20 MPa) |
| Elastic Modulus | 31800 MPa |
| Material Safety Factor | 1.50 |

Table 3.4 Steel reinforcement properties.

| Property | Value |
|---|---|
| Material Strength | S420 ($f_{yk}$ = 420 MPa, $f_{yd}$ = 365 MPa) |
| Elastic Modulus | 200000 MPa |
| Material Safety Factor | 1.15 |

## 3.4 Gravity Loads

The focus of the study is the seismic loads, the gravity loads are assumed by considering the values given in Example 7B (Yakut et al., 2018). The gravity loads are summarized in Table 3.5 and Table 3.6, and they are applied to all buildings considered in the study. The design of members for the gravity loads will be checked together with the seismic loads in the succeeding chapter.

Table 3.5 Roof gravity loads.

| Load Description | Load ($kN/m^2$) |
|---|---|
| Dead Load | 1.7 |
| Live Load | 0.8 |
| Snow Load | 1.2 |

Table 3.6 Floor gravity loads.

| Load Description | Load ($kN/m^2$) |
|---|---|
| Dead Load | 3.8 |
| Residential Live Load | 2.0 |
| Corridor/Stair Live Load | 3.5 |

## 3.5 Soil Properties

The soil considered under the building is defined as: “very dense sand, gravel, hard clay, and silty clay”. The definition is assigned to group (A) in Table 6.1, TEC 2007, from Table 6.2, TEC 2007, the soil class is obtained as Z1. For TBEC 2018, the soil class is defined as ZC for the considered definition.

# CHAPTER 4

# METHODOLOGY

The analysis and design of archetype structures are performed per the code's requirements. The member sizes are kept the same between the 2007 and 2018 codes at each structure with the same story for the sake of comparison. For all structures: the gravity loads are transferred by the slab to the beams, columns, and walls. The moment frames and shear walls carry the lateral earthquake loads and they are distributed to the lateral load resisting system by the diaphragm that is assumed as rigid. The foundation design is outside the scope of this thesis. The modeling assumptions are presented, lateral load calculation procedure is explained in detail for each code separately, and the necessary modifications are made to the seismic parameters, and the reasons are discussed.

## 4.1 Modeling Assumptions

The structures are modeled using ETABS v19. The beams and columns are modeled with frame elements. The slab and the shear walls are modeled as shell elements. A rigid diaphragm constraint is defined at each story. For TEC 2007 models, gross inertia values are used for all members. However, TBEC 2018 enforces the use of effective inertia values which are only applied for analysis performed according to TBEC 2018. The column bases are modeled with pin supports. Moment releases are assigned to the ends of the beams shown with red color in Figure 4.1 and their participation in the lateral moment resisting system is ignored.

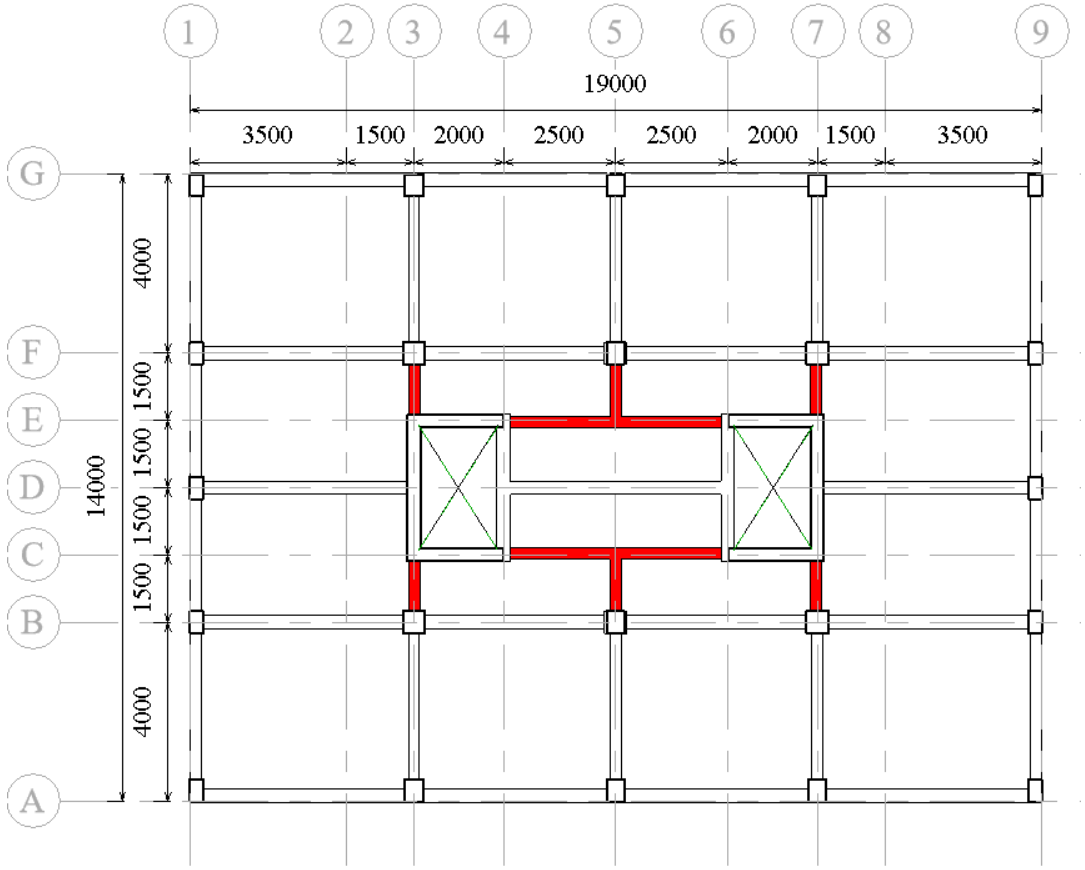


Figure 4.1. Beams with moment releases.

Additionally, modeling assumptions and reasonings are summarized:

a) The pin supports are used at bases of columns and shear walls. The effect of moment at the base of the columns is negligible since the main lateral resistance of moment frames comes from the tension-compression axial load couple on the columns (Figure 4.2). For the shear walls, assigning pin or fixed support at the ends of the shell elements does not matter since the behavior of the base still represents the fixed support.

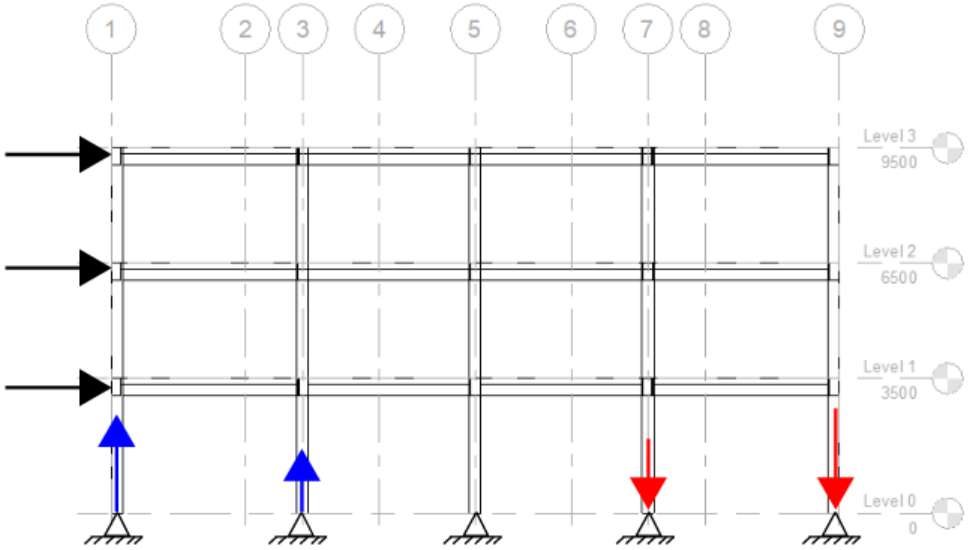


Figure 4.2. Moment frame representative reaction at the support to earthquake load.

b) Compared to the lateral stiffness of vertical elements, the reinforced concrete slab exhibits significantly more lateral stiffness; therefore, it is considered as rigid. A rigid diaphragm is assigned at each level assuming the diaphragm will distribute the lateral load with negligible in plane deformation. R. Pinho (2008) have found that when compared to other methods in the literature assigning a rigid diaphragm to the floor results in the closest agreement with their experimental data.

c) The slab thickness is taken as 14 cm from Example 7B (Yakut et al., 2018) and since rigid diaphragm assumption is made to distribute the lateral load, the only function of the slab in the model is to distribute the gravity loads to the beams and shear walls.

d) Initial member sizes are designed by considering the minimum requirements of TEC 2007 and TBEC 2018. The governing requirement (maximum or minimum member size limit) between the codes is used for analysis. Therefore, comparison eliminates the differences due to the minimum member size limits imposed by the codes and focuses on the applied seismic load and reduction factors.

## 4.2 Preliminary Design

The member size limits are imposed in both codes, and the differences between the requirements are shown and discussed for each member. The preliminary sizes are set to satisfy the minimum size limits, and the member sizes are increased to satisfy both codes' strength and serviceability requirements. The minimum column dimension limits are shown in Table 4.1.

Table 4.1. Minimum column dimension.

| Description | TEC 2007 (Section 3.3.1) | TBEC 2018 (Section 7.3.1) |
|---|---|---|
| Minimum allowable dimension for rectangular columns | 250 mm | 300 mm |
| Minimum allowable area | 75000 $mm^2$ | - |
| Minimum allowable area with respect to axial load | $A_{c,\,min} = N_{dm} / 0.5 * f_{ck}$ | $A_{c,\,min} = N_{dm} / 0.4 * f_{ck}$ |

The typical column size of 300x500 mm satisfies these requirements. The minimum area required with respect to the axial load on the column governs the column sizes for the 12-story structure. The decrease of the factor in the denominator from 0.5 to 0.4 results in TBEC 2018 governing the column sizes. The resultant difference is a 25% increase in the minimum required column area between the two codes.

The same column sizes are used in 12-story TEC 2007 to eliminate the variance when comparing other changes. The maximum load allowed on the column size is shown in Table 4.2 for both codes.

Table 4.2. Maximum allowed axial load with respect to the minimum area.

| Column Size | | Maximum Axial Load (kN) | |
|---|---|---|---|
| (mm) | (mm) | TEC 2007 | TBEC 2018 |
| 300 | 500 | 2250 | 1800 |
| 400 | 500 | 3000 | 2400 |
| 500 | 500 | 3750 | 3000 |

The minimum requirements for the beam dimensions are tabulated in Table 4.3.

Table 4.3. Minimum and maximum beam dimensions.

| Description | TEC 2007 (Section 3.4.1) | TBEC 2018 (Section 7.4.1) |
|---|---|---|
| Minimum width | 250 mm | 250 mm |
| Maximum width | $h_{beam} + b_{column}$ 450 + 300 = 750 mm | $h_{beam} + b_{column}$ 450 + 300 = 750 mm |
| Minimum depth | Max (300 mm, 3 * $t_{slab}$) Max (300 mm, 3 * 140 = 420 mm) | Max (300 mm, 3 * $t_{slab}$) Max (300 mm, 3 * 140 = 420 mm) |
| Maximum depth | 3.5 * $b_{beam}$ 3.5 * 250 = 875 mm | 3.5 * $b_{beam}$ 3.5 * 250 = 875 mm |

The typical beam size is 250x450 mm, and the 300x600 mm beams are used in the 12-story structure to limit the drifts. The differences between the drifts of the two codes will be discussed in the next chapter. The minimum and maximum limits for the beam dimensions have not changed.

The shear wall thickness and length limits are shown in Table 4.4.

Table 4.4. Minimum and maximum shear wall dimensions.

| Description | TEC 2007 (Section 3.6.1) | TBEC 2018 (Section 7.6.1) |
|---|---|---|
| Minimum wall thickness | Max (200 mm, $H_{story}$ / 20) Max (200 mm, 3500/ 20= 175 mm) = 200 mm | Max (250 mm, $H_{story}$ / 16) Max (250 mm, 3500/ 16= 219 mm) = 250 mm |
| Maximum wall thickness | $L/t \geq 7$ 2000/7 = 285 mm 3000/7 = 428 mm | $L/t \geq 6$ 2000/6 = 333 mm 3000/6 = 500 mm |

The limits for maximum and minimum dimensions of the wall have changed between the codes. In TBEC 2018, the minimum limit for the thickness has been increased

from 200 to 250 mm, and for the maximum limit, the L/t ratio has been changed to 6, which allows thicker walls to be used compared to TEC 2007.

The 250 mm thickness works for three and six-story structures, while 285 mm is required for twelve-story structures due to drift and strength limits.

The used member cross-sections are given in Figures 4.3 and 4.4 with minimum reinforcement, the reinforcement amount increases according to the demands of each member, and it will be given in the next chapter.

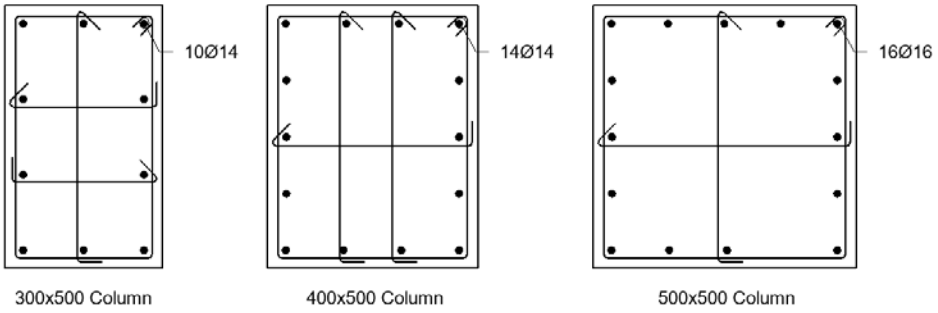


Figure 4.3. Column cross-sections with minimum reinforcement.

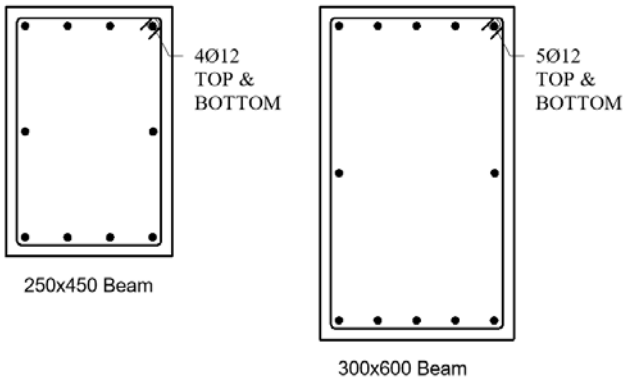


Figure 4.4. Beam cross-sections with minimum reinforcement.

## 4.3 Lateral Load Calculation for TEC 2007

The procedures defined in TEC 2007 are followed to calculate the lateral load on the archetype structure. The seismic zone map of Turkiye is used to identify the accelerations of each location. The seismic response spectrum is prepared, the

reduction factor calculations are given at all story configurations, and the results are discussed.

- Irregularities: The irregularity check is performed, and the twelve-story structure has a torsional irregularity (A1, Table 2.1, TEC 2007). For a given story, the ratio of maximum drift and average drift of the opposite corners must be less than 1.2. For the twelve-story structure, the maximum ratio is 1.27. The code requires the eccentricity to be amplified for floors where the ratio is exceeded.
- Effective Ground Acceleration Coefficient ($A_0$): The coefficient changes depending on the seismic zone. The seismic zones and corresponding accelerations ($A_0$) are tabulated in Table 4.5.

Table 4.5. Seismic zone and effective ground acceleration coefficients.

| Location | Seismic Zone | $A_0$ |
|---|---|---|
| Istanbul | 1 | 0.40 |
| Ankara | 3 | 0.20 |
| Adana | 2 | 0.30 |

- Building Importance Factor (I): The importance factor is chosen as 1 (4. Other Buildings, Table 2.3, TEC 2007).
- Site Class: The soil is assumed to be very dense soil which corresponds to (A) in soil groups (Table 6.1, TEC 2007) and Z1 in site class (Table 6.2, TEC 2007).
- Spectrum Coefficients: The site class is defined as Z1; therefore, the spectrum characteristic periods are $T_A = 0.10$ sec., $T_B = 0.30$ sec. (Table 2.4, TEC 2007). The spectrum plot is shown for each location per TEC 2007 in Figure 4.5.

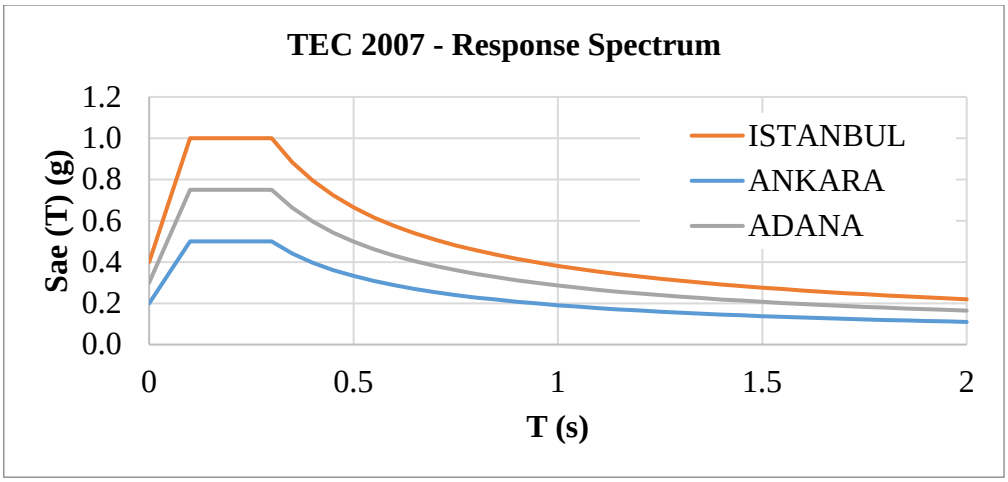


Figure 4.5. Response spectrum plot for TEC 2007 at three locations.

- Base Shear: The base shear and minimum base shear are defined in Equation 2.4, TEC 2007 as:

$$V_t = W * A(T_1) / R_a(T_1) \quad (4.1)$$

$$V_{t,\,min} = 0.1 * A_0 * I * W \quad (4.2)$$

Parameters given in the equations above are described in Table 4.6.

Table 4.6. Equations (4.1) and (4.2) parameter descriptions.

| Parameter | Description |
|---|---|
| $V_t$ | Total equivalent earthquake load (base shear force) acting on the building in the direction of the earthquake considered in the Equivalent Seismic Load Method. |
| W | Total weight of the building using the live load participation coefficient |
| $A(T_1)$ | Spectral Acceleration Coefficient |
| $T_1$ | The first natural vibration period of the building |
| $R_a$ | Earthquake Load Reduction Coefficient |
| $V_{t,\,min}$ | Minimum base shear force |
| $A_0$ | Effective Ground Acceleration Coefficient |
| I | Building Importance Factor |

The story mass includes the superimposed dead, self-weight, and 30% of snow load and live load (Equation 2.6, TEC 2007). The total weight is tabulated in Table 4.7 for each structure.

Table 4.7. Total structure weights of the archetype structure.

| Structure | Total (DL + 0.3*S/LL) (kN) |
|---|---|
| Three-story | 8151 |
| Six-story | 17062 |
| Twelve-story | 37314 |

The Spectral Acceleration Coefficient A (T) and Elastic Spectral Acceleration $S_{ae}$ (T) are defined by the following equations (Equation 2.1, TEC 2007):

$$A(T) = A_0 * I * S(T) \quad (4.3)$$

$$S_{ae}(T) = A(T) * g \quad (4.4)$$

Parameters given in the equations above are described in Table 4.8.

Table 4.8. Equations (4.3) and (4.4) parameter descriptions.

| Parameter | Description |
|---|---|
| S (T) | Spectrum Coefficient |
| $S_{ae}$ (T) | Elastic Spectral Acceleration ($m/s^2$) |
| g | Gravitational Acceleration (9.81 $m/s^2$) |

- Seismic Load Reduction Factor (R): The structure is cast-in-place reinforced concrete with moment frames and structural walls resisting the seismic load. To catch all the limitations of both codes, the structures will be attempted to be analyzed and designed as nominal (normal) ductility system. If the code does not allow nominal ductility, the system will be designed as a highly ductile structure, and the corresponding design requirements will be followed.

The seismic load reduction factor is a function of the first natural period vibration of the structure. Equation 2.3, TEC 2007:

$$R_a(T) = 1.5 + (R - 1.5) * T/T_A \quad \text{for} \quad 0 \leq T \leq T_A \qquad (4.5)$$

$$R_a(T) = R \quad \text{for} \quad T_A \leq T \qquad (4.6)$$

where $T_A$ is the first spectrum characteristic period. The parameters shown above apply to all structures, but the remaining items depend on the height and location of the structure. The following sections will go through each structure, and necessary modifications for the locations will be shown within each section.

#### 4.3.1.1 Three–Story Structure

The calculation of the base shear requires determining the natural period of vibration and the reduction factor chosen from Table 2.5, TEC 2007. The natural period of vibration is read from the structural model as: 0.218 seconds for the X-direction ($T_1$) and 0.147 seconds for the Y-direction ($T_3$). For the three-story structure, the mode shapes are given in Figures 4.6 and 4.7.

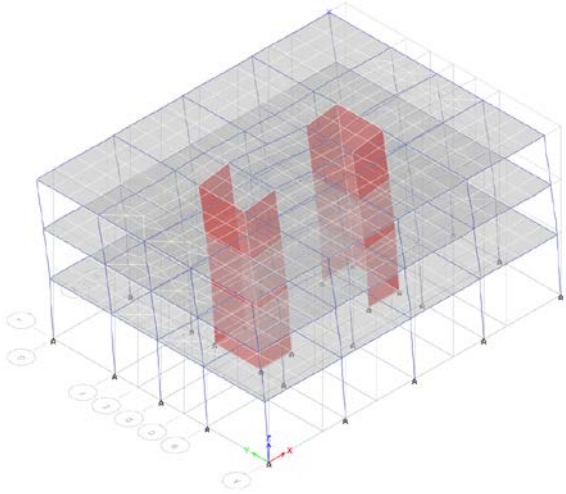

Figure 4.6. First mode shape of the three-story structure ($T_1$ = 0.218 s)

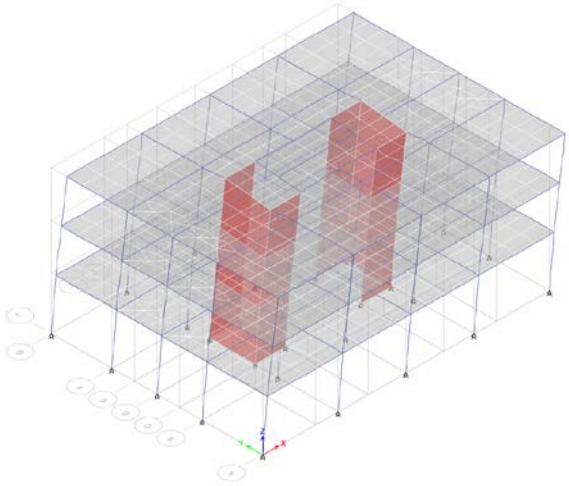

Figure 4.7. Third mode shape of the three-story structure ($T_3$ = 0.147 s)

The reduction factor (R) is chosen as normal ductility "For buildings that carry the seismic loads with shear walls and moment frames" which corresponds to category 1.4 in Table 2.5, TEC 2007. Therefore, R = 4 for three-story structures at all locations.

The code does not allow the use of a normal ductility system in the first or second SDC if the system only consists of moment frames. A dual system laterally supports the archetype building; therefore, this requirement is not applicable.

The equivalent force method is only allowed in the first and second SDC if the building has no torsional irregularity or soft stories within the structure. Additionally,

a height limit of forty meters is imposed, and the analyzed building satisfies these requirements; therefore, the equivalent force method can be used for seismic load application.

The periods from the model are used to calculate the spectral accelerations using Equation (4.4), and the results are tabulated in Table 4.9.

Table 4.9. Spectral acceleration parameters.

| Location | $S_{ae}$ ($T_1$ & $T_3$) |
|---|---|
| Istanbul | 1g |
| Ankara | 0.5g |
| Adana | 0.75g |

The periods in both directions are larger than $T_A$ (0.1 s) and smaller than $T_B$ (0.3 s); therefore, the reduction factors are not modified, and R = 4 is directly used per Equation (4.6). The base shears are calculated using Equations (4.1) and (4.2), and the results are tabulated in Table 4.10. The $V_t$ shown in Table 4.10 is the same for X and Y-direction.

Table 4.10. Base shears, three-story structure, TEC 2007

| Location | $V_{t,\,min}$ (kN) | $V_t$ (kN) |
|---|---|---|
| Istanbul | 326 | 2038 |
| Ankara | 163 | 1019 |
| Adana | 245 | 1528 |

#### 4.3.1.2 Six–Story Structure

The natural period of vibration is read from the structural model as: 0.561 seconds for the X-direction ($T_1$) and 0.373 seconds for the Y-direction ($T_3$). The mode shapes are given in Figures 4.8 and 4.9.

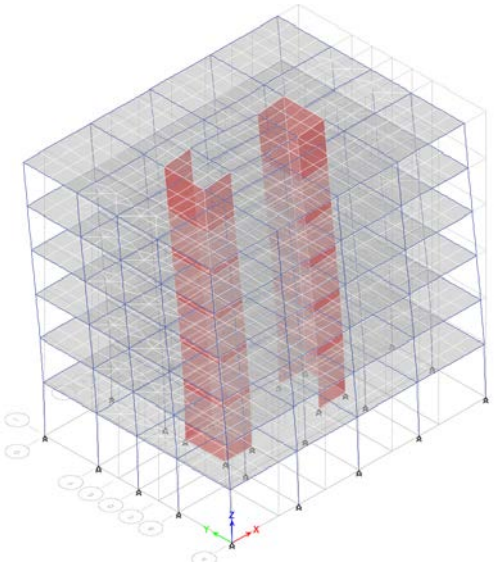

Figure 4.8. First mode shape of the six-story structure ($T_1$ = 0.561 s)

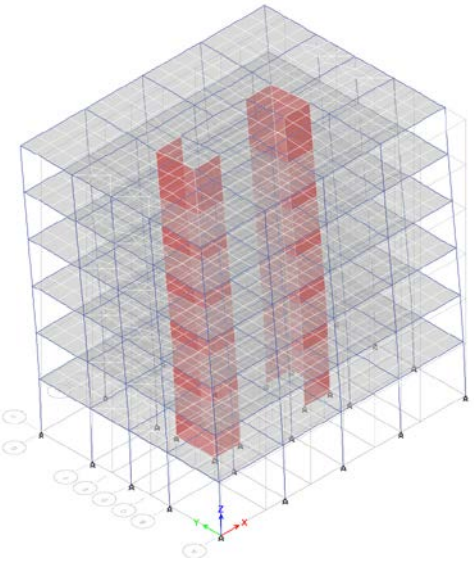

Figure 4.9. Third mode shape of the six-story structure ($T_3$ = 0.373 s)

The use of normal ductility is allowed in TEC 2007, but it will be shown in the next section that TBEC 2018 does not allow normal ductility for the six-story archetype building. Although it is allowed, analyzing the structure as normal ductility, and comparing it to a high ductility structure analyzed in TBEC 2018 would not yield results that are fit for comparison. Therefore, the buildings will be analyzed as high ductility, and R = 7 will be used with necessary modifications.

The height limit regarding the use of the equivalent force method discussed in the three-story structure is also satisfied for the six-story structure.

The reduction factor is initially chosen as R = 7 from the 1.4 high ductility system in Table 2.5, TEC 2007, but Section 2.5.2.1, TEC 2007, requires the shear at the base of the shear walls to be less than 75% of the overall base shear. The calculation for the base shear participation factor ($\alpha_s$) is performed assuming R = 7:

$$\alpha_s(x) = \frac{\text{Base Shear at Shear Walls}}{\text{Total Base Shear}} = \frac{1459}{1501} * 100\% = 97\% > 75\%$$

$$\alpha_s(y) = \frac{\text{Base Shear at Shear Walls}}{\text{Total Base Shear}} = \frac{2029}{2155} * 100\% = 94\% > 75\%$$

Section 2.5.2.2, TEC 2007 modifies the chosen reduction factor with Equation 4.7.

$$R = 10 - 4 * \alpha_s \tag{4.7}$$

$$R_x = 10 - 4 * 0.97 = 6.12$$

$$R_y = 10 - 4 * 0.94 = 6.24$$

The modification to the R factor in Equation (4.7), aims to capture the cases where the shear wall lateral stiffness dominates the stiffness of the dual system. The participation of more than 75% for the shear walls results in less ductile behavior since the moment frame systems have higher ductility than the shear wall systems. The R = 6 is used for systems with only high ductility shear walls; therefore, the equation above converges the reduction factor towards six if the contribution of the shear walls is high. The modified R factors are used to calculate the base shear for the high ductility six-story structure.

The periods from the model are used to calculate the spectral accelerations using Equation (4.4); for the six-story structure, the periods lie beyond $T_B$ (0.3 s); therefore, the spectral acceleration is different for X and Y directions. The results are tabulated in Tables 4.11 and 4.12.

Table 4.11. Spectral acceleration parameters.

| Location | $S_{ae}$ ($T_1$) | $S_{ae}$ ($T_3$) |
|---|---|---|
| Istanbul | 0.62g | 0.88g |
| Ankara | 0.31g | 0.44g |
| Adana | 0.46g | 0.66g |

Table 4.12. Base shears and reduction factors, six-story structure, TEC 2007

| Location | $V_{t,\,min}$ (kN) | $V_t$ (kN) - X | $V_t$ (kN) - Y | $R_x$ | $R_y$ |
|---|---|---|---|---|---|
| Istanbul | 682 | 1717 | 2417 | 6.12 | 6.24 |
| Ankara | 341 | 858 | 1209 | 6.12 | 6.24 |
| Adana | 512 | 1288 | 1813 | 6.12 | 6.24 |

#### 4.3.1.3 Twelve–Story Structure

The natural period of vibration is obtained from the structural model as: 1.105 seconds for the X-direction ($T_1$) and 0.872 seconds for the Y-direction ($T_3$). The mode shapes are given in Figures 4.10 and 4.11.

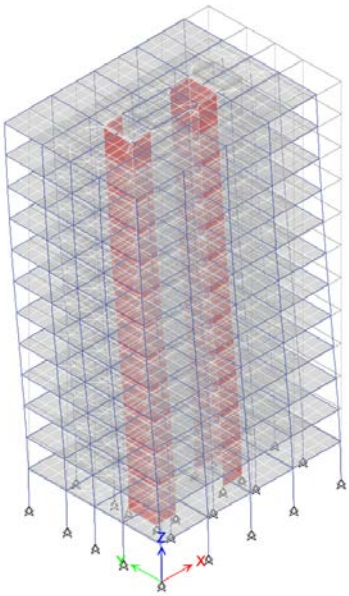

Figure 4.10. First mode shape of the twelve-story structure ($T_1$ = 1.105 s)

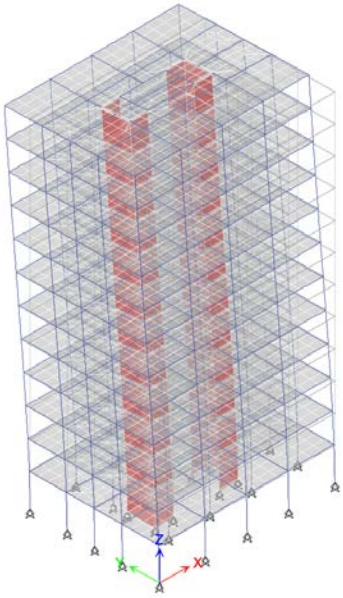

Figure 4.11. Third mode shape of the twelve-story structure ($T_3$ = 0.872 s)

For the twelve-story structure, normal ductility is allowed in TEC 2007. However, similar to the six-story structure, the TBEC 2018 does not allow the use of normal ductility. The details will be given in the upcoming section for the requirements of TBEC 2018.

The height limit regarding the use of the equivalent force method discussed in the three and six-story structure is also satisfied for the twelve-story structure.

The periods from the model are used to calculate the spectral accelerations using Equation (4.4); for the twelve-story structure, the periods lie beyond $T_B$ (0.3 s); therefore, the spectral acceleration is different for X and Y directions. The results are tabulated in Table 4.13.

Table 4.13. Spectral acceleration parameters.

| Location | $S_{ae}$ ($T_1$) | $S_{ae}$ ($T_3$) |
|---|---|---|
| Istanbul | 0.35g | 0.43g |
| Ankara | 0.18g | 0.22g |
| Adana | 0.27g | 0.33g |

The reduction factor is initially chosen as R = 7 from the 1.4 high ductility system in Table 2.5, TEC 2007, but Section 2.5.2.1, TEC 2007, requires the shear at the base of the shear walls to be less than 75% of the overall base shear. The calculation for the base shear participation factor ($\alpha_s$) is performed assuming R = 7:

$$\alpha_s(x) = \frac{\text{Base Shear at Shear Walls}}{\text{Total Base Shear}} = \frac{2250}{2308} * 100\% = 98\% > 75\%$$

$$\alpha_s(y) = \frac{\text{Base Shear at Shear Walls}}{\text{Total Base Shear}} = \frac{2841}{2855} * 100\% = 99\% > 75\%$$

The modified reduction factors are calculated as:

$$R_x = 10 - 4 * 0.98 = 6.08$$

$$R_y = 10 - 4 * 0.99 = 6.04$$

The base shear calculation results and reduction factors are tabulated in Table 4.14.

Table 4.14. Base shears and reduction factors, twelve-story structure, TEC 2007

| Location | $V_{t,\,min}$ (kN) | $V_t$ (kN) - X | $V_t$ (kN) - Y | $R_x$ | $R_y$ |
|---|---|---|---|---|---|
| Istanbul | 1493 | 2170 | 2685 | 6.08 | 6.04 |
| Ankara | 746 | 1085 | 1343 | 6.08 | 6.04 |
| Adana | 1119 | 1628 | 2014 | 6.08 | 6.04 |

## 4.4 Lateral Load Calculation for TBEC 2018

TBEC 2018 procedure uses the seismic hazard map of Türkiye to obtain the spectral accelerations according to the return period of the earthquake and, the site class. The seismic load is determined by following TBEC 2018, and the required parameters are obtained for all structures.

- Site Class: The site class is defined as very dense soil, corresponding to (ZC) in the site class table (Table 16.1, TBEC 2018).
- Ground motion data: The data is obtained from the seismic hazard map of Türkiye. The spectral acceleration coefficients are converted into design coefficients using Equation 2.1, TBEC 2018, and Table 2.1, TBEC 2018.

The tabulated data containing Design Spectral Acceleration Coefficient ($S_{DS}$) and 1 Second Period Design Spectral Acceleration Coefficient ($S_{D1}$) for all three locations are given in Table 4.15.

Table 4.15. Ground motion data, 475-year return period (DD-2)

| Location | $S_{DS}$ | $S_{D1}$ |
|---|---|---|
| Istanbul | 1.349 | 0.462 |
| Ankara | 0.477 | 0.155 |
| Adana | 0.723 | 0.212 |

The coefficients above are read for a seismic event with a return period of 475 years, classified as DD-2 in TBEC 2018.

Furthermore, 72-year return period seismic event ground motion data will be required to obtain the drift values. The obtained DD-3 spectral acceleration data is tabulated in Table 4.16 for each location.

Table 4.16. Ground motion data, 72-year return period (DD-3)

| Location | $S_{DS}$ | $S_{D1}$ |
|---|---|---|
| Istanbul | 0.556 | 0.171 |
| Ankara | 0.155 | 0.060 |
| Adana | 0.265 | 0.081 |

- Building Importance Factor (I): The importance factor is taken as 1 (Other Buildings, Table 3.1, TBEC 2018).
- Seismic Design Category (SDC): The Seismic Design Category is a function of the Design Spectral Acceleration Coefficient ($S_{DS}$) and Building Importance Factor (I) (Table 3.2, TBEC 2018). The data given in the tables above are used to tabulate the SDC for all three locations in Table 4.17.

Table 4.17. Seismic Design Category

| Location | SDC |
|---|---|
| Istanbul | 1 |
| Ankara | 3 |
| Adana | 2 |

- Spectrum Coefficients: The TBEC 2018 defines $T_A$ and $T_B$ coefficients as functions of $S_{DS}$ and $S_{D1}$ (Equation 2.3, TBEC 2018). The coefficients are given in Table 4.18.

Table 4.18. The Spectrum Coefficients

| Location | $T_A$ (sec.) | $T_B$ (sec.) |
|---|---|---|
| Istanbul | 0.07 | 0.34 |
| Ankara | 0.06 | 0.32 |
| Adana | 0.06 | 0.29 |

The response spectrum is constructed, and it is shown in Figure 4.12 for each location.

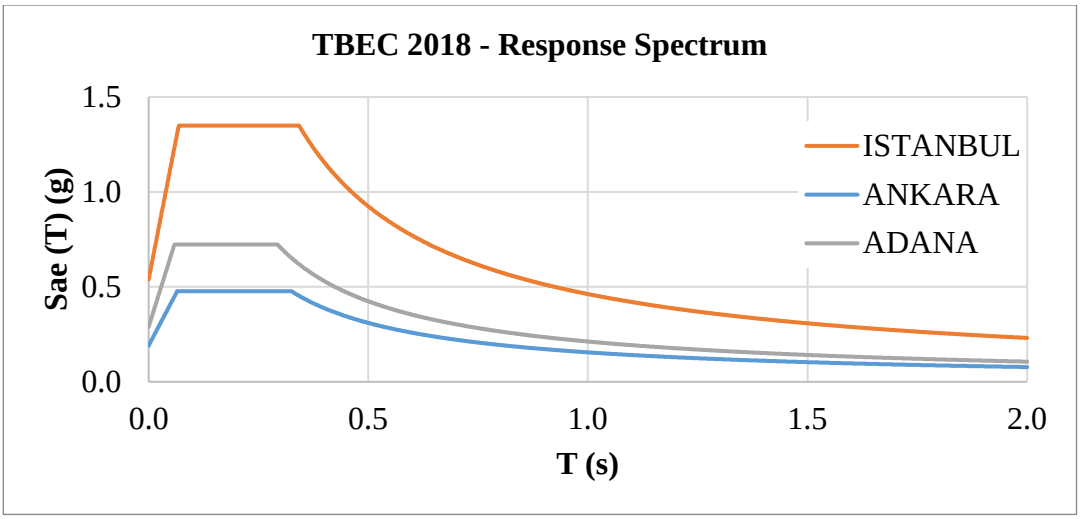


Figure 4.12. Response spectrum plot for TBEC 2018 at three locations.

- Modeling: The structure is modeled in ETABS. TEC 2007 does not enforce any factors for the modeling of members. However, in TBEC 2018, factors are used to reduce the member inertia to its cracked value. These factors are explained in Section 4.5 of the TBEC 2018 code, and they are shown in Table 4.19.

Table 4.19 Member Reduction Factors

| Member Type | Moment of Inertia Factor | Shear Factor |
|---|---|---|
| Columns | 0.70 | 1.00 |
| Beams | 0.35 | 1.00 |
| Shear Walls – In Plane | 0.50 | 0.50 |
| Shear Walls – Out of Plane | 0.25 | 1.00 |
| Slabs – In Plane | 0.25 | 0.25 |
| Slabs – Out of Plane | 0.25 | 1.00 |

- Building Height Class (BHC): The classes are given in Table 3.3, TBEC 2018. The BHC is a function of building height and SDC. The heights and classes are shown in Table 4.20 for each location and building.

Table 4.20. BHC for all structure heights and locations.

| | | BHC | | |
|---|---|---|---|---|
| Number of Stories | $H_N$ (m) | ISTANBUL | ANKARA | ADANA |
| 3 | 9.5 | 7 | 7 | 7 |
| 6 | 18.5 | 5 | 6 | 5 |
| 12 | 36.5 | 4 | 5 | 4 |

- Base Shear: The story weights were given in section 2.4.1 for TEC 2007 and are the same for TBEC 2018. The total base shear and minimum base shear values are given in Equation 4.19, TBEC 2018:

$$V_{tE}^{(X)} = m_t * S_{aR} * \left(T_p^{(X)}\right) \quad (4.8)$$

$$V_{t,min} = 0.04 * m_t * I * S_{DS} * g \quad (4.9)$$

The parameters given in the equations above are described in Table 4.21.

Table 4.21. Equations (4.8) and (4.9) parameter descriptions.

| Parameter | Description |
|---|---|
| $V_{tE}^{(X)}$ | Total equivalent earthquake load affecting the whole building in the X-direction (base shear force) (kN) |
| $m_t$ | The total mass of the upper part of the building above the basements (t) |
| $S_{aR}$ | Reduced design spectral acceleration (g) |
| $T_p^{(X)}$ | the dominant natural vibration period of the building in the X-direction (s) |
| $S_{DS}$ | Short period design spectral acceleration coefficient |

- Reduction Factor (R): The seismic load reduction factor is a function of the structure's X and Y direction natural period of vibration. Equation 4.1a and 4.1b, TBEC 2018:

$$R_a(T) = R/I \quad \text{for} \quad T > T_B \quad (4.10)$$

$$R_a(T) = D + (R/I - D) * T/T_B \quad \text{for} \quad T \leq T_B \quad (4.11)$$

The introduced parameters in Equation (4.11) are given in Table 4.22.

Table 4.22. Equation (4.11) parameter descriptions.

| Parameter | Description |
|---|---|
| D | Overstrength Factor |
| $T_B$ | Horizontal elastic design acceleration spectrum corner period |

In TBEC 2018, the reduction factor choice depends on the building height category (BHC), seismic design category (SDC), and the ductility of the system. For dual systems, the code imposes additional limits depending on the overturning moment participation ratios of the shear walls and moment frames. The system ductility, reduction factor, overstrength factor, and building height category limits given in Table 4.1, TBEC 2018 are shortened to only contain the applicable systems for the studied building in Table 4.23. The following sections will go through each structure, and reduction factors will be assigned accordingly.

Table 4.23. Building lateral system ductility definitions and factors.

| Building Lateral System | R | D | BHC limit |
|---|---|---|---|
| **A15.** Lateral earthquake load resisting system of combined high ductility reinforced concrete moment frames and shear walls. | 7 | 2.5 | BHC $\geq$ 2 |
| **A22.** Lateral earthquake load resisting system of combined limited ductility reinforced concrete moment frames and high ductility shear walls. | 5 | 2.5 | BHC $\geq$ 4 |
| **A33.** Lateral earthquake load resisting system of combined limited ductility reinforced concrete moment frames and shear walls. | 4 | 2 | BHC $\geq$ 6 |

#### 4.4.1.1 Three–Story Structure

The natural period of vibration is read from the structural model as: 0.318 seconds for the X-direction ($T_1$) and 0.211 seconds for the Y-direction ($T_3$). The mode shapes are given in Figures 4.13 and 4.14 for each direction.

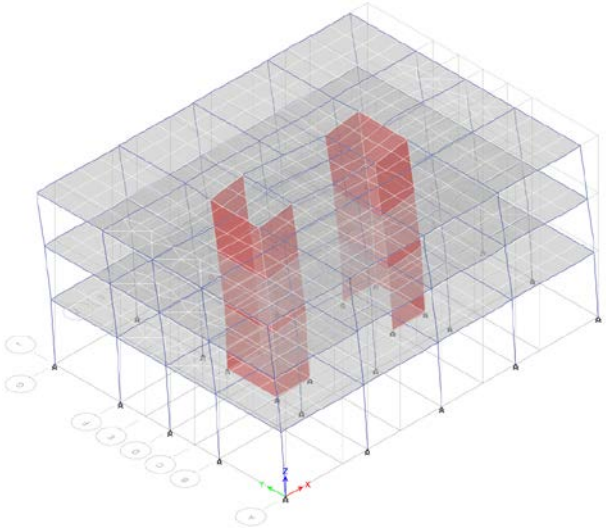

Figure 4.13. First mode shape of the three-story structure ($T_1$ = 0.318 s)

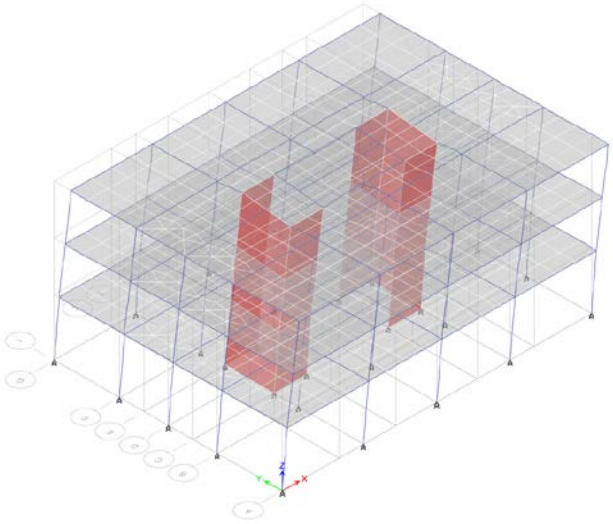

Figure 4.14. Third mode shape of the three-story structure ($T_3$ = 0.211 s)

A33 in Table 4.1, TBEC 2018 gives the reduction and overstrength factors for structures with limited (referred to as "normal" in TEC 2007) ductility frames and shear walls. The limiting factor is that the BHC must be larger than or equal to six.

For the three-story structure, the BHC = 7 for all locations, allowing the use of limited ductility frames and shear walls. Therefore, three-story structures will be solved using R = 4 and D = 2. The $T_A$ and $T_B$ periods depend on the seismic acceleration parameters, which change according to the location. For some locations, the calculated structure period is less than the $T_B$ value, which results in the modification of the reduction factor. The reduction factors are modified and tabulated in Table 4.24 with spectral accelerations for each location.

Table 4.24. Spectral accelerations and modified reduction factors, three-story, TBEC 2018

| Location | Sae(T) | R-x | R-y |
|---|---|---|---|
| Istanbul | 1.35g | 3.86 | 3.24 |
| Ankara | 0.48g | 3.96 | 3.30 |
| Adana | 0.71g | 4.00 | 3.45 |

The reduction factors and accelerations are combined with the total weight to obtain the base shears (Table 4.25).

Table 4.25. Base shears, three-story structure, TBEC 2018

| Location | $V_{t,\,min}$ (kN) | $V_x$ (kN) | $V_y$ (kN) |
|---|---|---|---|
| Istanbul | 440 | 2851 | 3396 |
| Ankara | 156 | 983 | 1177 |
| Adana | 236 | 1440 | 1710 |

#### 4.4.1.2 Six–Story Structure

The natural period of vibration is read from the structural model as: 0.829 seconds for the X-direction ($T_1$) and 0.547 seconds for the Y-direction ($T_3$). The mode shapes are given in Figures 4.15 and 4.16 for each direction.

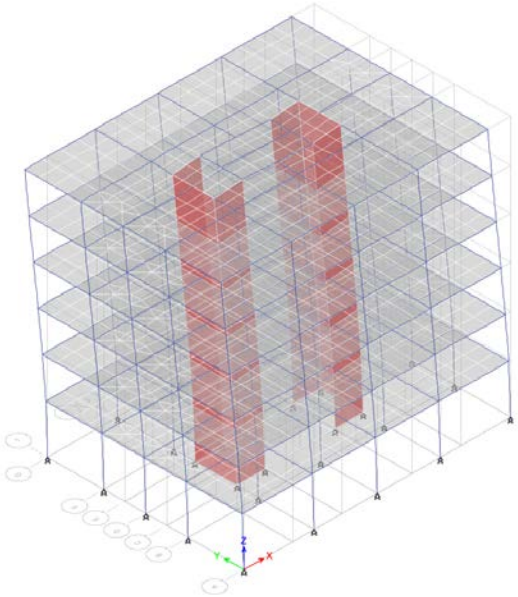

Figure 4.15. First mode shape of the six-story structure ($T_1$ = 0.829 s)

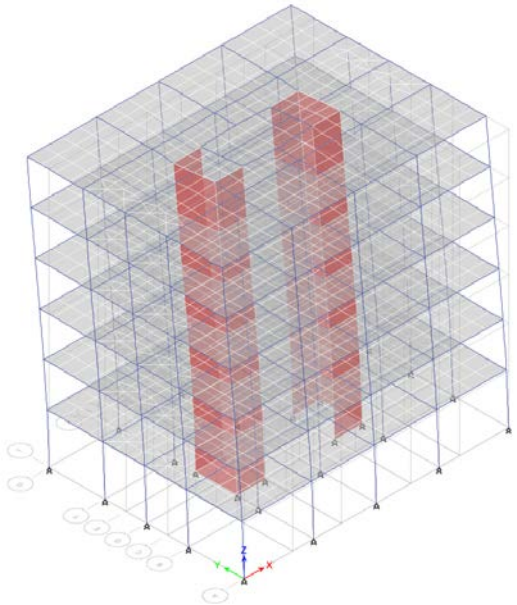

Figure 4.16. Third mode shape of the six-story structure ($T_3$ = 0.547 s)

The six-story structures have BHC equal to five for Istanbul and Adana, and six for Ankara. A33 in Table 4.1, TBEC 2018, cannot be used for this building height category. Therefore, the minimum allowed section for the structure is A22, which corresponds to the mixed ductility system with limited ductility frames and high ductility shear walls. However, this section requires the shear walls to carry at least

75% of the overall overturning moment. The overturning moment participation is calculated below for each direction using R = 5:

$$\sum M_o \geq 75\%$$

$$M_{o,x} = \frac{13541}{25116} * 100\% = 54\% < 75\%$$

$$M_{o,y} = \frac{25228}{38051} * 100\% = 66\% < 75\%$$

For both directions, the requirement is not satisfied; therefore, Section 4.3.4.6, TBEC 2018, prohibits the usage of mixed ductility systems and instead refers the user to the factors given for a system with limited ductility frames. The use of reduction factors defined for only limited ductility frames is prohibited for the current structure since the BHC requirement is not satisfied (the limit is BHC $\geq$ 7, and for the six-story structure, BHC = 5 or 6). Therefore, the structure must be solved with high ductility frames and shear walls, A15, Table 4.1, TBEC 2018. The corresponding factors are R = 7, D = 2.5, and the building height category limit is BHC $\geq$ 2, which satisfies the BHC limit for all locations.

An additional requirement for high ductility shear wall and moment frame system is to have the shear walls carry between 40% and 75% of the total seismic overturning moment. The calculated percentages for X and Y directions were 54% and 66%, respectively. The requirement is satisfied, and the factors are used directly from A14. The spectral accelerations and reduction factors are given in Table 4.26.

Table 4.26. Spectral accelerations and reduction factors, six-story, TBEC 2018

| Location | Sae(T) - x | Sae(T) - y | $R_x$ and $R_y$ |
|---|---|---|---|
| Istanbul | 0.56g | 0.84g | 7 |
| Ankara | 0.19g | 0.28g | 7 |
| Adana | 0.26g | 0.39g | 7 |

The reduction factors and accelerations are used together with the total weight calculated to obtain the base shears (Table 4.27).

Table 4.27. Base shears, six-story structure, TBEC 2018

| Location | $V_{t,\,min}$ (kN) | $V_x$ (kN) | $V_y$ (kN) |
|---|---|---|---|
| Istanbul | 921 | 1358 | 2059 |
| Ankara | 326 | 456 | 691 |
| Adana | 493 | 623 | 945 |

#### 4.4.1.3 Twelve–Story Structure

The natural period of vibration is read from the structural model as: 1.618 seconds for the X-direction ($T_1$) and 1.224 seconds for the Y-direction ($T_3$). The mode shapes are shown in Figures 4.17 and 4.18 for each direction.

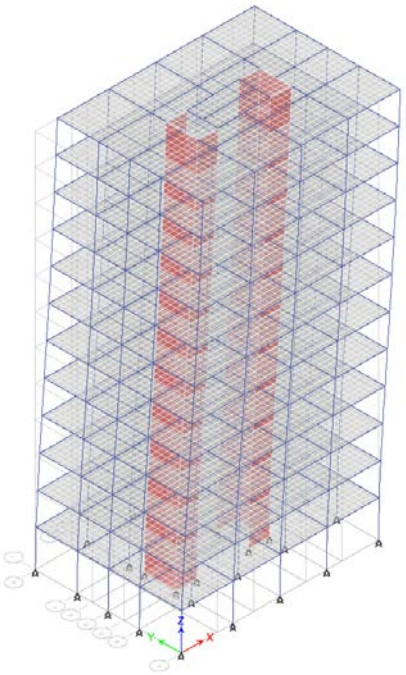

Figure 4.17. First mode shape of the twelve-story structure ($T_1$ = 1.618 s)

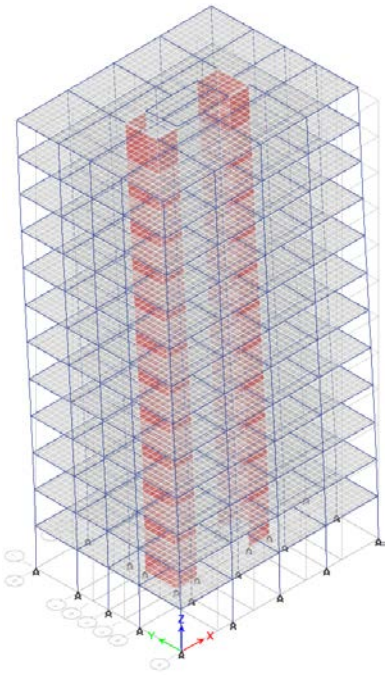

Figure 4.18. Third mode shape of the twelve-story structure ($T_3$ = 1.224 s)

The twelve-story structures have BHC equal to four for Istanbul and Adana, and five for Ankara. The minimum allowed system for the twelve-story structure is A22,

Table 4.1, TBEC 2018. As discussed for the six-story structure, this system requires the shear walls to carry at least 75% of the overall overturning moment. The overturning moment participation is calculated below for each direction using R = 5:

$$\sum M_o \geq 75\%$$

$$M_{o,x} = \frac{10669}{60193} * 100\% = 18\% < 75\%$$

$$M_{o,y} = \frac{26970}{72875} * 100\% = 37\% < 75\%$$

The requirement is not satisfied, and the use of limited ductility frames is not allowed due to the BHC restriction. Therefore, the structure must be solved with high ductility frames and shear walls, A15, Table 4.1, TBEC 2018. The corresponding factors are R = 7, D = 2.5, and the building height category limit is $BHC \geq 2$, which satisfies the BHC limit for all locations.

An additional requirement for high ductility shear wall and moment frame system is to have the shear walls carry between 40% and 75% of the total seismic overturning moment. The calculated percentages for the X and Y directions were 18% and 37%, respectively. The requirement is not satisfied, but Section 4.3.4.5, TBEC 2018, states that if the lower limit is not satisfied, the reduction factors can be directly used by considering the BHC limit that is increased by one. The BHC limit is changed from two to three, which is still satisfied for the twelve-story structure since the lowest BHC is equal to four in Istanbul and Adana. The reduction factors and spectral acceleration values are tabulated in Table 4.28.

Table 4.28. Spectral accelerations and modified reduction factors, twelve-story, TBEC 2018

| Location | Sae(T) - x | Sae(T) - y | $R_x$ & $R_y$ |
|---|---|---|---|
| Istanbul | 0.32g | 0.33g | 7 |
| Ankara | 0.11g | 0.11g | 7 |
| Adana | 0.15g | 0.15g | 7 |

The reduction factors and accelerations are used together with the total weight calculated to obtain the base shears (Table 4.29).

Table 4.29. Base shears, twelve-story structure, TBEC 2018

| Location | $V_{t,\,min}$ (kN) | $V_x$ (kN) | $V_y$ (kN) |
|---|---|---|---|
| Istanbul | 2013 | 1693* | 1764* |
| Ankara | 712 | 568* | 592* |
| Adana | 1079 | 777* | 810* |

The minimum base shear governs at all locations and will be used to perform further calculations.

# CHAPTER 5

# COMPARISON AND DISCUSSION OF RESULTS

The comparisons are made on the analysis and design results of the archetype structures. The effect of changes in response spectra, base shear, reduction factor, and effective moment inertia are discussed. The drifts will be calculated for both codes and the results will be compared. Additionally, the detailing requirements are given for each member type and differences are demonstrated. The total rebar weights are found at all building locations and stories according to the final design sizes, the comparisons will show the change in the rebar weight between the codes.

## 5.1 Seismic Parameters and Base Shear

TEC 2007 divides the country into five seismic regions, and the acceleration values given for each region are constant across the defined area. The corner periods of the response spectrums depend solely on the soil group and do not change between the regions. The given acceleration values are only for the seismic event with a return period of 475 years.

TBEC 2018 uses a seismic hazard map that presents site-specific seismic acceleration values that depend on specific coordinates provided in the DEMC online map tool. The corner periods and spectral accelerations depend on the site-specific data, and each location's response spectrum is unique. Additionally, the spectral accelerations can be obtained for seismic events with a return period of 2475, 475, 72, and 43 years.

### 5.1.1 Three-Story Structure

The elastic response spectrums are plotted for each location for both codes on the same plot (Figure 5.1).

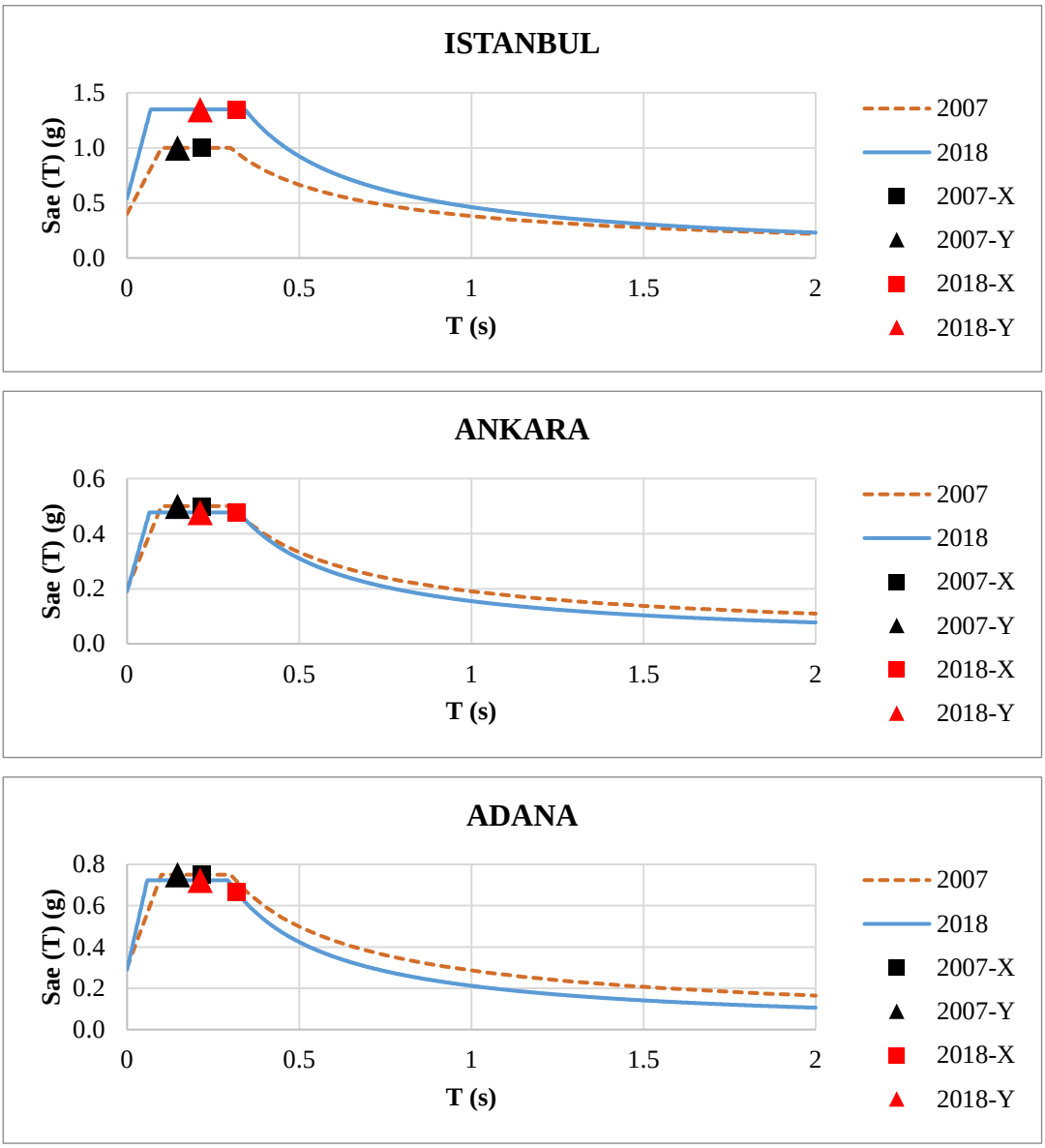


Figure 5.1. Elastic response spectrums, three-story structure.

The reduction factor is modified in TEC 2007 if the structure period is smaller than the first corner period $T_A$. It is shown in Figure 5.1 that for the current structure, the periods in both directions are larger than $T_A$; therefore, the reduction factors are directly used as R.

The reduction factor is modified in TBEC 2018, if the structure period is smaller than the second corner period $T_B$. It is shown in the figure above that for the current structure, the periods in both directions are smaller than $T_B$ except for Adana X-direction; therefore, the reduction factors are modified accordingly. Tables 5.1, 5.2, and 5.3 summarize the seismic parameters.

Table 5.1. Period of vibration comparison, three-story structure.

| TDY2007 | | TBDY2018 | |
|---|---|---|---|
| $T_1$ – X (s) | $T_3$ – Y (s) | $T_1$ – X (s) | $T_3$ – Y (s) |
| 0.218 | 0.147 | 0.320 | 0.210 |

Table 5.2. Response spectrum corner period comparison, three-story structure.

| | TDY2007 | | TBDY2018 | |
|---|---|---|---|---|
| Location | $T_A$ (s) | $T_B$ (s) | $T_A$ (s) | $T_B$ (s) |
| Istanbul | 0.1 | 0.3 | 0.07 | 0.34 |
| Ankara | 0.1 | 0.3 | 0.06 | 0.32 |
| Adana | 0.1 | 0.3 | 0.06 | 0.29 |

Table 5.3. Elastic spectral acceleration comparison, three-story structure.

| | TEC 2007 | | TBEC 2018 | | |
|---|---|---|---|---|---|
| Location | A(T) | R | Sae(T) | R-x | R-y |
| Istanbul | 1 | 4 | 1.35 | 3.86 | 3.24 |
| Ankara | 0.5 | 4 | 0.48 | 3.96 | 3.30 |
| Adana | 0.75 | 4 | 0.67 | 4.00 | 3.45 |

The comparison is made for the design spectral accelerations, which are the elastic spectral accelerations divided by the corresponding R factors for each direction. The change in the design accelerations from TEC 2007 to TBEC 2018 is shown in Table 5.4 as a percentage.

Table 5.4. Design spectral acceleration comparison, three-story structure.

| Location | $(S_{aR,\ TBEC\ 2018} / S_{aR,\ TEC\ 2007} - 1)$ | |
|---|---|---|
| | X-Direction | Y-Direction |
| Istanbul | 40% | 67% |
| Ankara | -4% | 15% |
| Adana | -6% | 9% |

For Istanbul, the initial accelerations were already higher per TBEC 2018, and using decreased reduction factors further increased the gap between the design accelerations.

For Ankara and Adana, the initial accelerations were almost identical for both codes; the design acceleration increased in TBEC 2018 due to the decreased reduction factors. The base shear is directly correlated with the design spectral accelerations; therefore, the base shears follow the same trend as the design spectral accelerations (Figure 5.2).

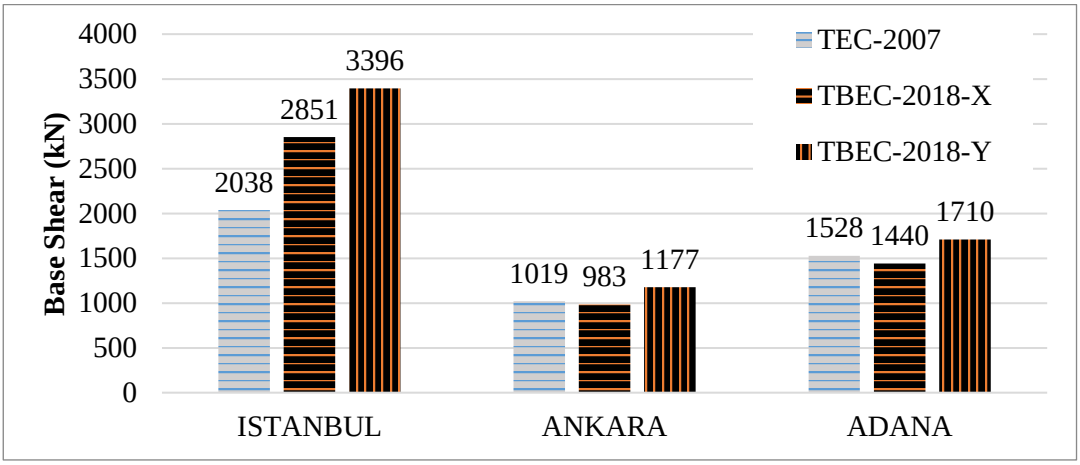


Figure 5.2. Base shear comparison, three-story structure.

Table 5.5 shows the difference from TBEC 2018 to TEC 2007 base shears in terms of percentage. The results show that the increased design acceleration in Istanbul together with the decreased reduction factor in TBEC 2018 results in significant increase in base shear. However, for Adana and Ankara the initial design accelerations are close since the site-specific corner periods defines the modification applied to the reduction factors which results in minor modification.

Table 5.5. Base shear comparison, three-story structure.

| Location | ($V_{TBEC\ 2018}$ / $V_{TEC\ 2007}$ − 1) | |
|---|---|---|
| | X-Direction | Y-Direction |
| Istanbul | 40% | 67% |
| Ankara | -4% | 15% |
| Adana | -6% | 12% |

### 5.1.2 Six-Story Structure

The elastic response spectrums are plotted for each location for both codes on the same plot (Figure 5.3).

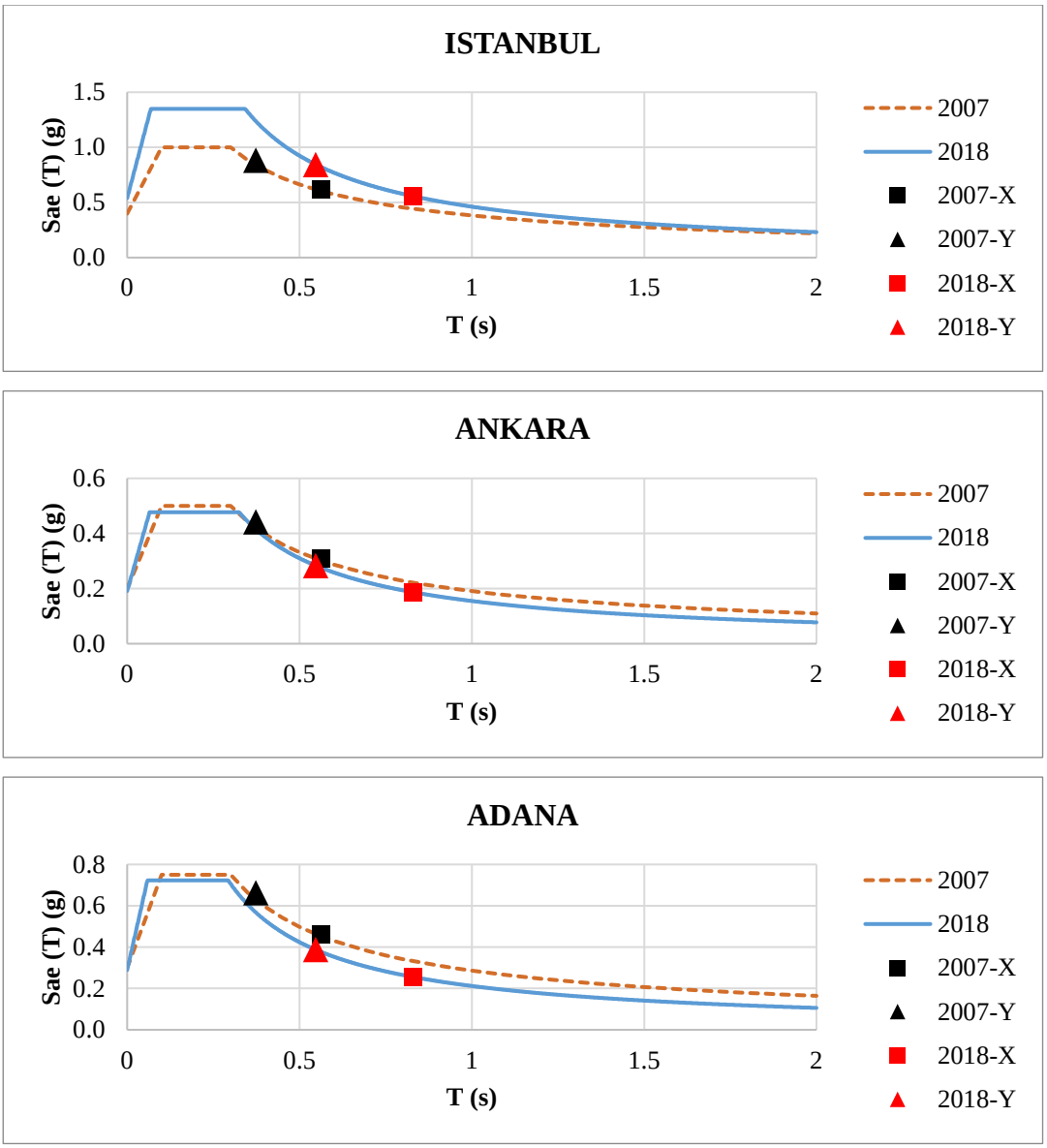


Figure 5.3. Elastic response spectrums, six-story structure

For both codes, the periods are larger than the corner period $T_B$, resulting in no need to modify the reduction factor due to the period's location on the response spectrum. The effect of using effective moment of inertias in TBEC 2018 can be observed in the response spectrums. The periods are larger in TBEC 2018 due to decreased stiffness of the structure, resulting in less acceleration applied to the structures in Ankara and Adana, while the accelerations are equalized for Istanbul. Tables 5.6 and 5.7 summarize the seismic parameters.

Table 5.6. Period of vibration comparison, six-story structure.

| TDY2007 | | TBDY2018 | |
|---|---|---|---|
| $T_1$ – X (s) | $T_3$ – Y (s) | $T_1$ – X (s) | $T_3$ – Y (s) |
| 0.561 | 0.373 | 0.829 | 0.547 |

Table 5.7. Elastic spectral acceleration comparison, six-story structure.

| | TEC 2007 | | | | TBEC 2018 | | | |
|---|---|---|---|---|---|---|---|---|
| Location | A(T) [x] | A(T) [y] | R [x] | R [y] | Sae(T) [x] | Sae(T) [y] | R [x] | R [y] |
| Istanbul | 0.62 | 0.88 | 6.12 | 6.24 | 0.56 | 0.84 | 7 | 7 |
| Ankara | 0.31 | 0.44 | 6.12 | 6.24 | 0.19 | 0.28 | 7 | 7 |
| Adana | 0.46 | 0.66 | 6.12 | 6.24 | 0.26 | 0.39 | 7 | 7 |

The comparison is made for the design spectral accelerations, which are the elastic spectral accelerations divided by the corresponding R factors for each direction. The reduction factors are smaller in TEC 2007 since the factors are modified according to the base shear participation of the shear walls. In TBEC 2018, the check is performed for the overturning moment participation, resulting in no modification to the reduction factor. The change in the design accelerations from TEC 2007 to TBEC 2018 is shown as a percentage in Table 5.8.

Table 5.8. Design spectral acceleration comparison, six-story structure.

| Location | $(S_{aR,\ TBEC\ 2018} / S_{aR,\ TEC\ 2007} - 1)$ | |
|---|---|---|
| | X-Direction | Y-Direction |
| Istanbul | -21% | -15% |
| Ankara | -47% | -43% |
| Adana | -52% | -48% |

Effective moment of inertias, which resulted in higher periods, decreased the elastic spectral accelerations for all locations. The reduction factor determination approach is different in TBEC 2018, further decreasing the design spectral accelerations.

The base shear is directly correlated with the design spectral accelerations; therefore, there is a significant decrease in base shears for Ankara and Adana, while the decrease is smaller but still significant for Istanbul (Figure 5.4 and Table 5.9).

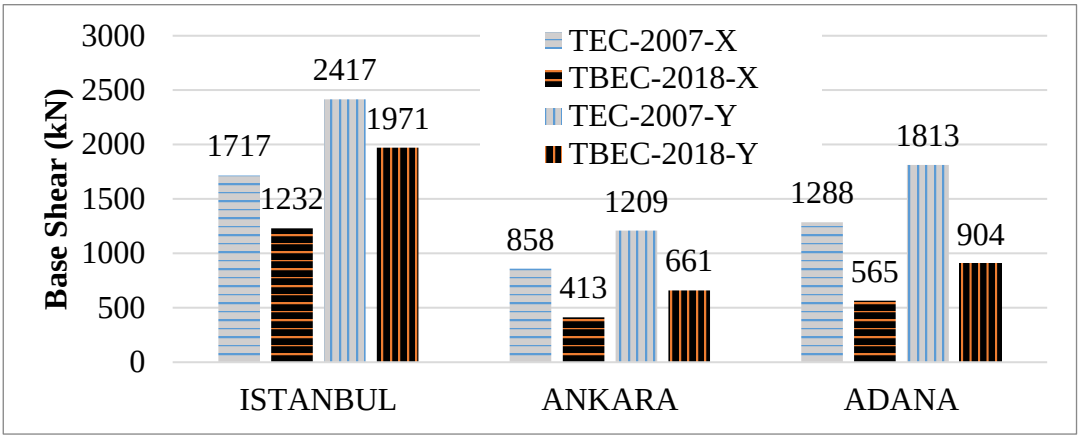


Figure 5.4. Base shear comparison, six-story structure.

Table 5.9. Base shear comparison, six-story structure.

| Location | $(V_{TBEC\ 2018} / V_{TEC\ 2007} - 1)$ | |
|---|---|---|
| | X-Direction | Y-Direction |
| Istanbul | -21% | -15% |
| Ankara | -47% | -43% |
| Adana | -52% | -48% |

### 5.1.3 Twelve-Story Structure

The elastic response spectrums are plotted for each location for both codes on the same plot (Figure 5.5).

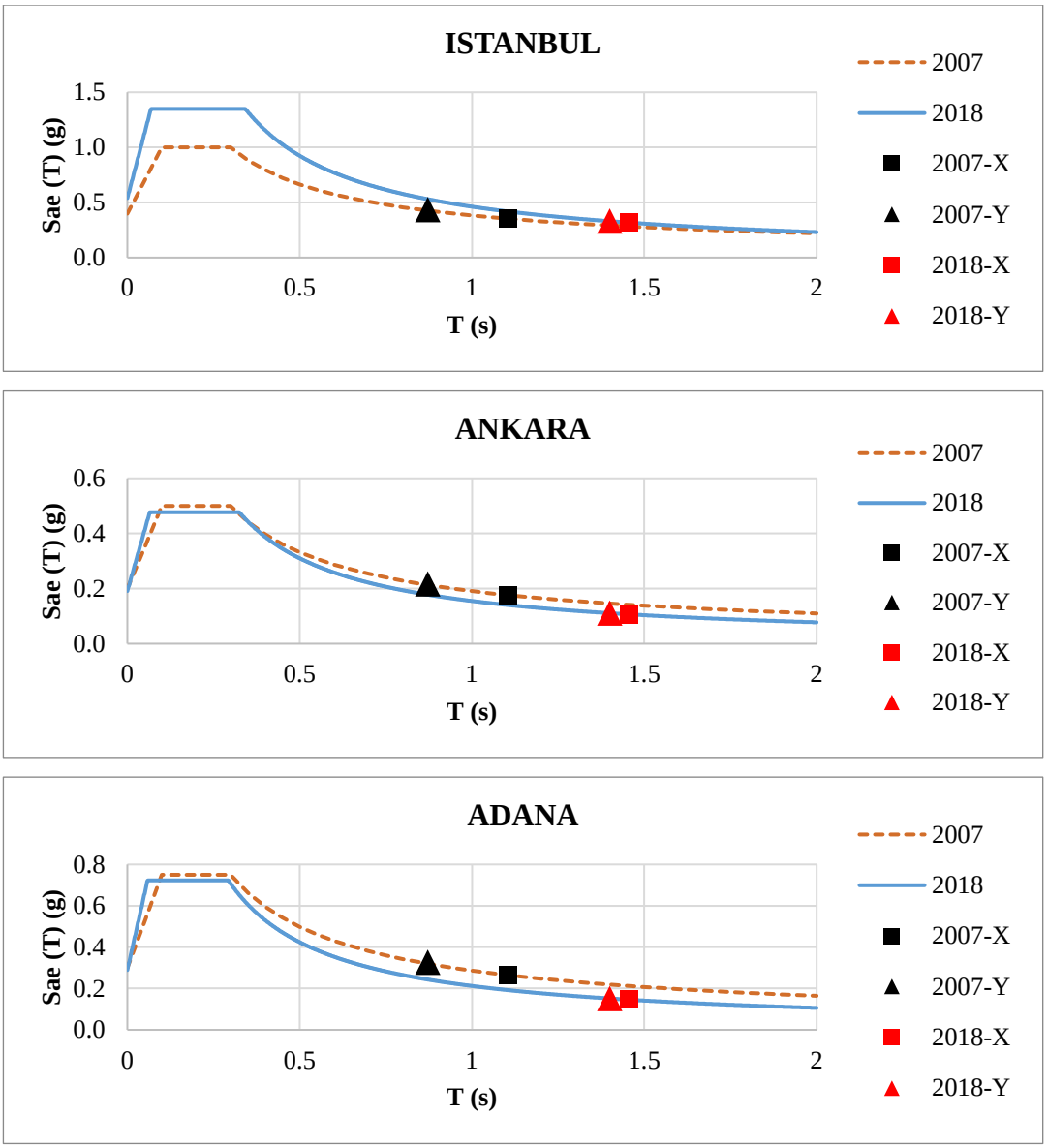


Figure 5.5. Elastic response spectrums, twelve-story structure.

The effective moment of inertia again increases the periods of TBEC 2018 structures. For 2018-X, the maximum allowed period governs; the limit is given in Section 4.7.3.2, TBEC 2018, with the following equations:

$$T_{pA} = C_t H_N^{0.75} = 0.07 * 36.5^{0.75} = 1.04 \text{ s.} \quad (5.1)$$

$$T_{max} \leq 1.4 * T_{pA} = 1.4 * 1.04 = 1.46 \text{ s.} \quad (5.2)$$

The parameters used in Equations (5.1) and (5.2) are given in Table 5.10.

Table 5.10. Equations (5.1) and (5.2) parameter descriptions.

| Parameter | Description |
|---|---|
| $T_{pA}$ | Empirical natural period of vibration (s) |
| $C_t$ | Coefficient for empirical natural period of vibration |
| $H_N$ | Total height of the building starting from the basement level (m) |

For the twelve-story structure, the period was obtained from the model as 1.618 seconds which is larger than the maximum allowable period of 1.46 seconds; therefore, $T_x$ = 1.46 seconds will be used for further calculations.

In TEC 2007, no empirical formula is defined for the period calculation; instead, the structure must be analyzed with fictional loads. Then, the story deflections from that analysis results are used together with the story masses to calculate the period. Section 2.7.4.1, TEC 2007 limits the periods to be used in the design with the following equations:

$$T_1 = 2\pi \left( \frac{\sum_{i=1}^{N} m_i d_{fi}^2}{\sum_{i=1}^{N} F_{fi} d_{fi}} \right)^{1/2} \tag{5.3}$$

$$F_i = (V_t - \Delta F_N) \frac{w_i H_i}{\sum_{j-1}^{N} w_j H_j} \tag{5.4}$$

The parameters used in Equations (5.3) and (5.4) are given in Table 5.11.

Table 5.11. Equations (5.3) and (5.4) parameter descriptions.

| Parameter | Description |
|---|---|
| $T_1$ | The first natural period of vibration of the building |
| $m_i$ | Mass of the i-th floor of the building ($m_i = w_i / g$) |
| $F_{fi}$ | The fictitious load acting on the i-th floor in the calculation of the first natural period of vibration |
| $d_{fi}$ | The displacement calculated according to the fictitious loads $F_{fi}$ on the i-th floor of the building |
| N | Total number of floors of the building from the top of the foundation |
| $F_i$ | Equivalent earthquake load acting on the i-th floor in the Equivalent Seismic Load Method |
| $\Delta F_N$ | Additional equivalent earthquake load acting on the N-th floor (top) of the building |
| $w_i$ | The weight of the i-th floor of the building calculated using the live load participation coefficient |
| $H_i$ | The height of the i-th floor of the building measured from the foundation |

Here the $(V_t - \Delta F_N)$ term is taken as 1 kN/m for both directions separately and applied to X and Y directions at all stories. The analysis is performed, story displacements are input into the formula, and the results are obtained as follows:

$$T_{max,\,X} = 1.38 \text{ seconds}$$

$$T_{max,\,Y} = 1.05 \text{ seconds}$$

The limiting periods in both directions are larger than those obtained from the modal analysis; therefore, the TEC 2007 limits for the periods are satisfied. Tables 5.12 and 5.13 compare the periods that are used.

Table 5.12. Period of vibration comparison, twelve-story structure.

| TDY2007 | | TBDY2018 | |
|---|---|---|---|
| $T_1$ – X (s) | $T_3$ – Y (s) | $T_1$ – X (s) | $T_3$ – Y (s) |
| 1.105 | 0.872 | 1.460 | 1.224 |

Table 5.13. Elastic spectral acceleration comparison, twelve-story structure.

| Location | TEC 2007 | | | | TBEC 2018 | | | |
|---|---|---|---|---|---|---|---|---|
| | A(T) [x] | A(T) [y] | R [x] | R [y] | Sae(T) [x] | Sae(T) [y] | R [x] | R [y] |
| Istanbul | 0.35 | 0.43 | 6.08 | 6.04 | 0.32 | 0.33 | 7 | 7 |
| Ankara | 0.18 | 0.22 | 6.08 | 6.04 | 0.11 | 0.11 | 7 | 7 |
| Adana | 0.27 | 0.33 | 6.08 | 6.04 | 0.15 | 0.15 | 7 | 7 |

The TEC 2007 reduction factor is reduced due to the shear participation factor of shear walls, which reduces the reduction factor towards the factor used for high ductility shear walls only, ignoring the ductility contribution of moment frames. The TBEC 2018 does not modify the reduction factor since the overturning moment contribution factor is satisfied. The change in the design accelerations from TEC 2007 to TBEC 2018 is shown in Table 5.14 as a percentage.

Table 5.14. Design spectral acceleration comparison, twelve-story structure.

| Location | $(S_{aR,\ TBEC\ 2018} / S_{aR,\ TEC\ 2007} - 1)$ | |
|---|---|---|
| | X-Direction | Y-Direction |
| Istanbul | -22% | -34% |
| Ankara | -48% | -56% |
| Adana | -52% | -60% |

The reasons discussed for the six-story structure also apply to the twelve-story structure. The effective moment of inertia increases the periods in TBEC 2018, and the increase in the reduction factors for high ductility systems further decreases the design spectral accelerations. The base shears are directly influenced by the spectral accelerations and the reduction factors (Figure 5.6).

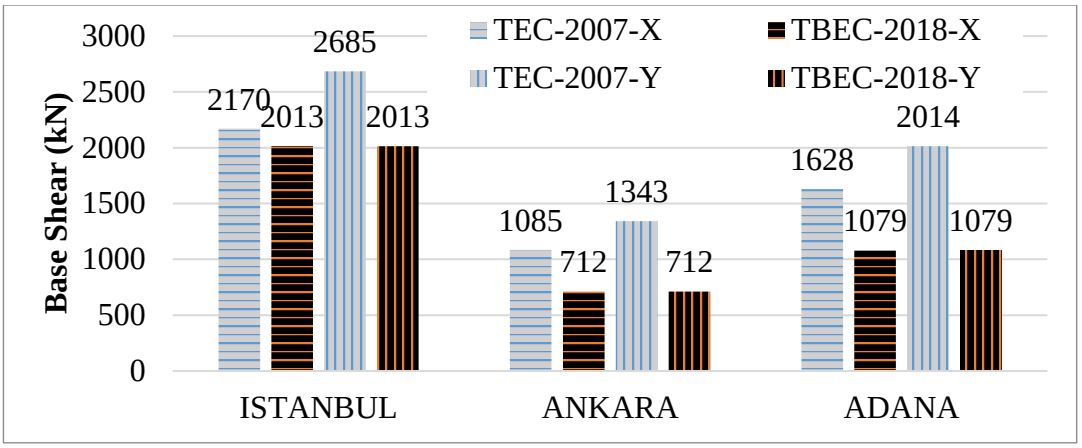


Figure 5.6. Base shear comparison, twelve-story structure.

The minimum base shear governs at all locations in TBEC 2018. The use of minimum base shear closes the gap between the seismic loads that are used in the design, but TEC 2007 is still larger. Table 5.15 shows that the difference is smaller compared to the design spectral accelerations shown in Table 5.14. The minimum base shear requirement depends on the short period design spectral acceleration, weight of the structure, and the building importance factor.

Table 5.15. Base shear comparison, twelve-story structure.

| Location | $(V_{TBEC\ 2018} / V_{TEC\ 2007} - 1)$ | |
|---|---|---|
| | X-Direction | Y-Direction |
| Istanbul | -7% | -25% |
| Ankara | -34% | -47% |
| Adana | -34% | -46% |

## 5.2 Member Forces

The member forces will be compared for beams, columns, and shear walls. In TBEC 2018, effective moment of inertias is used for all members. The comparison is performed to see the impact of spectral accelerations, base shear, and effective moment of inertias on the member forces.

The shown member forces will only include the seismic load case without modification. The percentages represent the change of force/moment from TEC 2007 to TBEC 2018, and they are calculated with the following formula:

$$\left(\frac{\text{TBEC 2018}}{\text{TEC 2007}} - 1\right) * 100\%$$

### 5.2.1 Beam Member Force Comparison

The beam members picked for comparison are located on the second story for three-story, the fifth for six-story, and the eleventh for twelve-story structures. The beam locations are chosen so that the effect of seismic load on the beam forces is prominent (Figure 5.7).

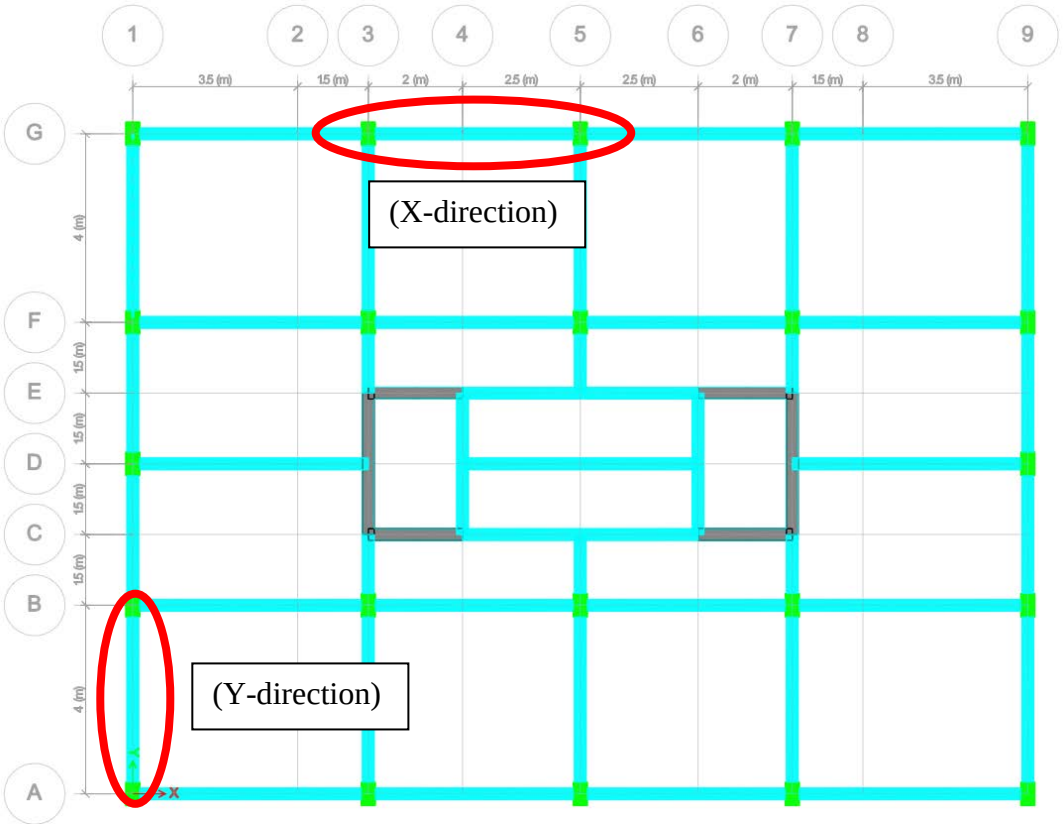


Figure 5.7. Beam member that is chosen for comparison.

Figures 5.8, 5.10, and 5.12 show the change in moment between the two codes of the selected beam that spans in the X-direction while Figures 5.9, 5.11, and 5.13

show the change for the beam spanning in the Y-direction. Additionally, the base shears are also shown on the plot to see the correlation between the moment and the base shears.

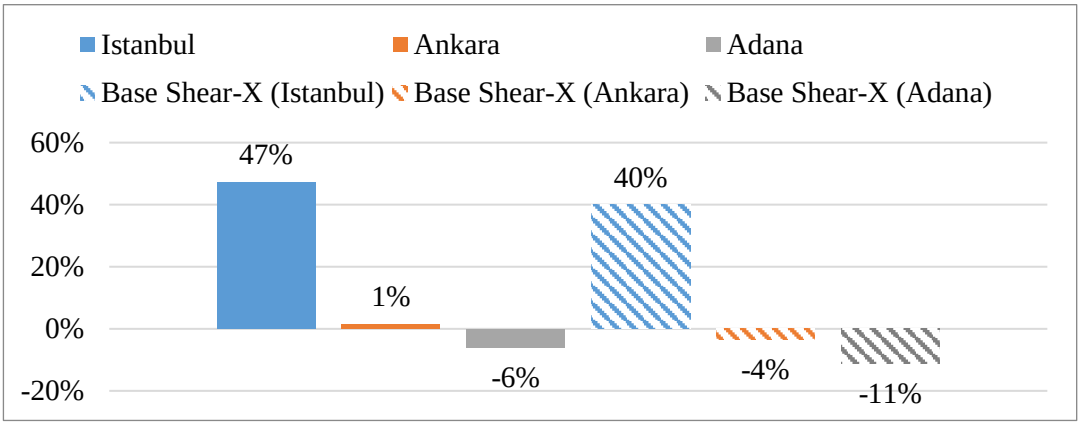


Figure 5.8. Beam – Change in Moment from TEC 2007 to TBEC 2018 (X-direction), three-story structure.

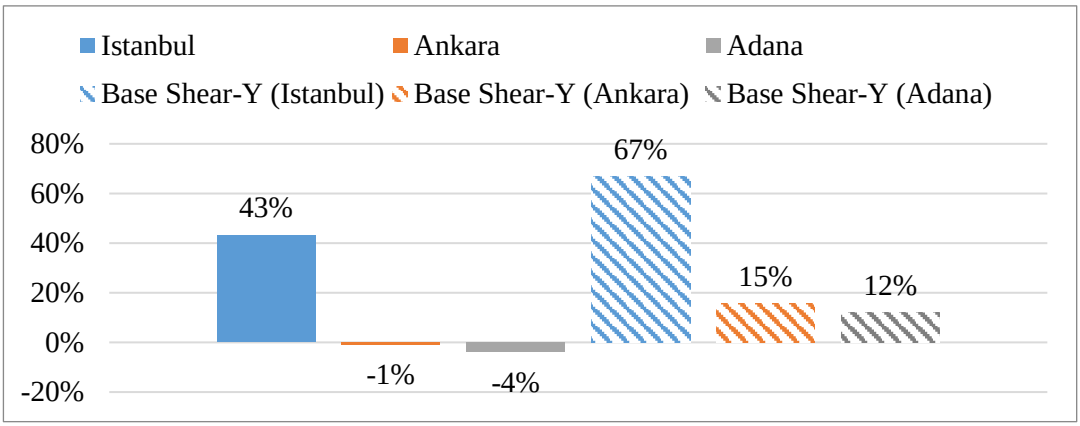


Figure 5.9. Beam – Change in Moment from TEC 2007 to TBEC 2018 (Y-direction), three-story structure.

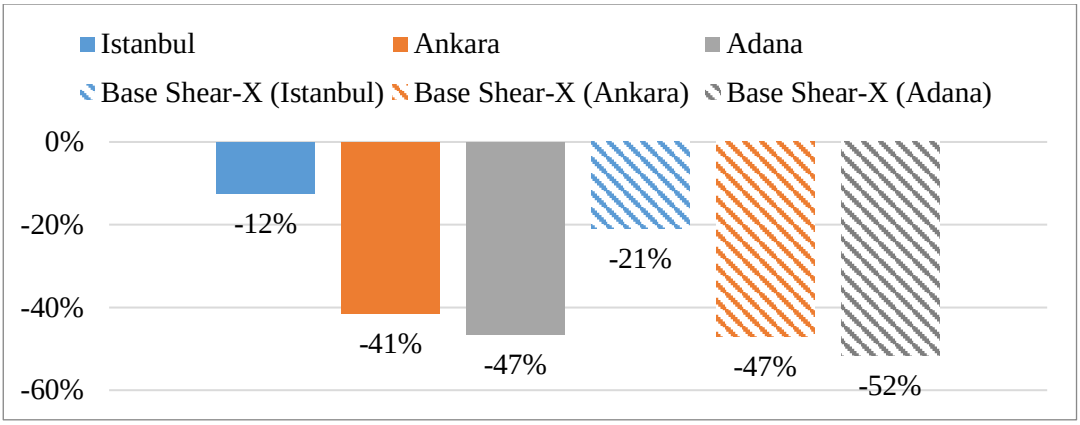


Figure 5.10. Beam – Change in Moment from TEC 2007 to TBEC 2018 (X-direction), six-story structure.

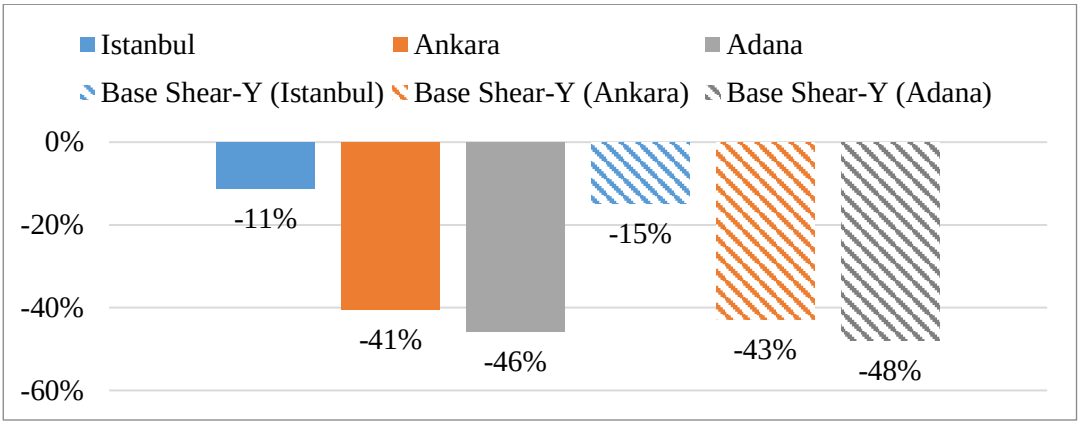


Figure 5.11. Beam – Change in Moment from TEC 2007 to TBEC 2018 (Y-direction), six-story structure.

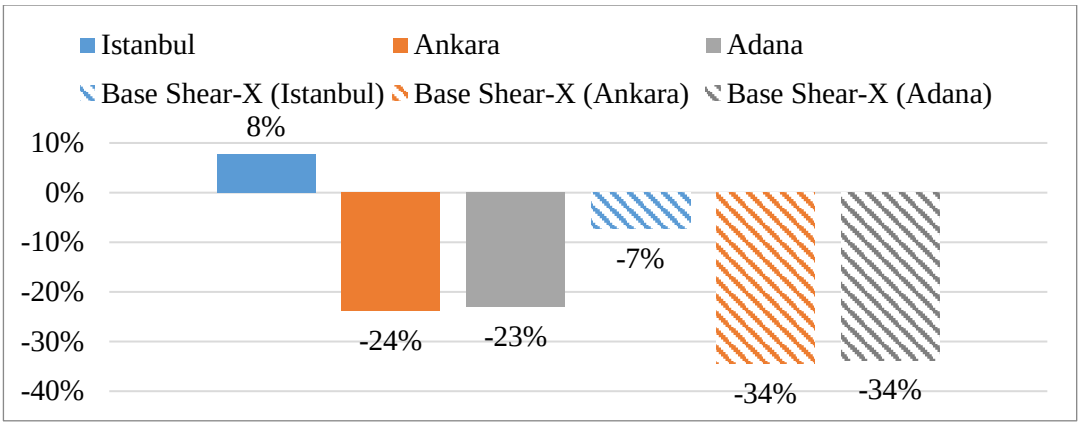


Figure 5.12. Beam – Change in Moment from TEC 2007 to TBEC 2018 (X-direction), twelve-story structure.

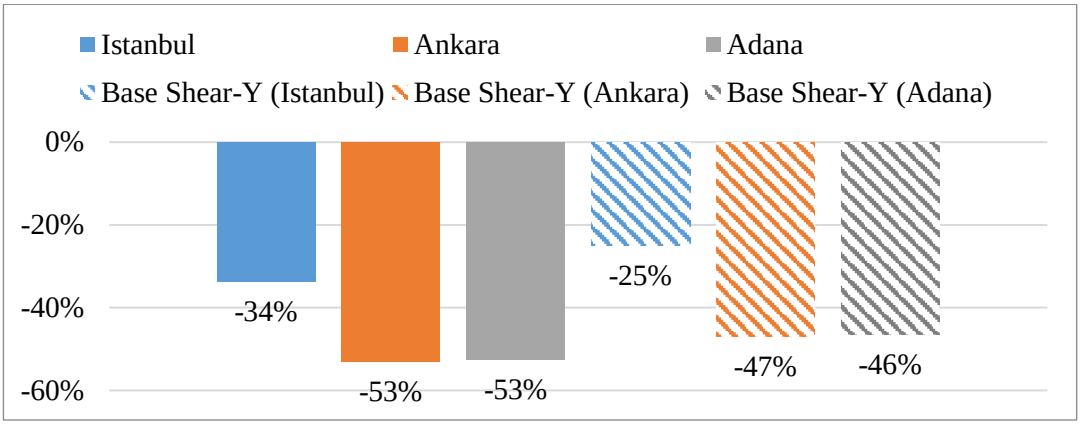


Figure 5.13. Beam – Change in Moment from TEC 2007 to TBEC 2018 (Y-direction), twelve-story structure.

The results show that the beam moment closely follows the change in the base shear. The slight difference between the relationship is attributed to the effective moment of inertias used in TBEC 2018 analysis. Using a 0.35 moment of inertia modifier for beams results in less force transferred to the beams. For the twelve-story structure, the base shears are close in the X-direction which results in the increase of moment in the chosen beam. The increase in the beam moment for the taller building is due to the increased participation of the moment frames.

### 5.2.2 Column Member Force Comparison

The column member picked for comparison is located on the third floor (grid line B3) for three-story structures, the sixth floor for six-story structures, and the twelfth floor for twelve-story structures. The column location is chosen so that its participation in the lateral resisting system is apparent in the member force results (Figure 5.11).

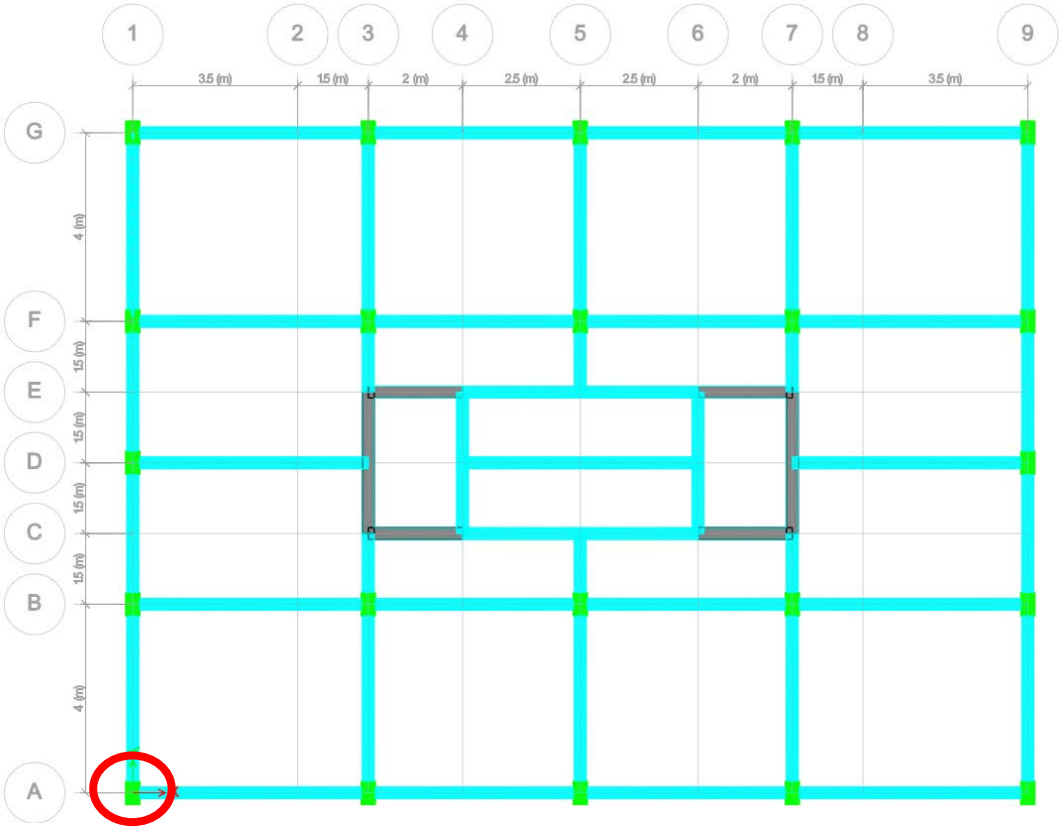


Figure 5.14. Column member that is chosen for comparison.

Figures 5.15, 5.17, and 5.19 show the moment comparison in the chosen column with respect to both codes as a percentage in the X-direction, and Figures 5.16, 5.18, 5.20 in the Y-direction.

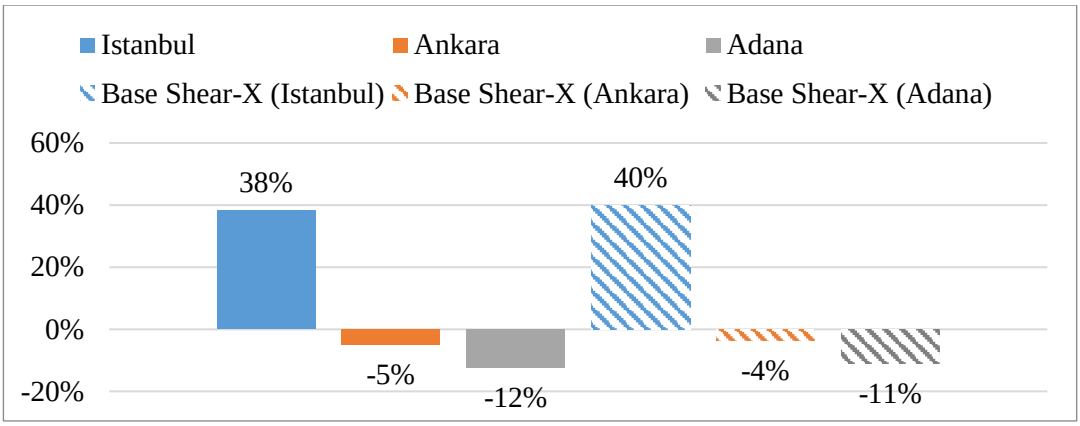


Figure 5.15. Column – Change in Moment from TEC 2007 to TBEC 2018 (X-direction), three-story structure.

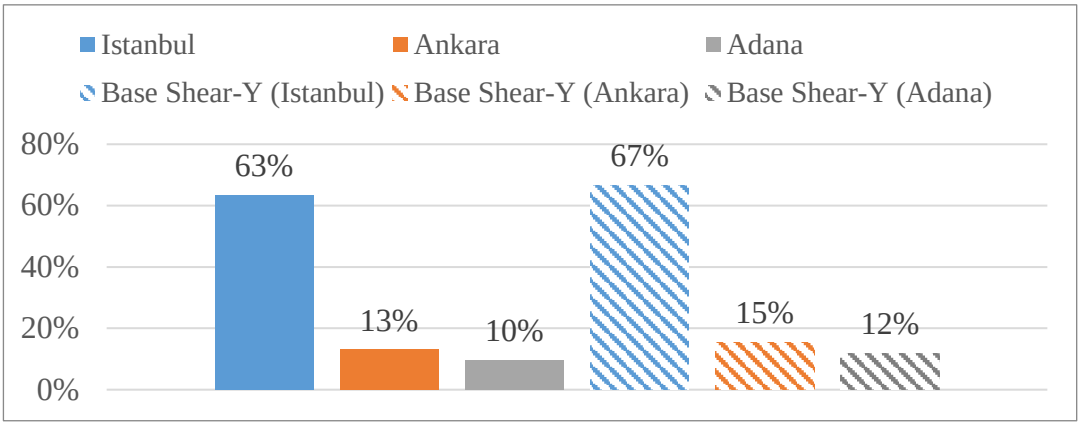


Figure 5.16. Column – Change in Moment from TEC 2007 to TBEC 2018 (Y-direction), three-story structure.

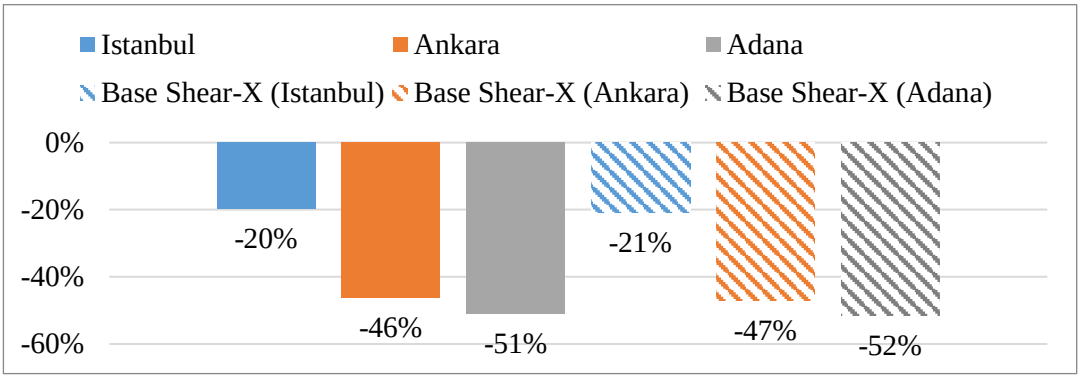


Figure 5.17. Column – Change in Moment from TEC 2007 to TBEC 2018 (X-direction), six-story structure.

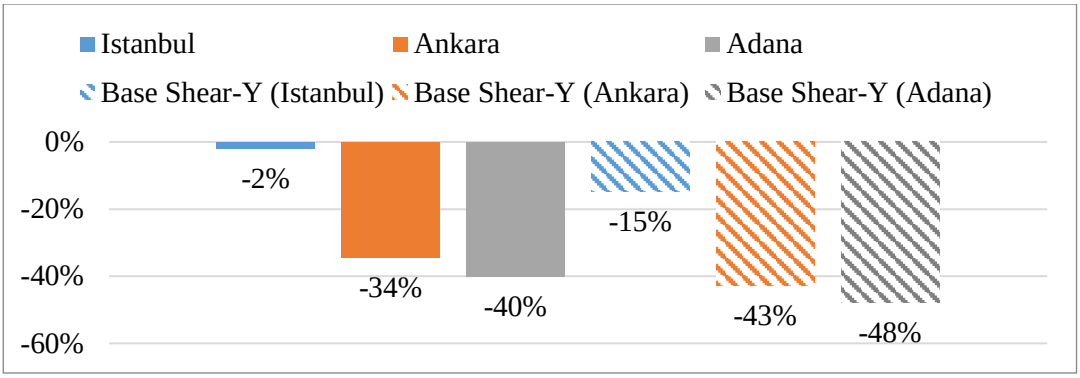


Figure 5.18. Column – Change in Moment from TEC 2007 to TBEC 2018 (Y-direction), six-story structure.

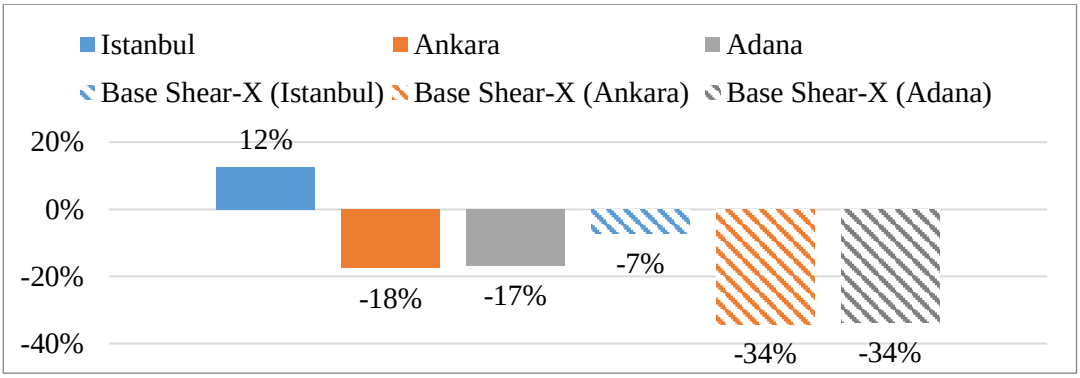


Figure 5.19. Column – Change in Moment from TEC 2007 to TBEC 2018 (X-direction), twelve-story structure.

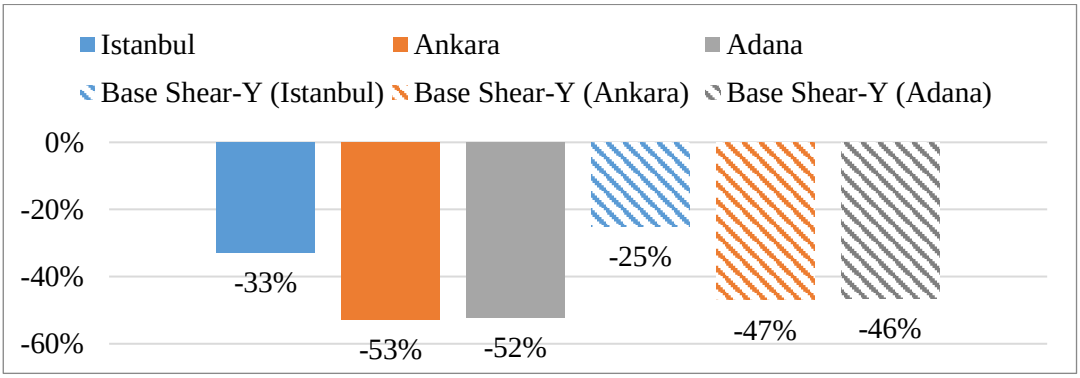


Figure 5.20. Column – Change in Moment from TEC 2007 to TBEC 2018 (Y-direction), twelve-story structure.

The effective moment of inertia factor was 0.7 for columns, 0.35 for beams, and 0.5 for shear walls. The columns are the members with the least amount of stiffness decrease, which results in columns participating in the lateral resistance system more

effectively. Their effectiveness is verified by comparing the change in column moments and base shears, which are closely correlated.

### 5.2.3 Shear Wall Member Force Comparison

The shear wall thickness is 250 mm for three- and six-story structures, while twelve-story structures have 285 mm shear walls. The walls are continuous through the stories with the same thickness. The U type shear wall that is picked for comparison is shown in Figure 5.15 and it is located at the first level for all structures.

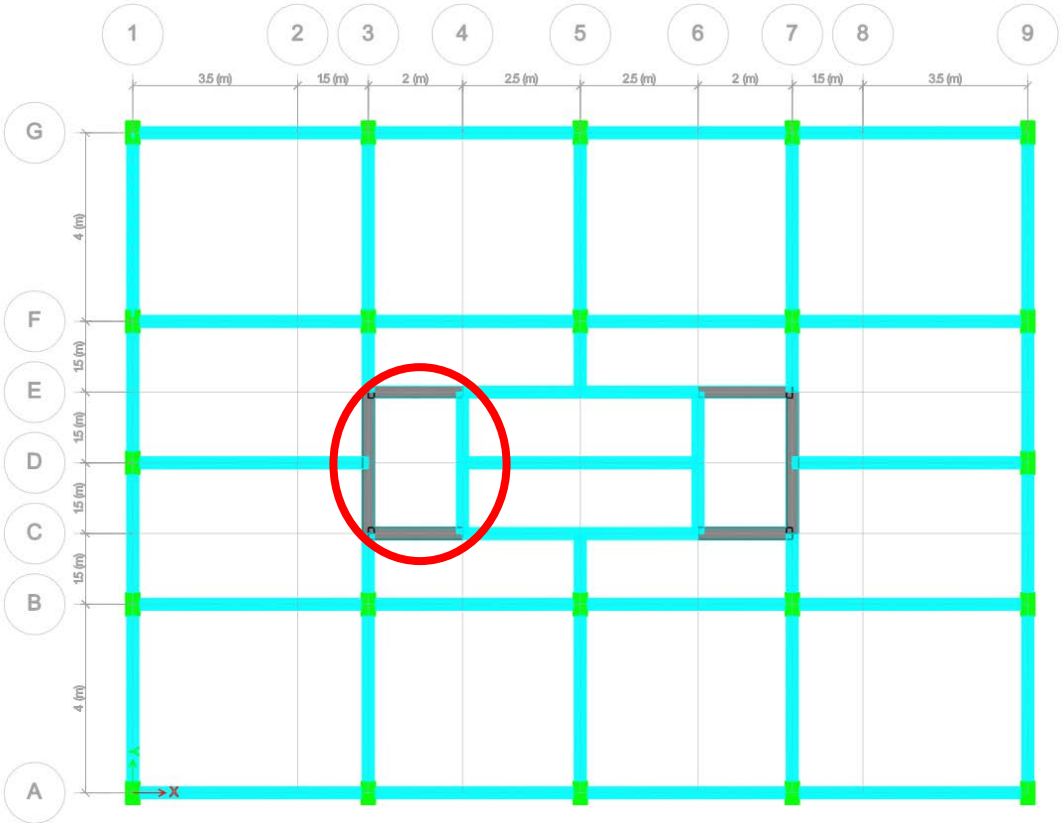


Figure 5.21. The U type shear wall that is chosen for comparison.

The shear forces obtained from the analysis results on the chosen shear wall are presented in Figures 5.22, 5.24, and 5.26 for the X-direction while Figures Figure 5.23, 5.25, and 5.27 . The base shears are also given for each location to visualize the correlation.

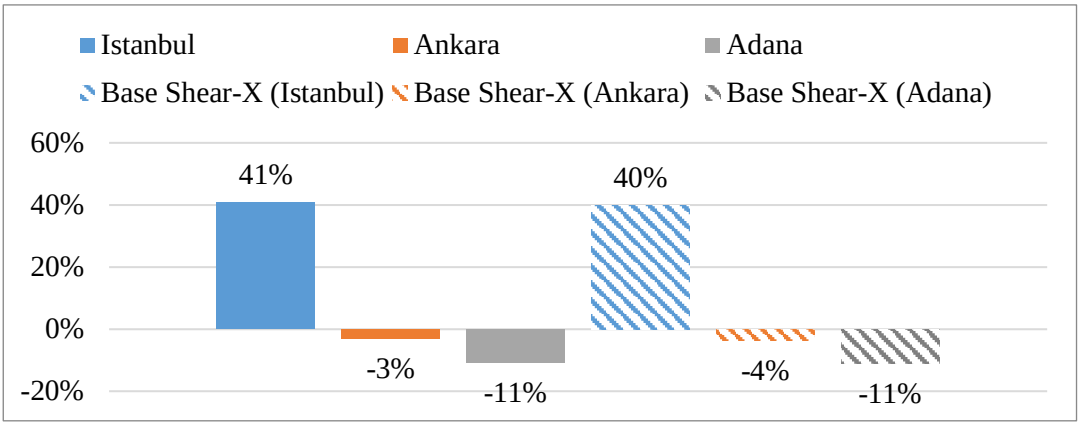


Figure 5.22. Wall – Change in Shear Force from TEC 2007 to TBEC 2018 (X-direction), three-story structure.

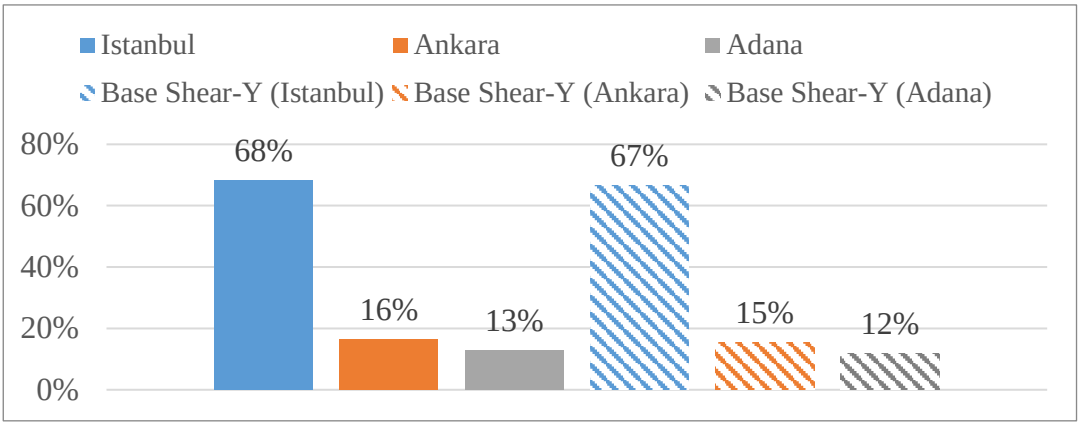


Figure 5.23. Wall – Change in Shear Force from TEC 2007 to TBEC 2018 (Y-direction), three-story structure.

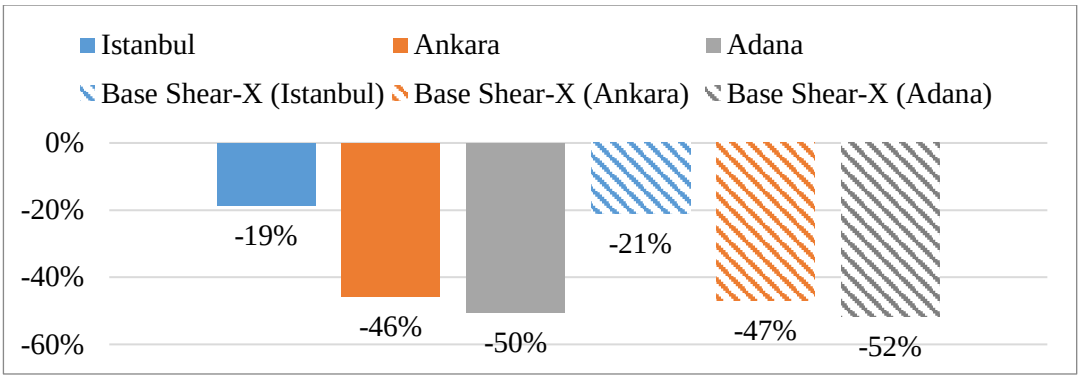


Figure 5.24. Wall – Change in Shear Force from TEC 2007 to TBEC 2018 (X-direction), six-story structure.

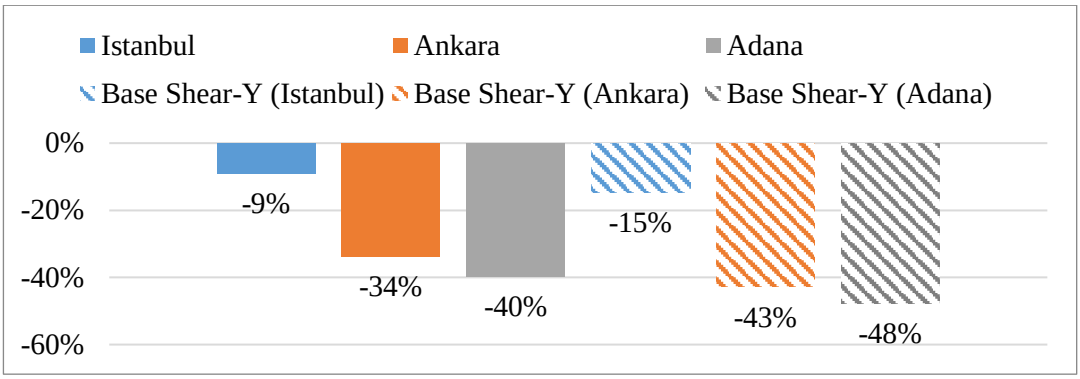


Figure 5.25. Wall – Change in Shear Force from TEC 2007 to TBEC 2018 (Y-direction), six-story structure.

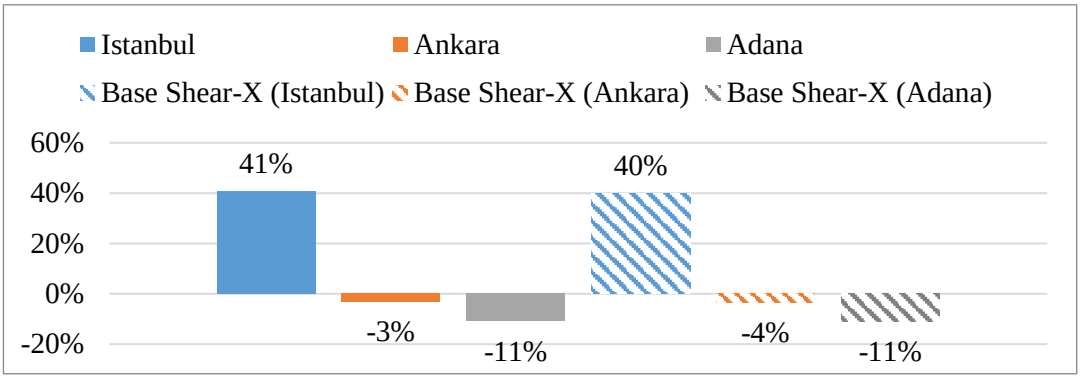


Figure 5.26. Wall – Change in Shear Force from TEC 2007 to TBEC 2018 (X-direction), twelve-story structure.

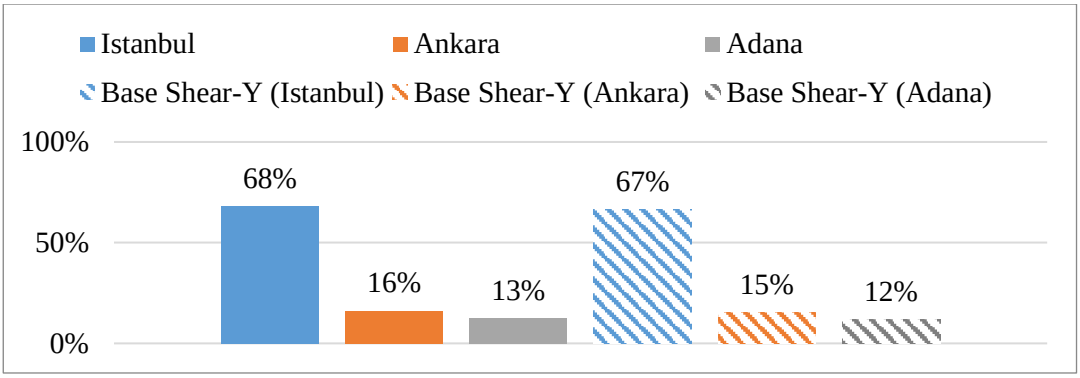


Figure 5.27. Wall – Change in Shear Force from TEC 2007 to TBEC 2018 (Y-direction), twelve-story structure.

The change in base shear is directly correlated with the change in the shear force on the walls since more than 90% of shear is resisted by the shear walls.

## 5.3 Drifts

The drifts and drift limits are calculated for both codes. There are differences in the approach between TEC 2007 and TBEC 2018, the changes are discussed, and results are shown.

The story drifts are defined in Section 2.10, TEC 2007. The relative displacement is calculated as follows:

$$\Delta_i = d_i - d_{i-1} \tag{5.5}$$

$$\delta_i = R * \Delta_i \tag{5.6}$$

$$\frac{(\delta_i)_{max}}{h_i} \leq 0.02 \tag{5.7}$$

The parameters used in Equations (5.5), (5.6), and (5.7) are given in Table 5.16.

Table 5.16. Equations (5.5), (5.6), and (5.7) parameter descriptions.

| Parameter | Description |
|---|---|
| $\Delta_i$ | Reduced relative floor drift at the i-th floor of the building |
| $d_i$ | Displacement calculated according to reduced seismic loads on the i-th floor of the building |
| $\delta_i$ | Effective relative floor drift at the i-th floor of the building |
| $h_i$ | Floor height of the i-th floor of the building |

The story drifts are defined in Section 4.9.1, TBEC 2018. The relative displacement is calculated as follows:

$$\Delta_i = d_i - d_{i-1} \tag{5.8}$$

$$\delta_i = \frac{R}{I} * \Delta_i \tag{5.9}$$

$$\lambda \frac{(\delta_i)_{max}}{h_i} \leq 0.008\kappa \tag{5.10}$$

$\kappa = 1$ for reinforced concrete structures, $\lambda$ is the ratio of service level spectral seismic acceleration coefficient (DD-3, 72-year return period) to the strength level spectral seismic acceleration coefficient. (DD-2, 475-year return period). The service to strength spectral acceleration coefficients is shown in Tables 5.17, 5.18, and 5.19.

Table 5.17. Service to strength seismic ratios, 3-Story

| Location | $\lambda$ |
|---|---|
| Istanbul | 0.41 |
| Ankara | 0.32 |
| Adana | 0.37 |

Table 5.18. Service to strength seismic ratios, 6-Story

| Location | $\lambda$ |
|---|---|
| Istanbul | 0.37 |
| Ankara | 0.39 |
| Adana | 0.38 |

Table 5.19. Service to strength seismic ratios, 12-Story

| Location | $\lambda$ |
|---|---|
| Istanbul | 0.41 |
| Ankara | 0.32 |
| Adana | 0.37 |

The calculation results for the X-direction drift of three, six, and twelve-story structures located in Istanbul are given in Figures 5.28, 5.29, and 5.30 . The rest of the drift results can be found in the Appendix A. The presented results are for the most critical location and direction.

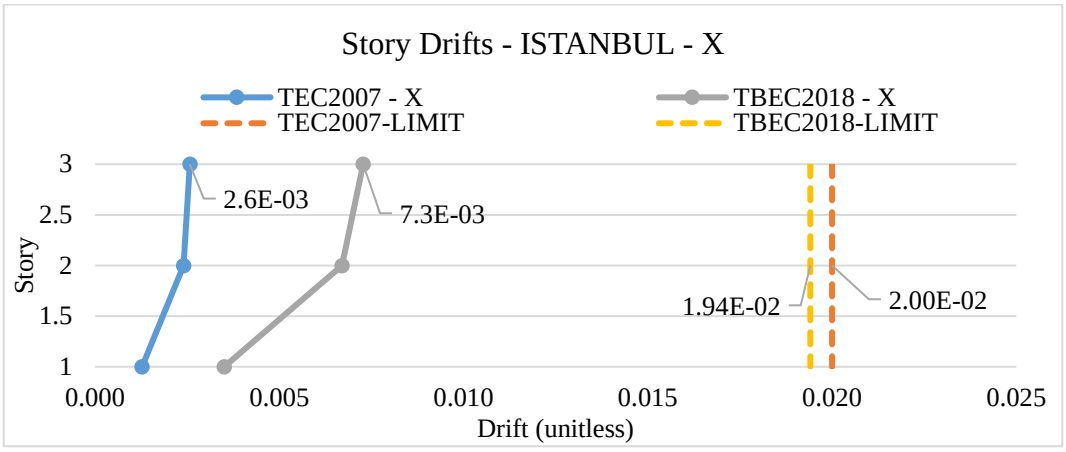


Figure 5.28. Drift comparison, Istanbul, three-story structure

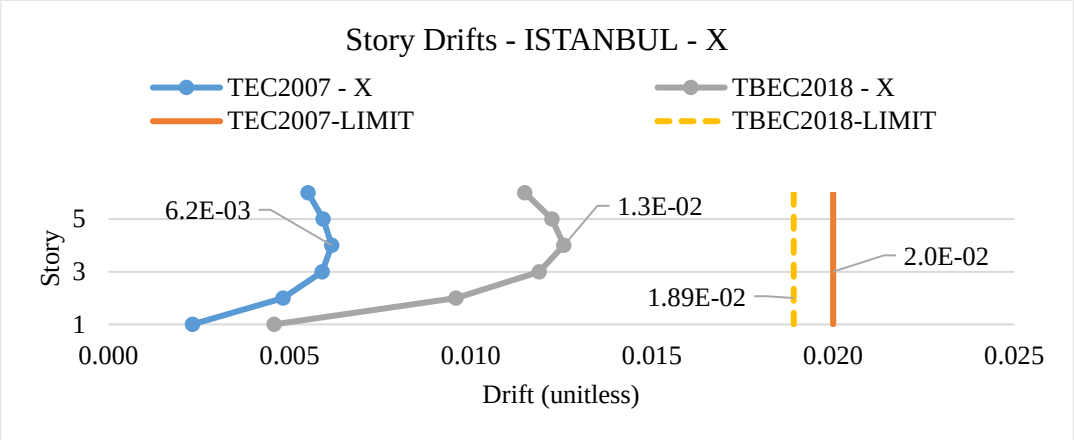


Figure 5.29. Drift comparison, Istanbul, six-story structure

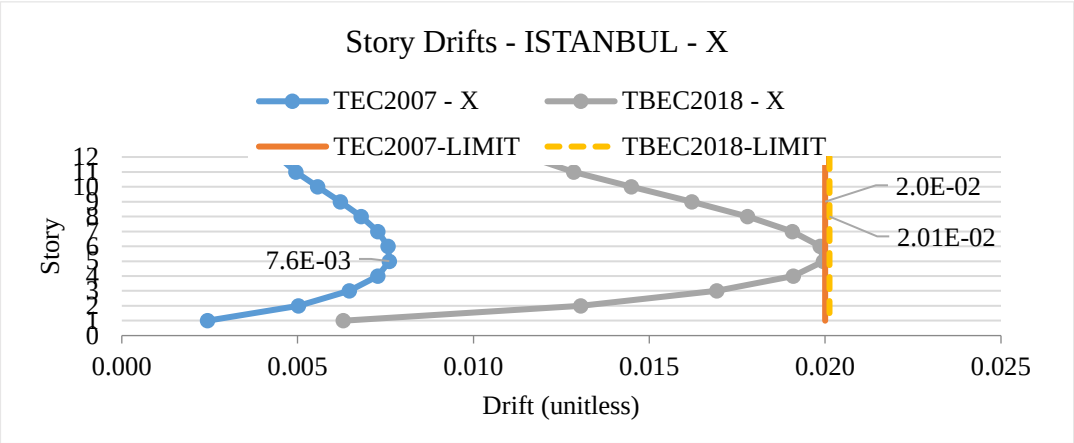


Figure 5.30. Drift comparison, Istanbul, twelve-story structure

At all locations and for all stories, the drifts increase from TEC 2007 to TBEC 2018 while the limits remain close between the codes. The increase in drifts is expected in TBEC 2018 since the member stiffnesses are decreased by effective moment of inertia factors resulting in a stiffness decrease for all members. The drift is larger in TBEC 2018 even for the six and twelve-story structure, where the base shears calculated for TEC 2007 were larger.

## 5.4 Member Reinforcement Detailing

This section will focus on reinforcement detailing and strength limit differences between the codes. The detailing and shear strength requirements have been updated

in TBEC 2018 according to the latest advancements in the structural members' seismic performance.

The reinforcement areas are obtained from the structural model, and the procedure is available in "Concrete Frame Design Manual – Turkish TS500-2000 with Seismic Code 2018" (CSI, 2020). The software procedure is verified by following the manual and ensuring that the code requirements are satisfied.

### 5.4.1 Columns

In addition to the 1% minimum reinforcement ratio, the minimum longitudinal reinforcement requirement given in TEC 2007 for rectangular columns was 4ϕ16 or 6ϕ14. This requirement was simplified in TBEC 2018; the new code only requires the minimum reinforcement size to be ϕ14, and the minimum ratio of 1% only limits the minimum number of bars.

TEC 2007 allows the lap of longitudinal bars at the base of the column with modifications to the original lap length. However, TBEC 2018 requires the laps to be within the middle one-third of the clear height of the column. The rule is enforced to ensure that the lap is within the minimum moment region of the column; therefore, the potential decrease in the column's moment capacity due to the lap is prevented.

For both codes, the top and bottom ends of the columns are required to have increased transverse reinforcement. In TBEC 2018, one of the limits for determining the length that defines the column confinement zone length was changed from the column's larger side to one and a half times the column's larger side. This increases the length of the confinement region at the ends of the columns. Additionally, one of the maximums for the spacing of the transverse reinforcements in this region is increased from 100 mm to 150 mm in TBEC 2018. The transverse reinforcement is considered for a 300x500 column with minimum allowed reinforcement and a ratio

is obtained to compare the minimum transverse reinforcement requirement of the codes (Figure 5.31 and Table 5.20).

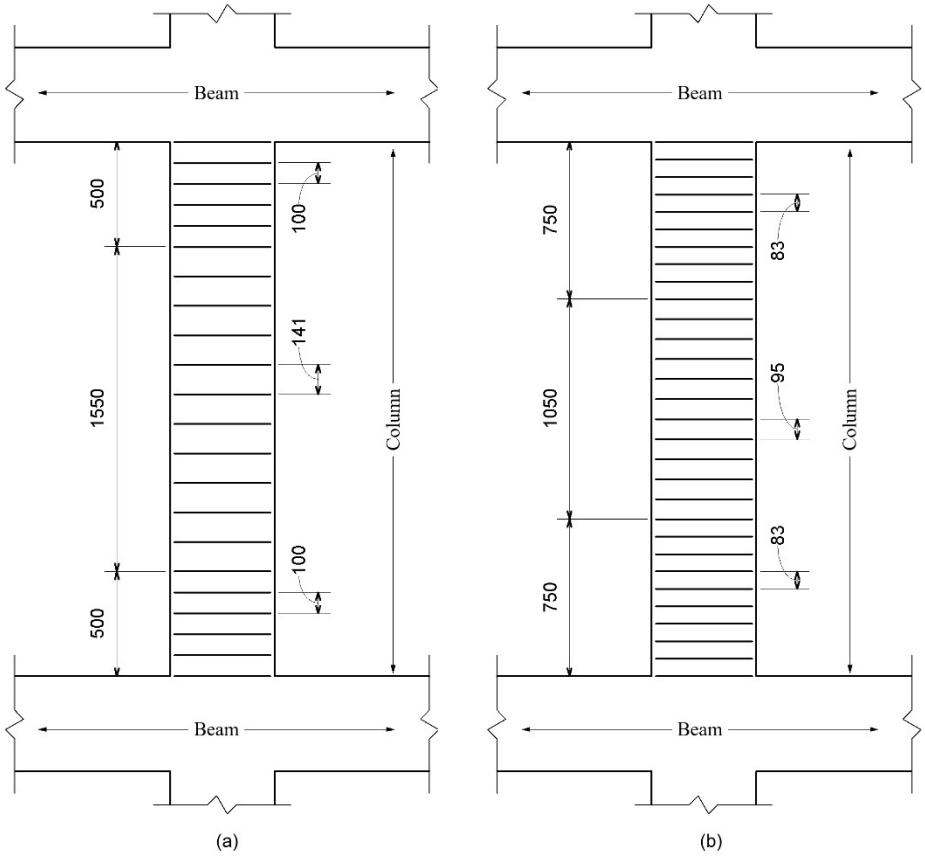


Figure 5.31. Transverse reinforcement requirement for the 300x500 column, (a) TEC 2007 (b) TBEC 2018.

Table 5.20. 300x500 Column, minimum transverse reinforcement comparison.

| | TEC 2007 | TBEC 2018 | TBEC 2018/TEC 2007-1 |
|---|---|---|---|
| Length, Confinement region | 500 | 750 | 50% |
| Spacing, Confinement region | 100 | 83 | -17% |
| **Number of Bars** | **6** | **10** | **67%** |
| Length, Lap region | 1550 | 1050 | -32% |
| Spacing, Lap region | 141 | 95 | -33% |
| **Number of Bars** | **10** | **10** | **0%** |
| **Total** | **16** | **20** | **25%** |

The increase in the length and decrease in the spacing for the confinement region results in a 25% increase in the minimum required transverse reinforcement amount from TEC 2007 to TBEC 2018.

The code defines a maximum shear force allowed on a column; if the shear force exceeds this value, the column size or concrete grade must be increased. Table 5.21 demonstrates the difference between the codes.

Table 5.21. Maximum shear force limit on a column

| TEC 2007 | TBEC 2018 |
|---|---|
| $0.22*A_w*f_{cd}$ | $0.85*A_w*\sqrt{f_{ck}}$ |

Table 5.22 shows the calculated multiplier of $A_w$ with respect to the concrete grade.

Table 5.22. The multiplier for the maximum allowed shear force

| Grade | TEC 2007 ($N/mm^2$) | TBEC 2018 ($N/mm^2$) |
|---|---|---|
| C25 | 3.67 | 4.25 |
| C30 | 4.40 | 4.66 |
| C40 | 5.87 | 5.38 |
| C50 | 7.33 | 6.01 |
| C60 | 8.80 | 6.58 |

The results show that while the limit is increased in TBEC 2018 for C25 and C30, for higher grade concrete, the limit is decreased, which increases the shear strength requirement for grades above C30.

The column design is performed by considering the axial load and moments on the column in both directions. The longitudinal reinforcement of the columns is determined by the three-dimensional interaction diagram. The interaction diagrams are obtained at 15-degree intervals rotated around the column cross-section. The longitudinal reinforcement is obtained by comparing the demand axial load and moment pairs with the obtained three-dimensional interaction diagram (Figure 5.32). The maximum allowed demand capacity ratio is set to 95% for all columns. If the required reinforcement due to the demand is less than the minimum reinforcement, then minimum reinforcement area is used for design.

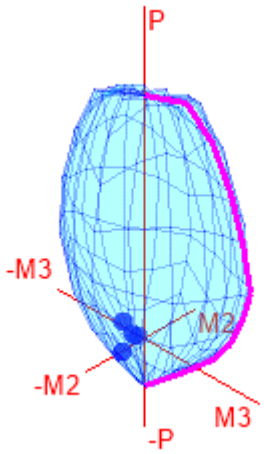


Figure 5.32. Three-dimensional interaction diagram for a column.

Additionally, both codes require the columns to be stronger than the beams at beam-column joints in each direction, as given in Section 3.3.5, TEC 2007, and Section 7.3.5, TBEC 2018. The requirement is satisfied for all beam-column joints that are designed as highly ductile moment frames. The limit is given with the following equation:

$$M_{rc,1} + M_{rc,2} = 1.2(M_{rb,1} + M_{rb,2}) \quad (5.11)$$

The parameters used in Equation (5.11) are given in Table 5.23 and Figure 5.33.

Table 5.23. Equation (5.11) parameter descriptions.

| Parameter | Description |
|---|---|
| $M_{rc,1}$ | Moment capacity calculated with respect to $f_{cd}$ and $f_{yd}$ at the top end of the free height of the column |
| $M_{rc,2}$ | Moment capacity calculated with respect to $f_{cd}$ and $f_{yd}$ at the lower end of the free height of the column |
| $M_{rb,1}$ | Positive or negative moment capacity calculated with respect to $f_{cd}$ and $f_{yd}$ on the column or shear face at the left end of the beam |
| $M_{rb,2}$ | Positive or negative moment capacity calculated with respect to $f_{cd}$ and $f_{yd}$ on the column or shear face at the right end of the beam |

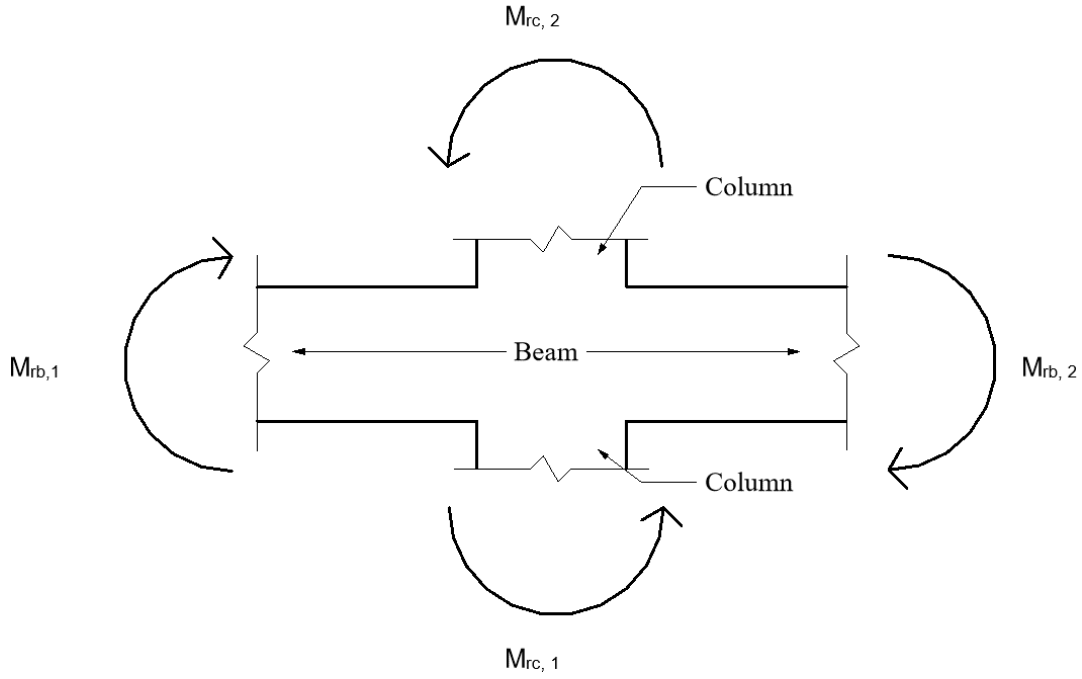


Figure 5.33. Moments considered in strong column, weak beam check.

### 5.4.2 Beams

For the transverse reinforcement at the end zones of the beams, TBEC 2018 adds a minimum bar diameter requirement of eight millimeters. The confinement region length and transverse reinforcement spacing limits are the same in both codes.

The maximum allowed shear force equation change shown in the column section is also applicable for beams by replacing the column's effective area with the beam's effective area.

Section 3.5.2.2, TEC 2007, and Section 7.5.2.2, TBEC 2018, limits the shear at the beam-column joints with the shown formulas in Table 5.24.

Table 5.24. Maximum shear force limits on beam-column joints

| TEC 2007 | | TBEC 2018 | |
|---|---|---|---|
| (a) | (b) | (a) | (b) |
| $0.6*b_j*h*f_{cd}$ | $0.45*b_j*h*f_{cd}$ | $1.7*b_j*h*\sqrt{f_{ck}}$ | $1.0*b_j*h*\sqrt{f_{ck}}$ |

The formula shown with (a) corresponds to joints that have beams on all four sides, and each beam has a width of at least ¾ of the column that it is connected to, (b) is for all other cases. Table 5.25 shows the factors that would be multiplied by the area for each concrete grade to obtain the shear force limit.

Table 5.25. Maximum shear force limits on beam-column joints

| Grade | TEC 2007 | | TBEC 2018 | |
|---|---|---|---|---|
| | a | b | a | b |
| C25 | 10.00 | 7.50 | 8.50 | 5.00 |
| C30 | 12.00 | 9.00 | 9.31 | 5.48 |
| C40 | 16.00 | 12.00 | 10.75 | 6.32 |
| C50 | 20.00 | 15.00 | 12.02 | 7.07 |
| C60 | 24.00 | 18.00 | 13.17 | 7.75 |

Table 5.25 shows that the maximum allowable shear force is significantly decreased at beam-column joints in TBEC 2018.

The longitudinal reinforcement is calculated by considering flexure about the major axis of the beam. The minor axis bending, and effect of the axial force is not checked, and they are negligible for the analyzed structure. The minimum size of the longitudinal reinforcement is Ø12 and at least two bars are required at top and bottom of the section.

For the beams, a reinforcement area plan is given at the top story of the twelve-story structure located in Istanbul to demonstrate the reinforcement area distributions

according to TEC 2007 (Figure 5.34). The same figure is given for the reinforcement design results of TBEC 2018 (Figure 5.35).

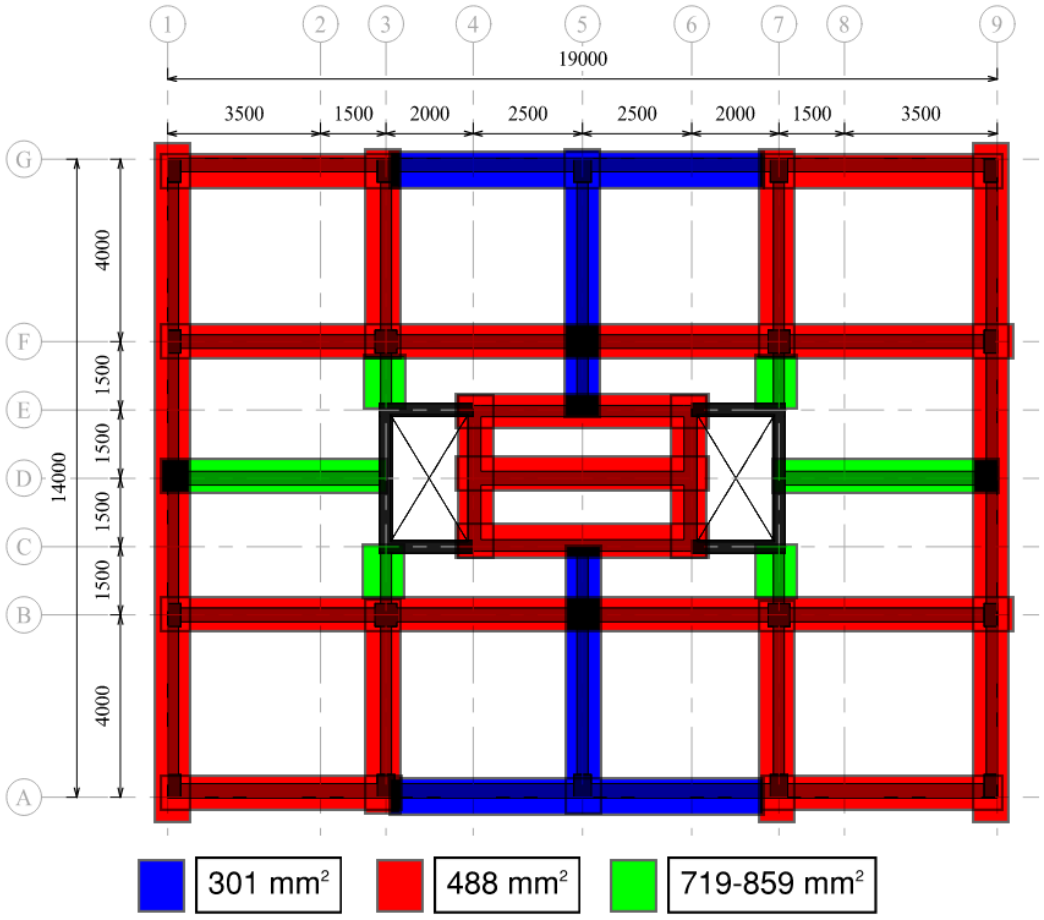


Figure 5.34. Twelve-story structure in Istanbul, beam reinforcement area groups per TEC 2007.

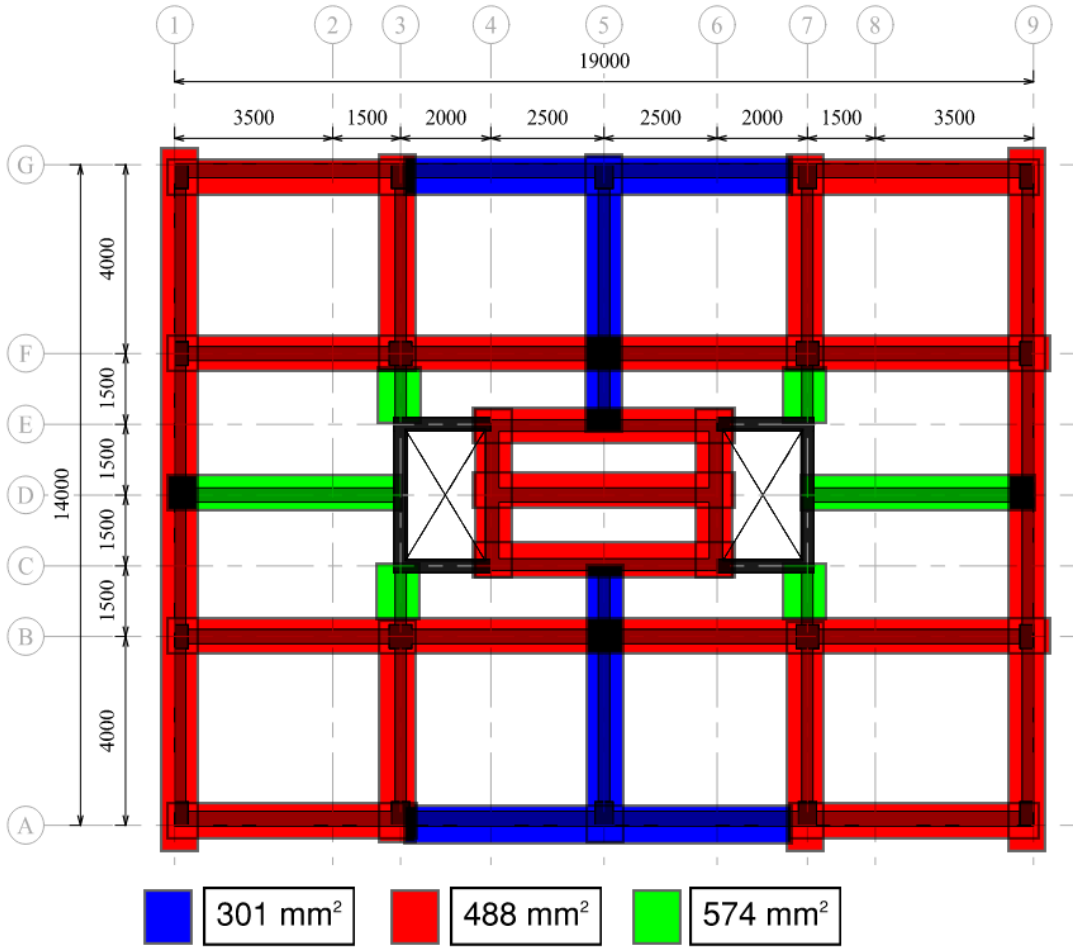


Figure 5.35. Twelve-story structure in Istanbul, beam reinforcement area groups per TBEC 2018.

### 5.4.3 Shear Walls

In Section 7.6.1.1, TBEC 2018, a new requirement is added for the maximum axial load on a shear wall:

$$A_c \geq N_{dm}/(0.35 * f_{ck}) \quad (5.12)$$

The parameters used in Equation (5.12) are given in Table 5.26.

Table 5.26. Equation (5.12) parameter descriptions.

| Parameter | Description |
|---|---|
| $A_c$ | Gross cross-sectional area of column or wall end zone |
| $N_{dm}$ | The largest of the axial compressive forces calculated under the combined effect of vertical loads and earthquake loads |
| $f_{ck}$ | Characteristic cylinder compressive strength of concrete |

The equation is similar to the equation given for the columns, but the factor is decreased from 0.4 to 0.35.

The minimum horizontal reinforcement area in Section 3.6.3.2, TEC 2007, increased from 0.0015 to 0.002 in TBEC 2018.

The change in the maximum allowable shear shown for beams and columns also applies to the shear walls with the same factors but with the shear wall's cross-sectional area.

The shear force and moment from the analysis are modified in both codes. TBEC 2018 introduces an overstrength factor to increase the shear demand on shear walls and modifies the maximum allowed shear load equation in TEC 2007. The procedure given in TBEC 2018 will be followed in this section, and differences will be discussed between the codes.

The shear force to be used in the design of the member is defined in Equation 5.13, TBEC 2018:

$$V_e = \beta_v \frac{(M_p)_t}{(M_d)_t} V_d \leq 1.2 * D * V_d \tag{5.13}$$

The parameters used in Equation (5.13) are given in Table 5.27.

Table 5.27. Equation (5.13) parameter descriptions.

| Parameter | Description |
|---|---|
| $V_e$ | Amplified design shear force |
| $\beta_v$ | Dynamic amplification factor, 1.5 for dual lateral systems. |
| $(M_p)_t$ | Plastic moment capacity of the shear wall section. Can be taken as: $1.25 * (M_r)_t$ |
| $(M_r)_t$ | Elastic moment capacity of the shear wall. |
| $(M_d)_t$ | Design moment at the shear wall from analysis. |
| $V_d$ | Design shear at the shear wall from analysis. |
| D | Overstrength factor. |

From the analysis, the following results are obtained for the chosen shear wall shown in Table 5.28.

Table 5.28. Analysis results of the selected shear wall.

| Parameter | Result |
|---|---|
| P | 4729 kN |
| $(M_d)_t$ | 10914 kNm |
| $(M_r)_t$ | 19264 kNm |
| $(M_p)_t$ | $1.25 * 19264 = 24080$ kNm |
| $V_d$ | 1192 kN |

$$V_e = 1.5 * \frac{24080}{10914} * 1192 = 3943 \text{ kN} \geq 1.2 * 2.5 * 1192 = 3574 \text{ kN}$$

The amplified shear force is more than the limit of "$1.2 * D * V_d$"; therefore, the amplified shear force is ignored, and the limit is directly used to determine the shear reinforcement of the chosen shear wall.

The shear capacity of the wall is calculated using the following formula:

$$V_r = A_c * \left(0.65 * 0.35 * \frac{\sqrt{f_{ck}}}{1.5} + \rho_{shear} * f_{ywk}\right) \quad (5.14)$$

$A_c$ is the cross-sectional area of the shear wall in the shear direction, and $\rho_{shear}$ is the shear reinforcement ratio.

$$V_r = (2000 * 285 + (3000 - 285 * 2) * 285) *$$

$$* \left(0.65 * 0.35 * \frac{\sqrt{30}}{1.5} + 0.006 * 420\right) = 6141 \text{ kN}$$

The demand capacity ratios of the shear wall are given in Table 5.29.

Table 5.29. Demand capacity ratios of the chosen shear wall.

| **Parameter** | **Result** |
|---|---|
| Moment Demand/Capacity | 10914/19264 = 0.57 |
| Shear Demand/Capacity | 3574/6141 = 0.58 |

The shear reinforcement ratio of 0.006 is chosen to satisfy the maximum spacing requirement of the seismic code. In terms of detailing, there are no differences between the codes but, TBEC 2018 introduces an overstrength factor for the maximum shear demand ($V_d$) which leads to an increase in the shear force demand in cases where the amplified shear exceeds the demand limit.

The cross-section and detailing of the chosen shear wall is given in Figure 5.36.

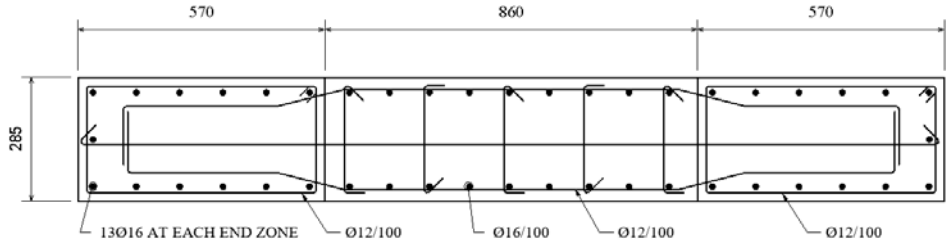


Figure 5.36. Shear wall cross-section with detailing for the chosen shear wall.

Figures 5.37 and 5.38 show the pier name assignments for reinforcement detailing purpose.


Figure 5.37. Plan view of the shear wall design group name.

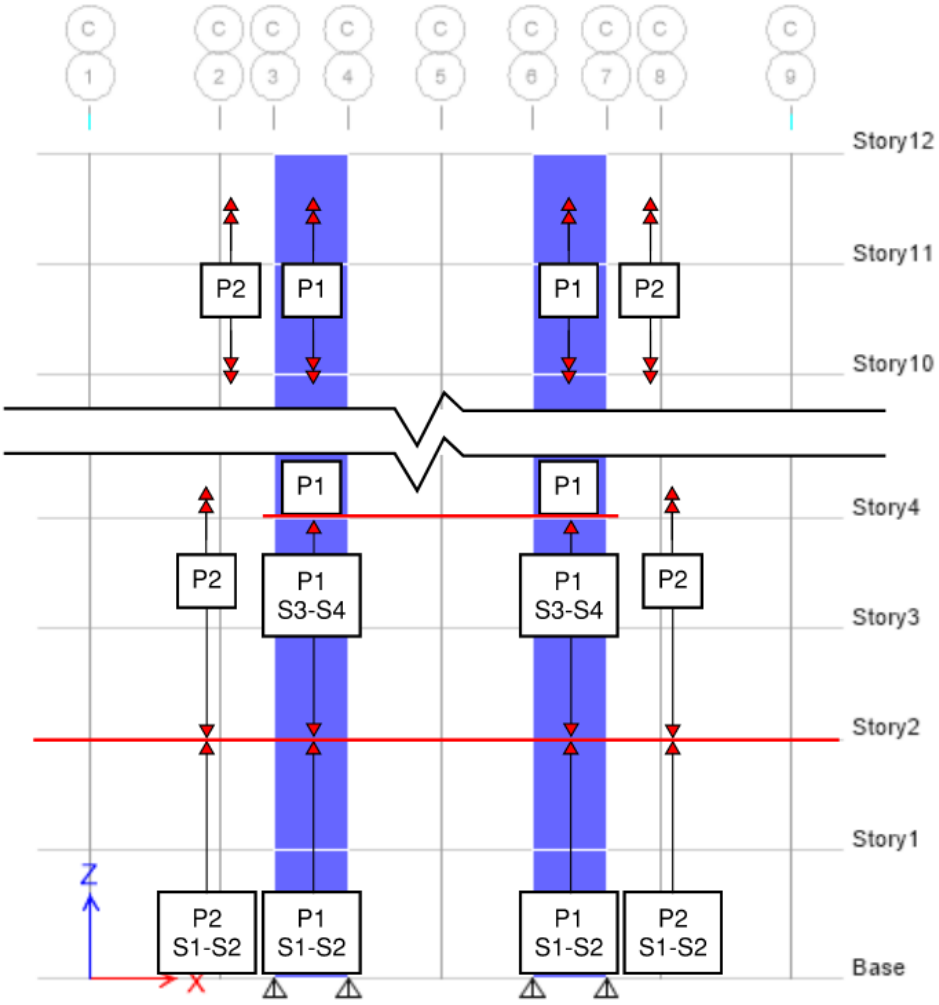


Figure 5.38. Shear wall section change with respect to the story.

The reinforcement information which is obtained from the design procedure is given in the Figures 5.39, 5.40, 5.41, 5.42, and 5.43 for each shear wall section in Istanbul and according to the results of TBEC 2018.

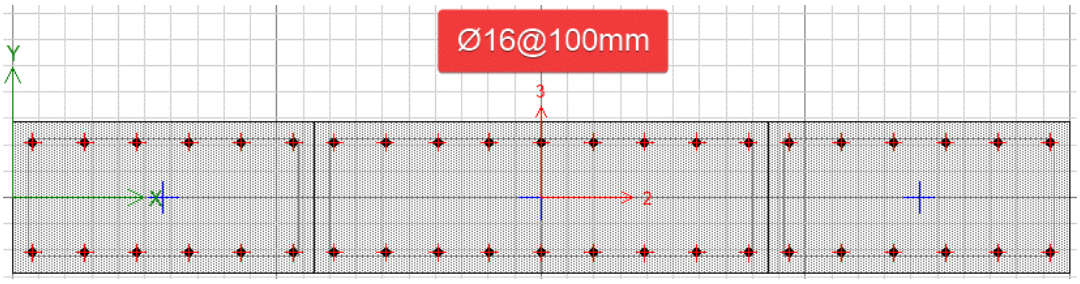


Figure 5.39. P1 (S1-S2) shear wall section reinforcement.

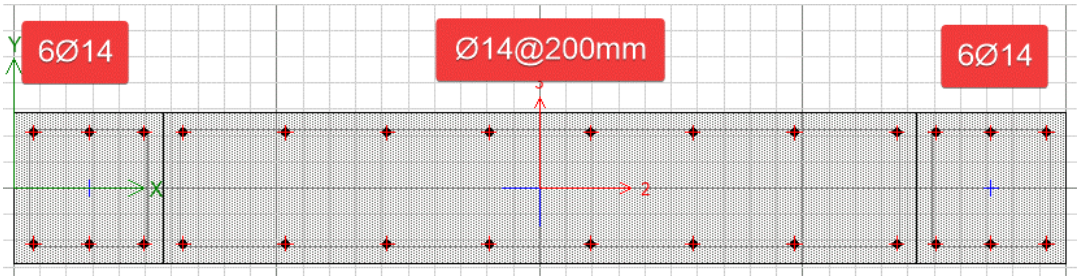


Figure 5.40. P1 (S3-S4) shear wall section reinforcement.

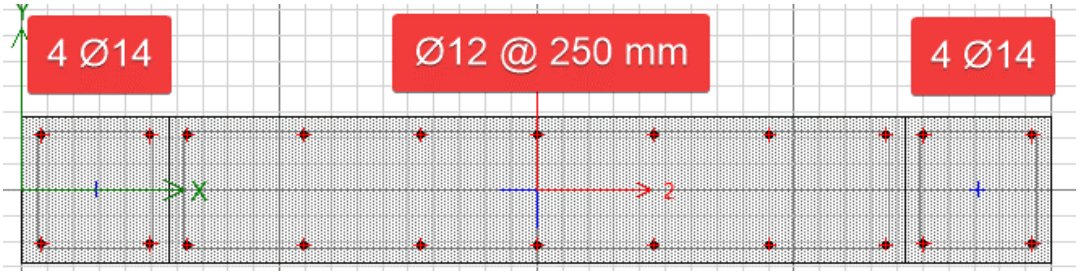


Figure 5.41. P1 shear wall section reinforcement.

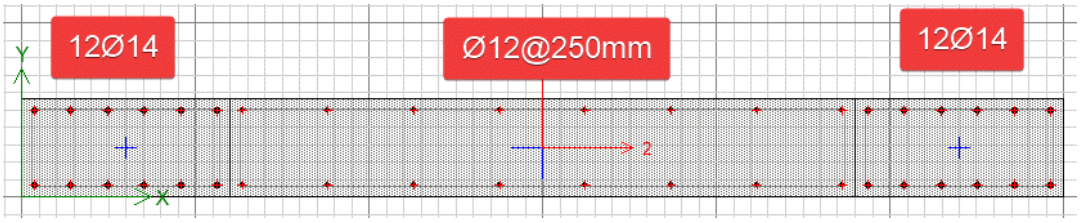


Figure 5.42. P2 (S1-S2) shear wall section reinforcement.

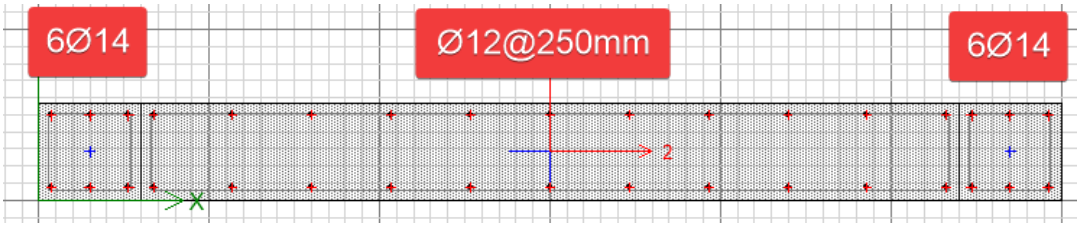


Figure 5.43. P2 shear wall section reinforcement.

## 5.5 Final Member Sizes

The minimum allowed sizes are used as a starting point for each member. The beams, columns, and shear walls are set to 250x450 mm, 300x500 mm, and 250 mm thick, respectively. The design is performed for all locations and story configurations. The plan view (Figure 5.44) shows the designed sections for three and six-story structures.

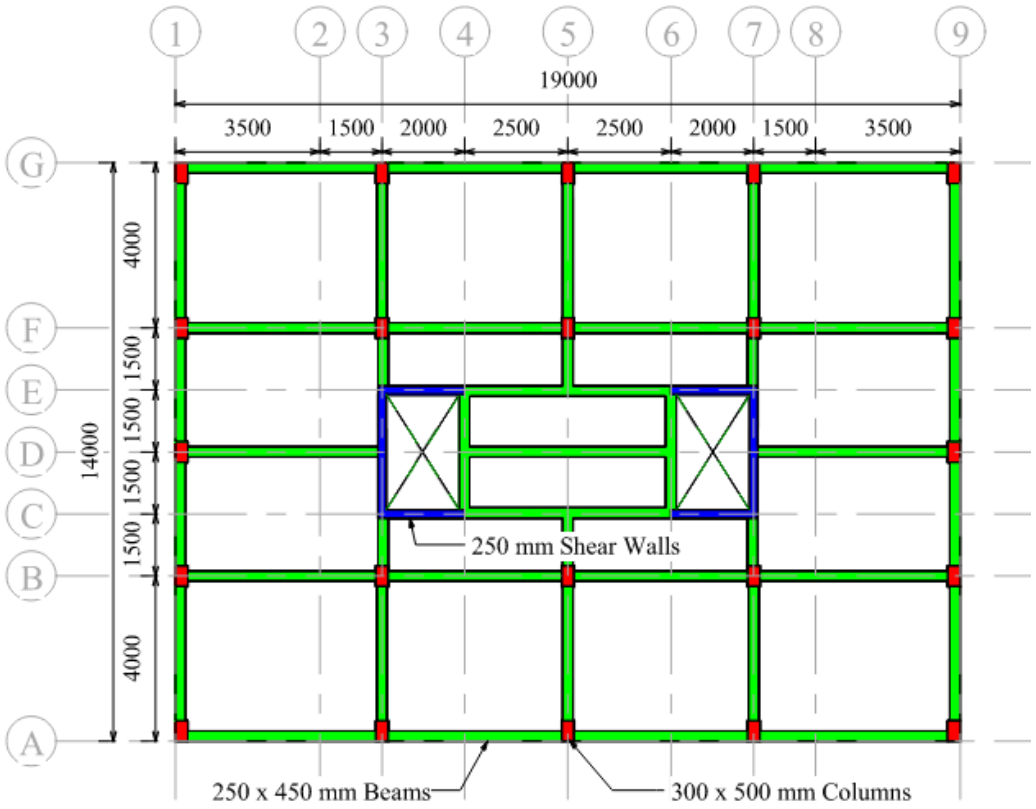


Figure 5.44. Designed member sizes for three and six-story structures.

For the twelve-story structure, the design of columns is governed by the minimum column size enforcement of TBEC 2018 that was discussed in Section 4.1.3 of this thesis. Additionally, an iterative design procedure is followed to obtain the required sizes that satisfies the limit discussed in Section 5.6. The shear wall thickness is limited by the length and thickness ratio given in TEC 2007, to satisfy the drift limit in X-direction, the beam and column sizes are increased in the moment frames

spanning east to west. The designed sizes for the combined requirements of TEC 2007 and TBEC 2018 is given in Figure 5.45.

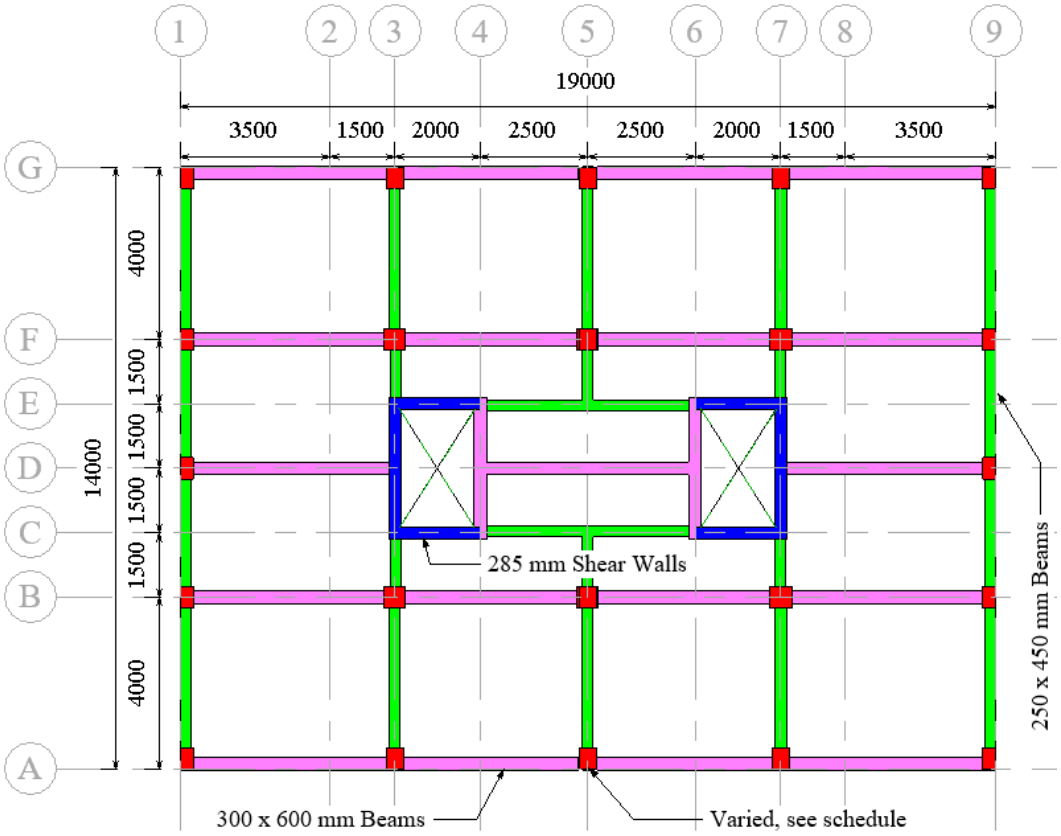


Figure 5.45. Designed member sizes for the twelve-story structure.

The graphical column schedule is given below to visualize the changing column sizes according to the gridline and story (Figure 5.46).

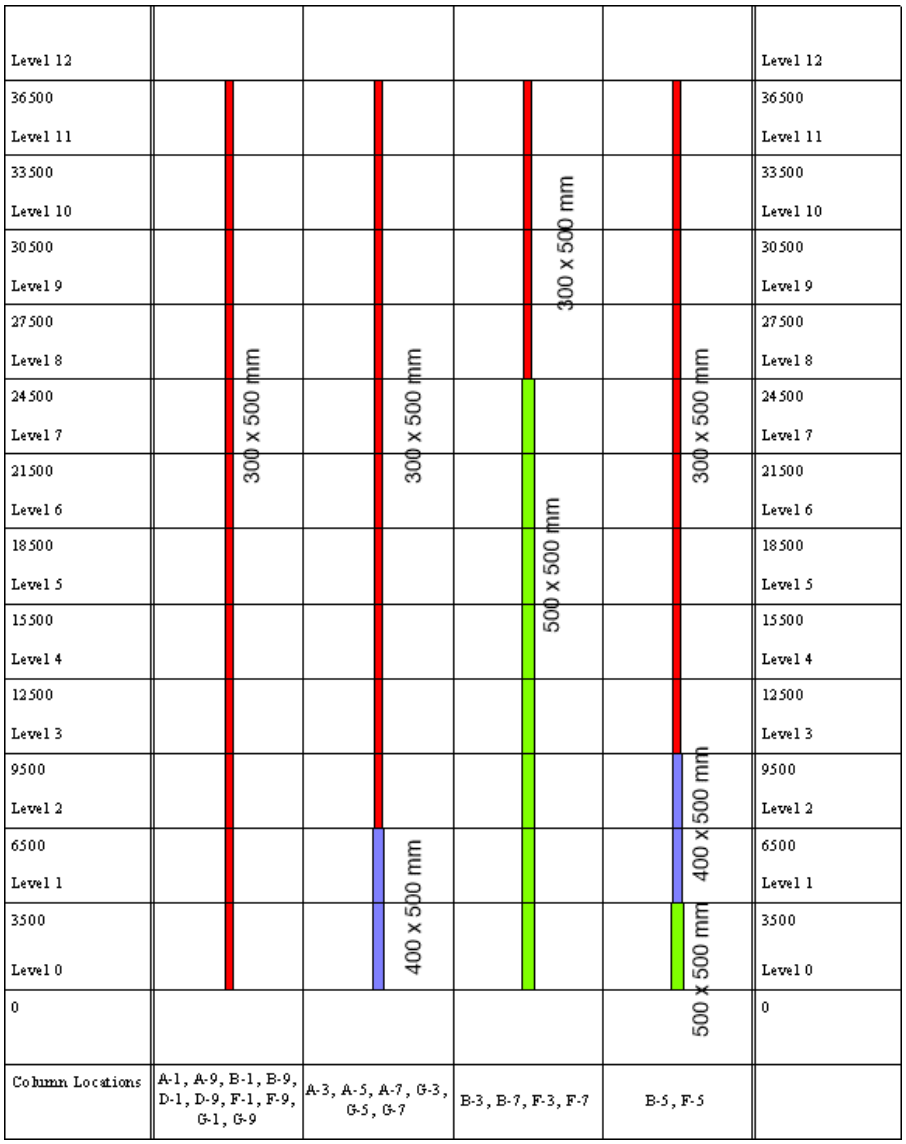


Figure 5.46. Graphical column schedule, twelve-story structure.

## 5.6 Total Rebar Weights

The total rebar weights are calculated using the analysis and design results obtained from the finite element model. The strength requirements of members are checked according to TS500 and both seismic codes. The minimum reinforcement requirements defined in the seismic codes are also considered in the total rebar weights.

The figures below summarize the changes between the total rebar weights of three, six, and twelve-story structures. The figures are shown at each location separately by comparing rebar weights.

For beams, the required reinforcement area is increased in TBEC 2018. The slight increase agrees with the increase in the beam member force discussed in the previous section. For columns, the minimum reinforcement governs the design of all members. For shear walls, the change in reinforcement is correlated with the change in the base shears.

Figures 5.47, 5.48, and 5.49 show the total reinforcement weight in units of tons. The total weight is compared for each code and location, the discussions are made underneath each figure.

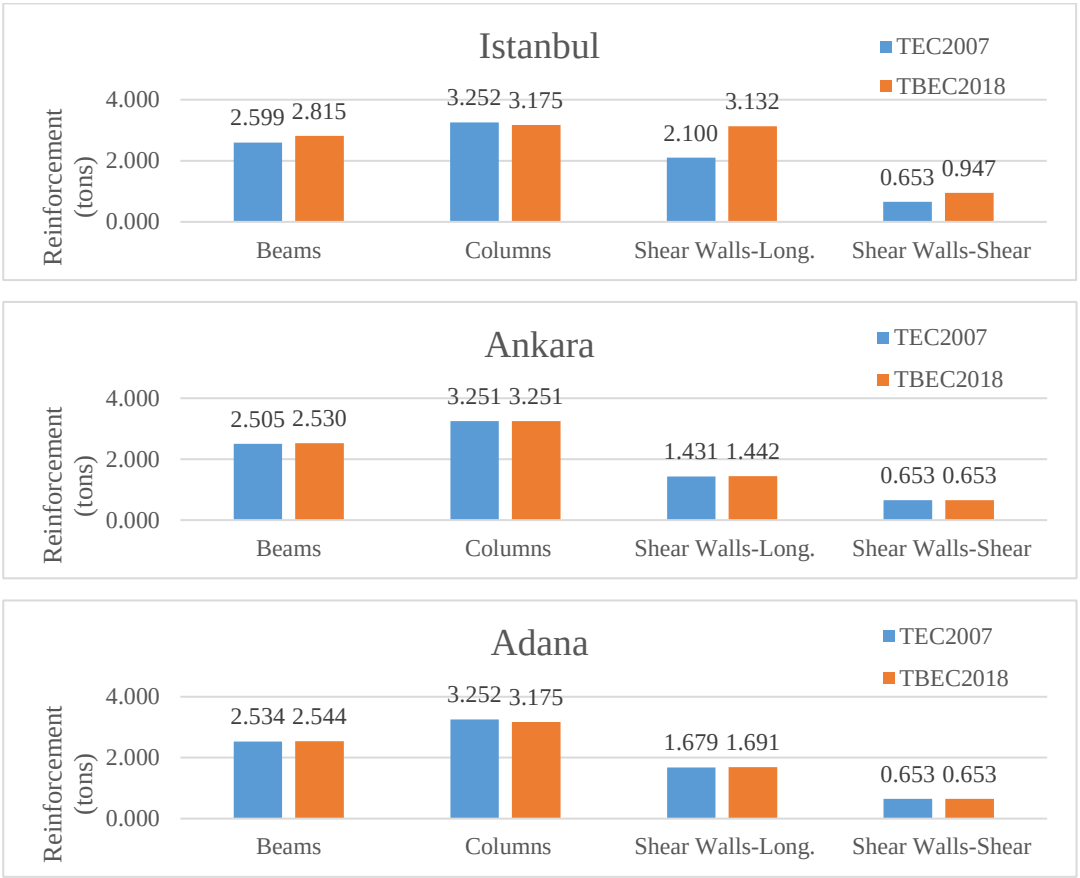


Figure 5.47. Total reinforcement weights, three-story structure.

The difference is only noticeable for the structure located in Istanbul for the three-story structure where the spectral design acceleration is increased, and the reduction

factor is decreased from TEC 2007 to TBEC 2018. The results show that the effect of these differences is mainly absorbed by the increase in the reinforcement of shear walls. For shorter structures shear behavior is expected which explains the difference in the shear wall reinforcement. For Ankara and Adana, the design spectral acceleration is close; therefore, the difference in reinforcement areas is minimal.

For the six-story structure, the following results are obtained (Figure 5.48). The decrease in the seismic load for the six-story structure in TBEC 2018 resulted in a decrease in total reinforcement weight for all members. Some of the decreases are limited by the minimum reinforcement.

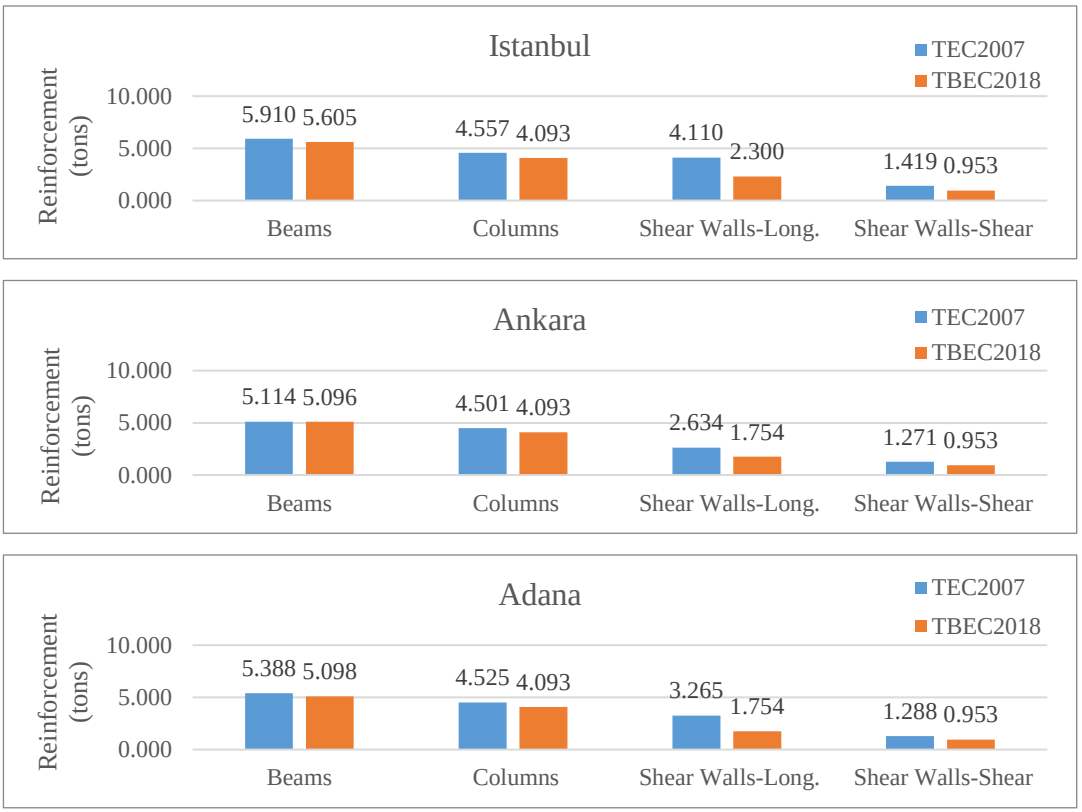


Figure 5.48. Total reinforcement weights, six-story structure.


Figure 5.49. Total reinforcement weights, twelve-story structure.

The results in Figure 5.49 show that for the twelve-story structure, the decrease in the loads from TEC 2007 to TBEC 2018 is observed in the decrease in the total reinforcement weight of beams and shear walls. For the columns, the minimum reinforcement and gravity loads govern the design; therefore, the change in seismic load barely influences the results.

Additionally, the total reinforcement cost (TRC) difference can be obtained with the information presented in this section. Assuming a per ton price of reinforcement to be 15500 TL, TRC difference is calculated by subtracting the TEC 2007 TRC from TBEC 2018 TRC. The results are presented in Figure 5.50.

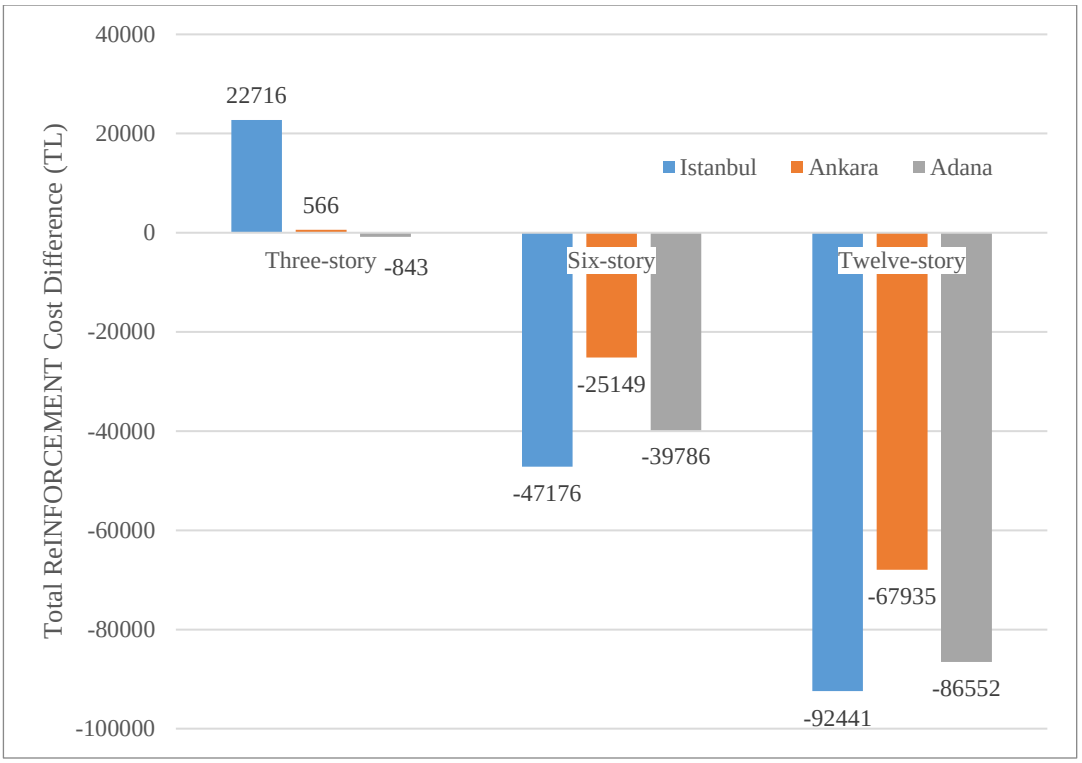


Figure 5.50. Total reinforcement cost difference between TBEC 2018 and TEC 2007.

The results presented in Figure 5.50 shows that TBEC 2018 procedures have decreased the cost of total reinforcement for six and twelve-story structures while the cost has increased for the three-story structure. The increase in the reinforcement cost for the three-story structure is attributed to the initially higher acceleration in Istanbul, and the change in the modification procedures of the seismic load reduction factor. The decrease in the cost for the six and twelve-story structure is due to the usage of effective moment of inertia factors which increases the periods of structures leading to smaller design spectral acceleration. Additionally, the reduction factor determination procedure further decreases the design spectral accelerations leading to the total reinforcement weight/cost decrease in TBEC 2018.

The cost calculation is calculated again including the cost of concrete to obtain the total material cost difference. The C30 concrete price is assumed as 1460 TL/m$^3$. Figure 5.51 demonstrates the change in total material cost between the two codes in terms of percentage. The resulting percentages show that the differences due to the reinforcement discussed above affect the total material costs up to 5%.

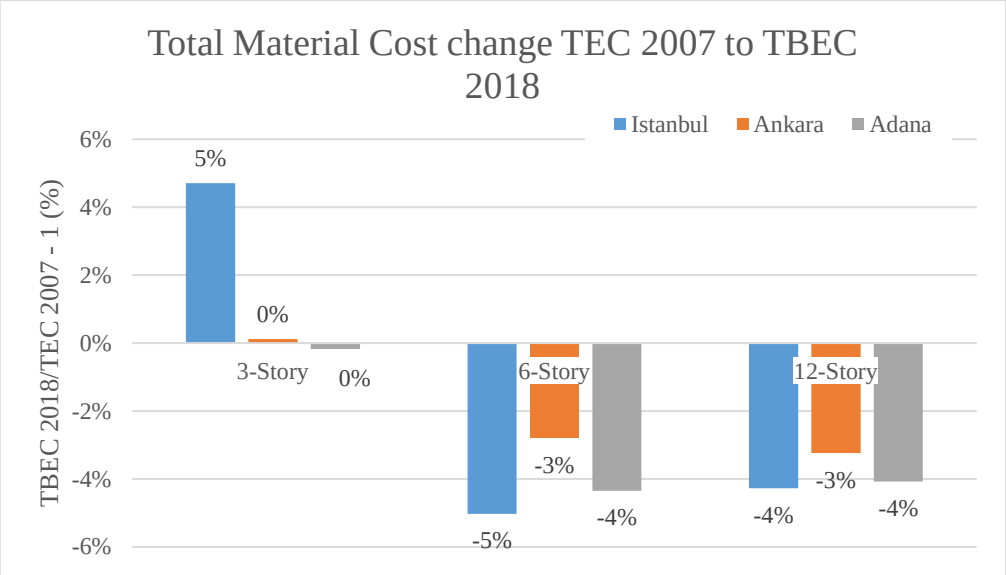


Figure 5.51. Total material cost change in terms of percentage.

# CHAPTER 6

# CONCLUSION

This study compared archetype buildings at three different seismic zones of Türkiye with three, six, and twelve stories. The analysis and design of these structures shows that the changes introduced to TBEC 2018 affect all aspects of the structures' seismic design. The spectral accelerations, base shears, reduction factor, member forces, drifts, and total reinforcement weights have been compared with linear analysis and design according to both codes. The following conclusions are derived:

- Spectral Acceleration: the root of the difference between the codes is the determination of the ground acceleration at each location. TEC 2007 divides the country into seismic regions without regard for local site conditions. Four acceleration values are defined for these regions. However, TBEC 2018 completely changes the process by introducing a seismic hazard map and providing site-specific data dependent on the coordinates of the structure.
- Seismic Load Reduction Factors: the methodology with which the reduction factors are chosen for the structural system has been changed in TBEC 2018. This study showed that while a ductility requirement was met for TEC 2007 with the same structure, the requirements of TBEC 2018 could not be satisfied. This results in a comparison of structures with different reduction factors. The use of different reduction factors changes the reinforcement demand of all members. TBEC 2018 uses the overturning moment participation to determine the shear wall’s stiffness contribution while TEC 2007 uses base shear participation. As a result, the reduction factor in TBEC 2018 is not modified from R = 7 but for TEC 2007 the reduction factor is reduced from R = 7 to R = 6 due to high participation of shear walls.

- Modeling: TBEC 2018 requires the use of effective moment of inertia factors on members; the decreased stiffness results in higher periods for the analyzed structures. The increase in periods decreases the accelerations, and when combined with differences in the seismic load reduction factors, the results for both codes further diverge from each other by decreasing the forces on the structures designed for TBEC 2018. TBEC 2018 absorbs some of the decrease in the base shear by applying overstrength factors to brittle member failures. Additionally, shear strength formulas have been revised in TBEC 2018 to impose stringier requirements on all member types for higher grade concrete.
- Reinforcement: the total reinforcement weights show that for columns mostly minimum reinforcement governs. For beams, the total weight changes according to the change in seismic load. The most change is observed in the shear wall reinforcements since they comprise the majority of the lateral load resistance. The difference in the total cost shows that the change in the reinforcement areas increases the total material cost up to 5% in three-story structure while it decreases the cost up to 5% for six and twelve-story structures.
- Drifts: the drift comparisons show that the change to the determination of the drift limit in TBEC 2018 imposes a minor change to the limit given TEC 2007, but the drift found in the new code has significantly increased due to the use of effective moment of inertia factors for all members. The results indicate that the drift demand on buildings designed using TBEC 2018 has increased compared to TEC 2007.

## 6.1 Future Studies and Recommendations

Further studies are suggested for the following aspects of this thesis:

- Linear analysis and design using modal response spectrum analysis may yield different results than the equivalent lateral force method.

- The ductility and reduction factor relationship can be studied for buildings with different lateral resisting systems and materials.
- The comparative analysis can be repeated for other soil/site class conditions to observe the effect of soil parameters to the design.
- Nonlinear analysis can be utilized to assess the performance of structures designed according to TBEC 2018.

## REFERENCES


Akansel, Vesile & Soysal, B. Feyza & Kadaş, Koray & Gülkan, Polat. (2019). AN EVALUATION OF THE 2019 SEISMIC HAZARD MAP OF TURKEY ON THE BASIS OF SPECTRUM INTENSITY.

Akkar, S., Azak, T., Çan, T. et al. Evolution of seismic hazard maps in Turkey. Bull Earthquake Eng 16, 3197–3228 (2018). https://doi.org/10.1007/s10518-018-0349-1

Aksoylu, C., Mobark, A., Arslan, M. H., & Erkan, I. H. (2020). A comparative study on ASCE 7-16, TBEC-2018, and TEC-2007 for reinforced concrete buildings. *Revista de La Construccion*, *19*(2), 282–305. https://doi.org/10.7764/RDLC.19.2.282

Ay, B. Ö. (2012). Scaling and Selection of Ground Motion Records for Nonlinear Response History Analysis of Structures. 15th World Conference on Earthquake Engineering, Lisbon, Portugal, 24 - 28 Eylül 2012. https://hdl.handle.net/11511/70734

Büyüksaraç, A., Işık, E., & Bektaş, Ö. (2022). A Comparative Evaluation of Earthquake Code Change on Seismic Parameter and Structural Analysis; A case of Turkey. *Arabian Journal for Science and Engineering*. https://doi.org/10.1007/s13369-022-07099-4

Chopra, A. K. (2023). *Dynamics of Structures: Theory and applications to earthquake engineering*. Pearson.

CSI Analysis Reference Manual (SAP 2000, ETABS and CSI Bridge), Computers and Structures Inc., USA.

Disaster and Emergency Management Center (2020), Seismic Hazard Map of Türkiye. Ankara, Türkiye. Available at: https://tdth.afad.gov.tr/TDTH/main.xhtml

G. Dok , H. Öztürk , A. Demir and N. Çağlar , "Investigation of Effective Bending Rigidity Considering Different Code Approaches", Academic Platform Journal of Natural Hazards and Disaster Management, vol. 1, no. 1, pp. 35-48, Jun. 2020

Işık, E. (2021). A comparative study on the structural performance of an RC building based on updated seismic design codes: case of Turkey. Challenge Journal of Structural Mechanics, 7(3), 123-134. doi:http://dx.doi.org/10.20528/cjsmec.2021.03.002

Leissa, A. W. (2005). The historical bases of the Rayleigh and Ritz methods. Journal of Sound and Vibration, 28(4), 961-978. https://doi.org/10.1016/j.jsv.2004.12.021

Nemutlu, Ömer & Sari, Ali. (2018). Comparison of Turkish Earthquake Code in 2007 With Turkish Earthquake Code in 2018.

R. Pinho, C. Bhatt, S. Antoniou, & R. Bento (2008). MODELLING OF THE HORIZONTAL SLAB OF A 3D IRREGULAR BUILDING FOR NONLINEAR STATIC ASSESSMENT. In 14th World Conference on Earthquake Engineering, October 12-17, 2008, Beijing, China: Innovation, practice, safety. Beijing; World Conference on Earthquake Engineering Retrieved 2022.

TBEC 2018: Turkish Building Earthquake Code. (2018). *T.C. Resmi Gazete. Ankara, Türkiye*.

TEC 2007: Turkish Earthquake Code. (2007). *T.C. Resmi Gazete. Ankara, Türkiye*.

Wilson, E. L. (2000). *Three dimensional static and dynamic analysis of structures: A physical approach with emphasis on earthquake engineering*. Computers and Structures.

Yakut, A., Binici, B., Topkaya, C., Canbay, E., Sucuoğlu, H., Tuncay, K., Yılmaz, M. T., & Gülkan, P. (2018). ÖRNEK 7B. In *Türkiye Bina Deprem Yönetmeliği Örnekler Kitabi* (pp. 25–48). essay, T.C. İçişleri Bakanlığı Afet ve Acil Durum Yönetimi Başkanlığı.

# A. APPENDIX

The following figures show the remaining drift comparisons from the linear analysis of three, six, and twelve-story archetype buildings in Istanbul, Ankara, and Adana.

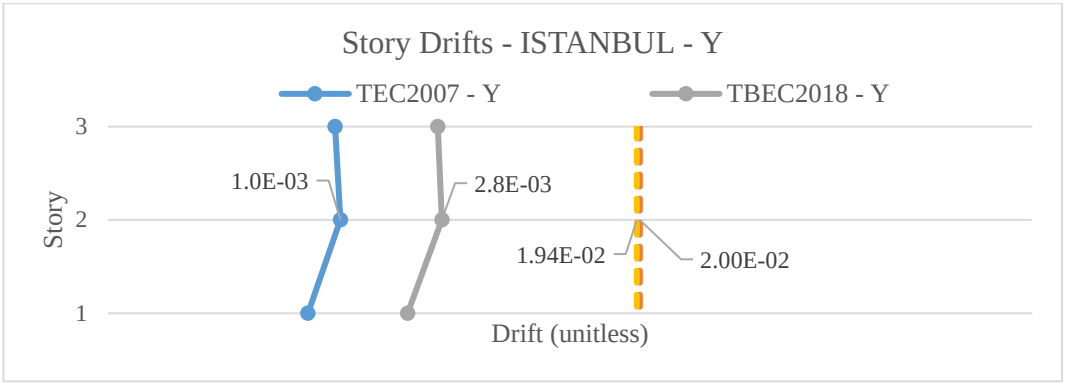


Figure A.1. Drift comparison, Istanbul, three-story structure.

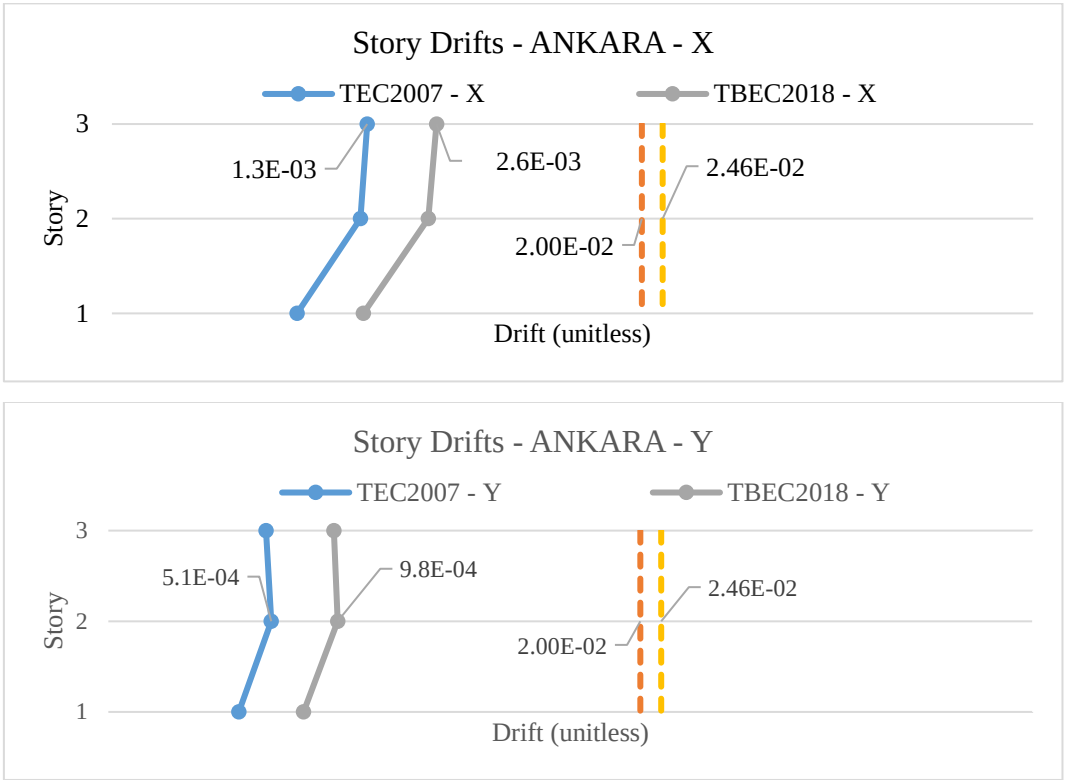


Figure A.2. Drift comparison, Ankara, three-story structure.

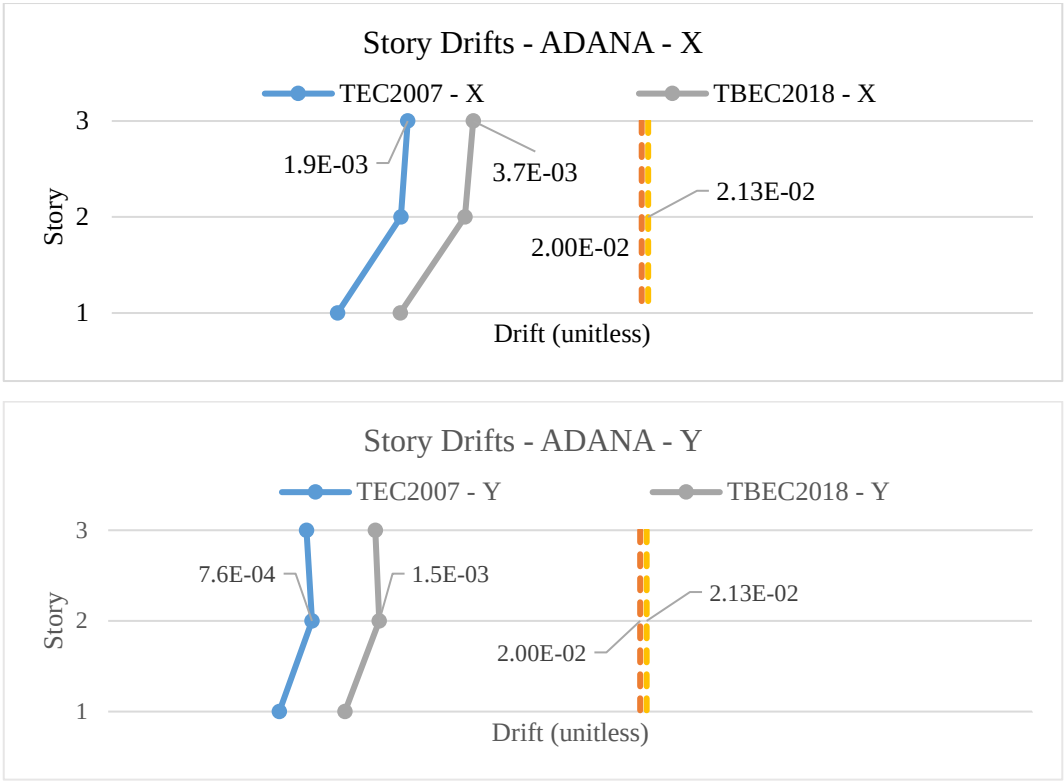


Figure A.3. Drift comparison, Adana, three-story structure

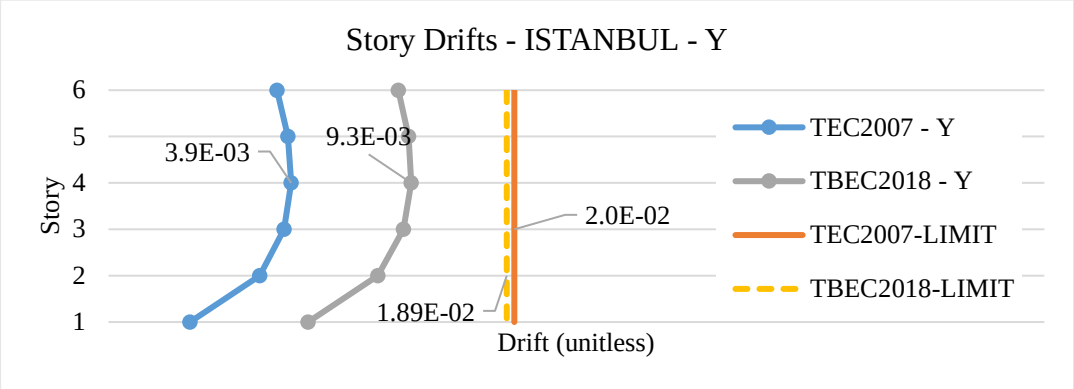


Figure A.4. Drift comparison, Istanbul, six-story structure

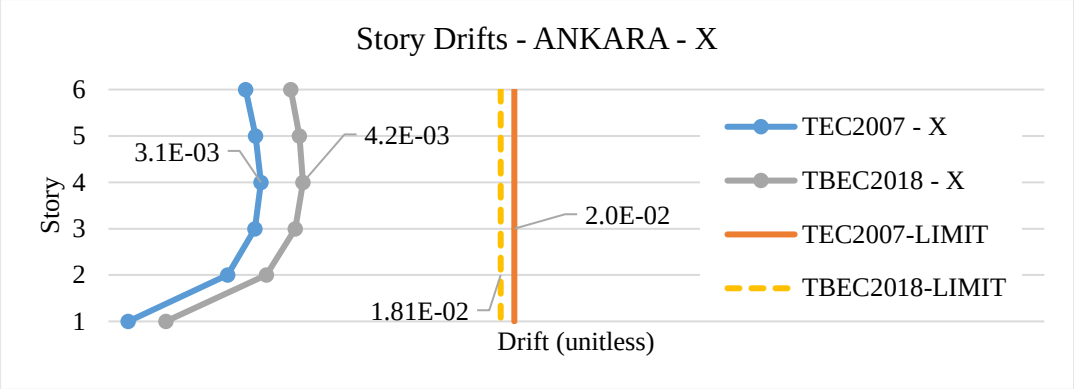


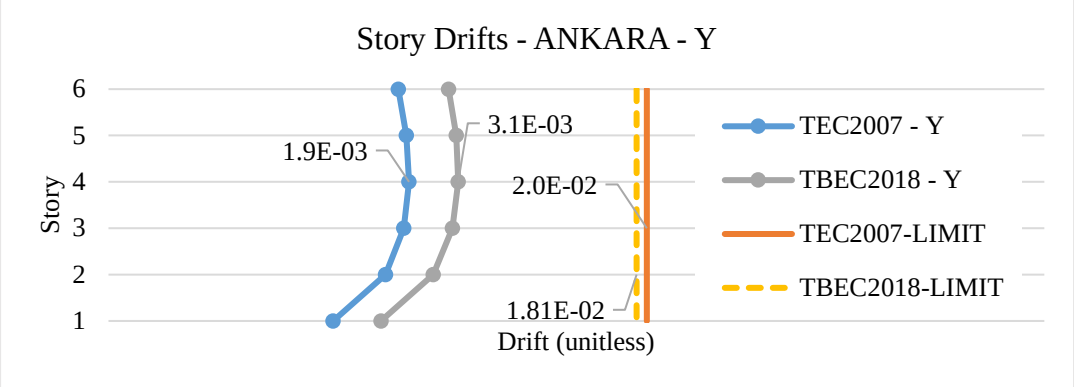


Figure A.5. Drift comparison, Ankara, six-story structure.

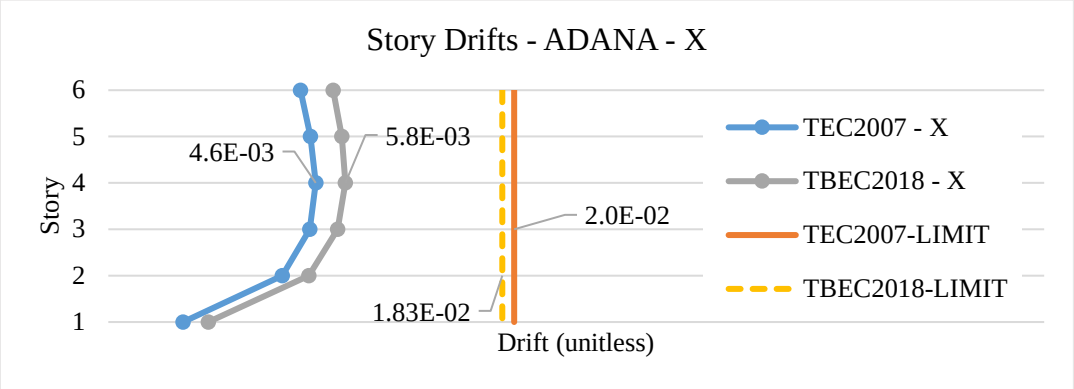


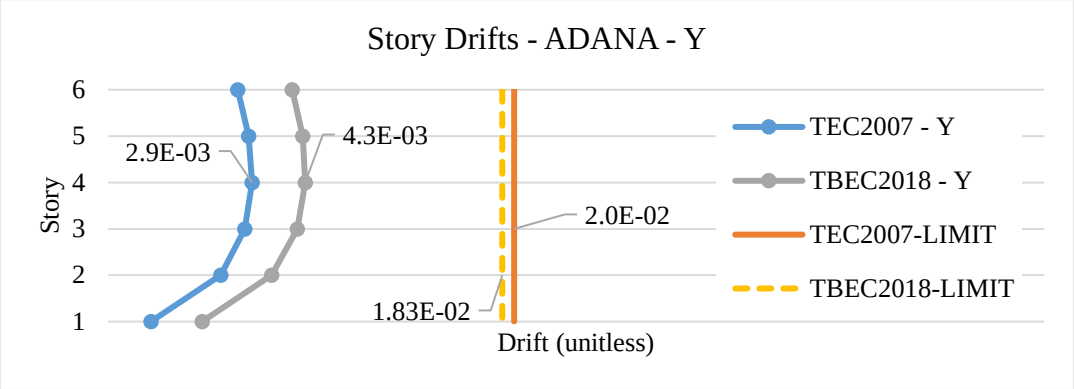


Figure A.6. Drift comparison, Adana, six-story structure.

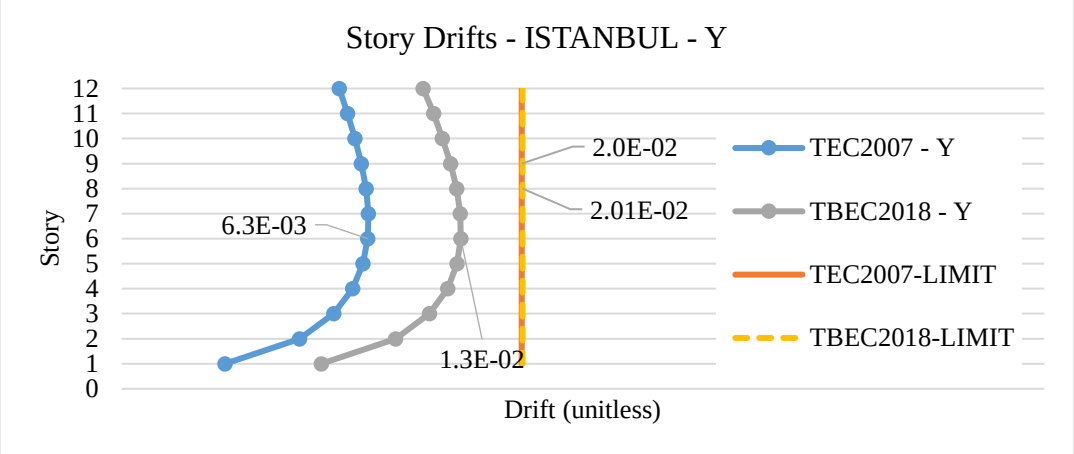


Figure A.7. Drift comparison, Istanbul, twelve-story structure

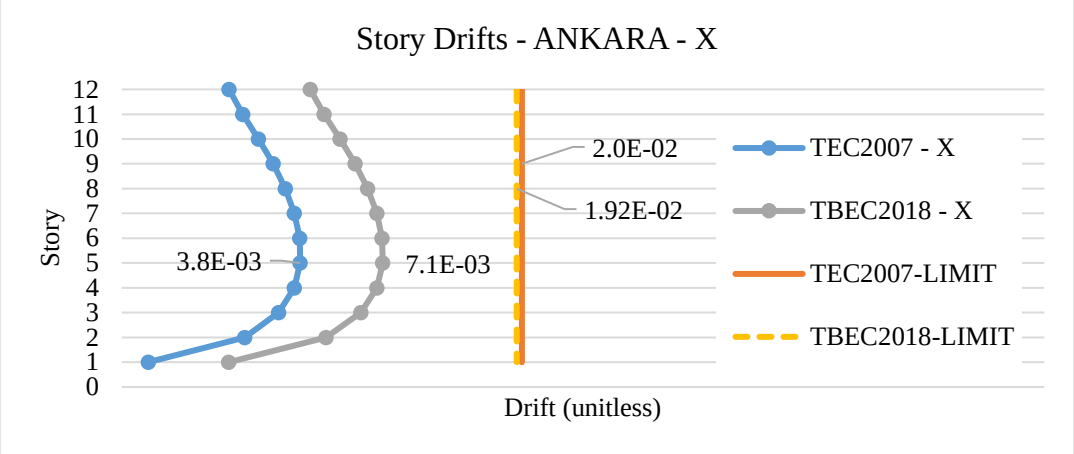


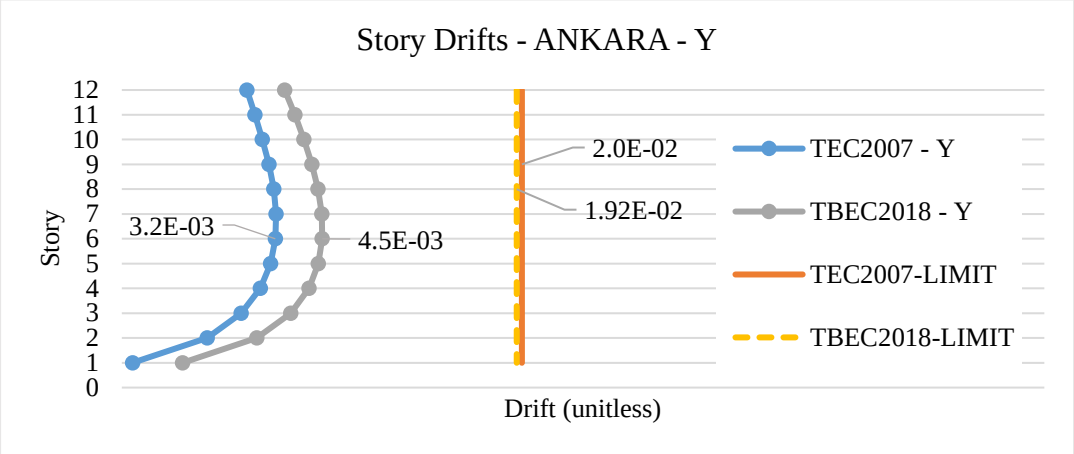


Figure A.8. Drift comparison, Ankara, twelve-story structure.

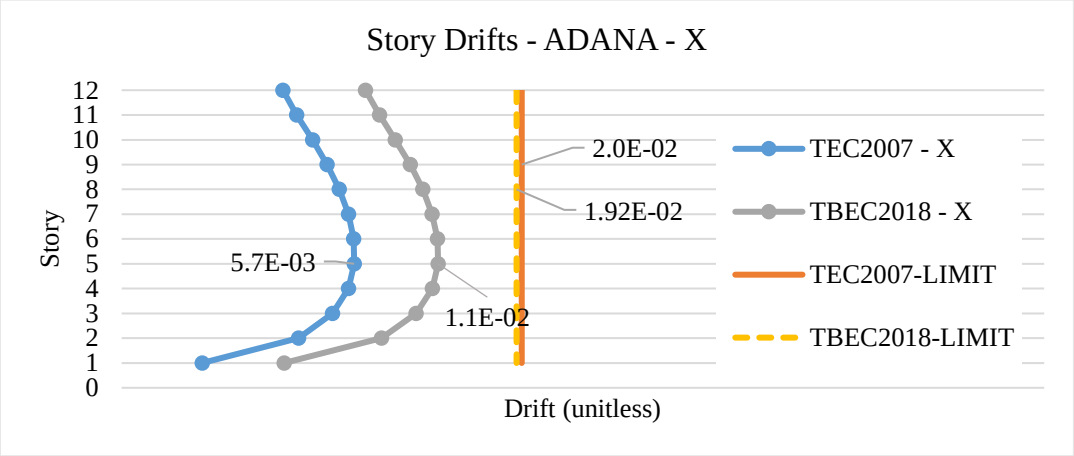


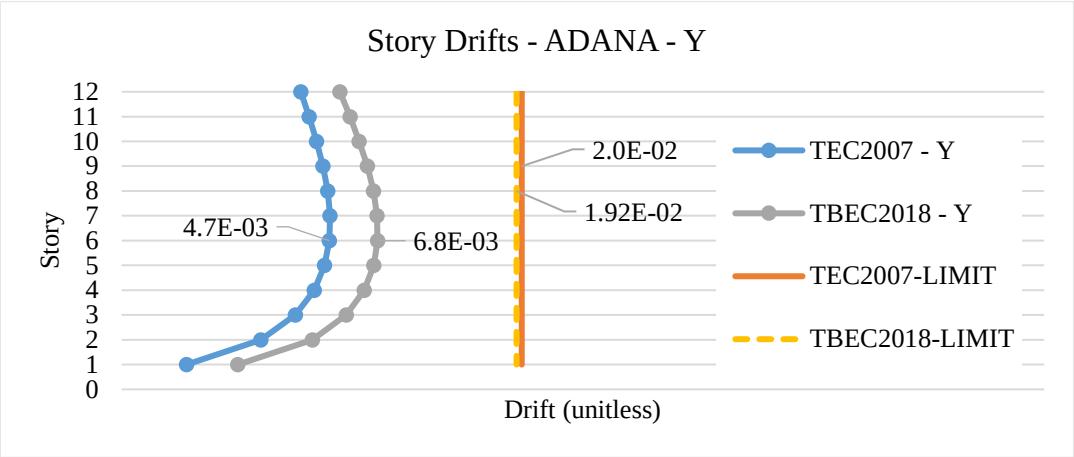


Figure A.9. Drift comparison, Adana, twelve-story structure.